2021

Sustained CA2+ mobilizations: a quantitative approach to predict their importance in cell-cell communication

BOSTON UNIVERSITY

SCHOOL OF MEDICINE

Dissertation

SUSTAINED CA2+ MOBILIZATIONS: A QUANTITATIVE APPROACH TO PREDICT THEIR IMPORTANCE IN CELL-CELL COMMUNICATION

by

YOONJOO KATHERINE LEE

B.S., Yale College, 2012

Submitted in partial fulfillment of the

requirements for the degree of

Doctor of Philosophy

2019

Approved by

First Reader _____

Vickery Trinkaus-Randall, Ph.D.
Professor of Biochemistry, Ophthalmology

Second Reader _____

Christopher V. Gabel, Ph.D.
Associate Professor of Physiology & Biophysics

Third Reader _____

Keith Tornheim, Ph.D.
Associate Professor of Biochemistry

DEDICATION

I would like to dedicate this work to my family and friends who have supported me through the years.

ACKNOWLEDGMENTS

I would not have made it this far without the help of many people along the way. I want to thank my mentor Dr. Vickery Trinkaus-Randall, who has been a supportive backbone for the entirety of my graduate school career. It has been such a pleasure to work with her over the past four years, especially after I had been struggling to find a lab and mentor that was a good fit for me right after my qualifying exams. I am grateful for the opportunity to have learned from her what is to be a scientist, teacher, and mentor. I would like to thank Celeste Rich for teaching me lab techniques and for offering help or give scientific advice. Her meticulous approach to experimental design and lab techniques has been a great influence.

I would also like to thank my thesis committee for all their advice and scientific insight: Dr. Shelley Russek, Dr. Christopher Gabel, Dr. Keith Tornheim, and Dr. Katya Ravid. I would especially like to thank Dr. Gabel for acting as my second reader and offering excellent critique in my experiments and work. I would like to thank Dr. Tornheim for his excellent advice and mentorship both in and outside of the lab. Finally I would like to Dr. Russek for being my committee chair and helping me navigate through the scientific process of my project and offering me excellent advice.

I would like to thank the members of the Trinkaus-Randall lab for welcoming me into the lab, which has been a supportive and enjoyable workplace environment. I would like to thank Dr. Martin Minns and Gregory Teicher for all the work they did on P2X7 and Ca^{2+} live-cell imaging, which contributed greatly to the conceptualization of my

project. I would like to thank Jenna Meyer and Dr. Obianamma Onochie for being good friends and lab partners for the first years I was in lab. I would like to thank Anwuli Onyejose and Garrett Rhodes for being great co-workers and friends for the past few years. I would like to thank Mintae Kim and Sung Jun Son for spending time out of their busy medical school schedules to contribute to the project. I would also like to thank Zhonghao Dai and Anne Londregan for their contributions for the project as undergraduate researchers.

I would like to thank all the faculty and staff of the MD/PhD program and the Departments of Pharmacology and Biochemistry for creating a supportive environment for students, and I would like to especially thank the co-directors Dr. Vickery Trinkaus-Randall and Dr. Steven Borkan for their mentorship and guidance. I would like to thank Dr. Vijaya Kolachalama and Cody Karjadi for their feedback and collaboration on the computer programming aspect of the project. I would like to thank all my friends from Pharmacology, Biochemistry, and other departments. I would also like to thank my friends in the MD/PhD Department for being a support network during difficult times.

Most of all, I thank my family and especially my parents, Max Myungsoo and Gumsun Lee, and my brother Anthony Gunho Lee. This work is dedicated to you, and I absolutely could not have made it without your unconditional love and support.

SUSTAINED CA2+ MOBILIZATIONS: A QUANTITATIVE APPROACH TO PREDICT THEIR IMPORTANCE IN CELL-CELL COMMUNICATION AND WOUND HEALING

YOONJOO KATHERINE LEE

Yale University, 2012

Ph.D. degree requirements completed in 2019

Dual M.D./Ph.D. degrees expected in 2021

Major Professor: Vickery Trinkaus-Randall Ph.D., Professor of Biochemistry

ABSTRACT

Epithelial wound healing requires the coordination of cells to migrate as a unit over the basement membrane after injury. An excellent model tissue is the corneal epithelium, which is an avascular stratified squamous tissue that responds to growth factors and nucleotides when the epithelial barrier is damaged. One signal that has a ubiquitous response in epithelial wound healing is the cellular release of the nucleotide ATP, which may occur because of mechanics forces and/or change in cell shape. Within milliseconds to seconds after injury, extracellular ATP binds to purinoreceptors and triggers a transient Ca^{2+} wave, which is used by cells to transduce mechanical signals into chemical signals and alter signaling pathways. To understand the process of this coordinated movement, it is critical to study the dynamics of cell-cell communication.

In this study we developed a novel method to identify and characterize the degree of cell-cell communication that occurs through sustained Ca^{2+} mobilizations after injury, which are concentrated along the epithelial wound edge and reduced in cells distal to the injury. Using MATLAB analyses, we generated profiles of the sustained Ca^{2+} mobilizations, and demonstrated that the Ca^{2+} response was replicated in ex vivo organ culture models. The sustained Ca^{2+} mobilizations were present also after stimulation with either BzATP or UTP, which are agonists of P2X7 and P2Y2 respectively. The probability that cells would communicate was greater in response to BzATP compared to UTP. The specificity of these ligands was demonstrated using competitive inhibitors of P2Y2 and P2X7 receptors, AR-C 118925XX and A438079, respectively. An inhibitor of pannexin-1, 10Panx, attenuated both wound closure and BzATP agonist-initiated response. These sustained mobilizations are correlated with changes in cellular morphology and motility, which were prominent in cells at the leading edge of the wound during cell migration. Together, our results demonstrate that the sustained Ca^{2+} mobilizations mediated by purinoreceptors and pannexins are a vital component in regulating the long-term response to injury, as studied in organ culture.

TABLE OF CONTENTS

LIST OF FIGURES

LIST OF ABBREVIATIONS

ANOVA ..... analysis of variance

ADP ..... adenosine 5'-diphosphate

AMP ..... adenosine 5'-phosphate

ATP ..... adenosine 5'-triphosphate

βME 2-mercaptoethanol

BzATP ..... 3’-O-(4’-benzoyl)benzoyl ATP

Ca2+..... calcium

$CaCl_2$ ..... calcium chloride

CONX ..... connexin

CSK buffer ..... "cytoskeletal" buffer

Da ..... dalton (unit of mass)

DAG ..... diacylglycerol

DAPI ..... 4',6-diamidino-2-phenylindole

DIO ..... diet-induced obesity

DMEM ..... Dulbecco's modified Eagle medium

DMSO ..... dimethyl sulfoxide

DNA ..... deoxyribonucleic acid

DTT ..... dithiothreitol

EGF(R) ..... epithelial growth factor (receptor)

EGTA ..... ethylene glycol tetraacetic acid

EDTA ..... ethylenediaminetetraacetic acid

ER ..... endoplasmic reticulum

F-actin ..... filamentous actin

FAK ..... focal adhesion kinase

FBS ..... fetal bovine serum

FIJI ..... FIJI is just ImageJ

FRAP ..... fluorescence recovery after photobleaching

GPCR ..... G protein-coupled receptor

GJ ..... gap junction

HCl ..... hydrochloric acid

HCLE cells ..... human corneal limbal epithelial cells

HEPES ..... 4-(2-hydroxyethyl)piperazine-1-ethanesulfonic acid

HRP ..... horseradish peroxidase

IP_3(R) ..... inositol (1,4,5) trisphosphate (receptor)

kDa ..... kilodalton

K-SFM ..... keratinocyte serum-free media

$MgCl_2$ ..... magnesium chloride

mRNA ..... messenger ribonucleic acid

µg ..... microgram

µM ..... micromolar

µL ..... microliter

mg ..... milligram

mL ..... milliliter

mM ..... millimolar

ng..... nanogram

nM ..... nanomolar

NaCl ..... sodium chloride

oxATP ..... oxidized ATP (adenosine 5'-triphosphate 2',3'-dialdehyde)

P1 ..... class 1 purinergic receptor (adenosine receptor)

P2Y ..... class 2 purinergic receptor, family Y

P2X ..... class 2 purinergic receptor, family X

PAGE ..... polyacrylamide gel electrophoresis

PANX ..... pannexin

PBS (-T) ..... phosphate-buffered saline (with Tween-20)

PCR ..... polymerase chain reaction

PFA ..... paraformaldehyde

PIP_2 ..... phosphatidylinositol (4,5) bisphosphate

PIPES ..... 1,4-piperazinediethanesulfonic acid

PKC ..... protein kinase C

PLC ..... phospholipase C

PMSF ..... phenylmethanesulfonyl fluoride

PMCA ..... plasma membrane calcium ATPase

Pro ..... proline (amino acid)

rRNA ..... ribosomal ribonucleic acid

RIPA ..... radiolabeled immunoprecipitation assay

SDS ..... sodium dodecyl sulfate

SERCA ..... smooth endoplasmic reticulum calcium ATPase

SR ..... sarcoplasmic reticulum

T2D ..... type 2 diabetes mellitus

TBS(-T) ..... tris-buffered saline (with Tween-20)

TNF(R) ..... tumor necrosis factor (receptor)

Tris ..... tris(hydroxymethyl)aminomethane

UTP ..... urindine 5'-triphosphate

CHAPTER ONE: INTRODUCTION

Epithelial wound healing requires the coordination of cells to migrate as a unit over the basement membrane after injury. This process requires coordination between cells to migrate over the basement membrane by forming adhesion complexes to stabilize the tissue. This collective movement of cells as an epithelial sheet is more complex than the migration of single cells, such as observed in fibroblasts. The release of ATP is a ubiquitous response that occurs after cell injury in multiple tissue systems such as the bronchial and corneal epithelia, or an alteration in force such as in glaucoma (Barrios et al., 2017; Klepeis et al., 2001; Lu et al., 2015). This extracellular ATP binds to purinoreceptors and triggers a transient Ca^{2+} wave within milliseconds to seconds after injury. This Ca^{2+} mobilization is used by cells to transduce mechanical signals into chemical signals and alter signaling pathways (Adinolfi 2013; Boucher et al., 2007; Burnstock 2009; Kehasse et al., 2013; Yin et al., 2007).

To understand the process of this coordinated movement, it is critical to study the dynamics of cell-cell communication. We developed a method to characterize the injury-induced sustained Ca^{2+} mobilizations that travel between cells for periods of time up to several hours. These events of communication are concentrated along the wound edge and are reduced in cells further away from the wound. Our goal was to delineate the role and contribution of these sustained mobilizations and using MATLAB analyses, we determined the probability of cell-cell communication events in in vitro models and ex vivo organ culture models. We demonstrated that the injury response was complex and

represented the activation of a number of receptors. In addition, we found that pannexin channels mediated the cell-cell communication and motility. Furthermore, the sustained Ca^{2+} mobilizations are associated with changes in cell morphology and motility during wound healing. The results demonstrate that both purinoreceptors and pannexins regulate the sustained Ca^{2+} mobilization necessary for cell-cell communication in wound healing.

1-1: The Cornea and Corneal Injury

Anatomy of the eye and the cornea

The eye is the organ that interprets incoming light into neuronal signals that are processed in the brain as visual images. This process allows organisms to visually interact and respond to environmental stimuli (Jakus, 1961). The cornea is the most anterior structure of the eye that covers the lens and iris; it also transmits and refracts light to the lens to focus the light on the retina (Jakus, 1961) (Fig. 1-1A). The light-sensitive receptors in the retina then translate the light into signals through the optic nerve to relay them to the visual cortex of the brain (Jakus, 1961). To allow for maximum light passage, the cornea is avascular and clear, surrounded by conjunctival vascular cells in the sclera. The cornea accounts for 70-80% of total light refraction, indicating the health of the cornea is important for vision integrity (Jakus, 1961).

The cornea itself consists of several cell types in three distinct layers separated by two basement membranes: epithelium, Bowman’s layer, stroma, Descemet's membrane, and endothelium (Fig. 1-1B). The corneal epithelium is a pseudo-stratified, 5-7 layer of epithelial cells that are fed by the tear fluid on the apical surface of the cornea and blood

A

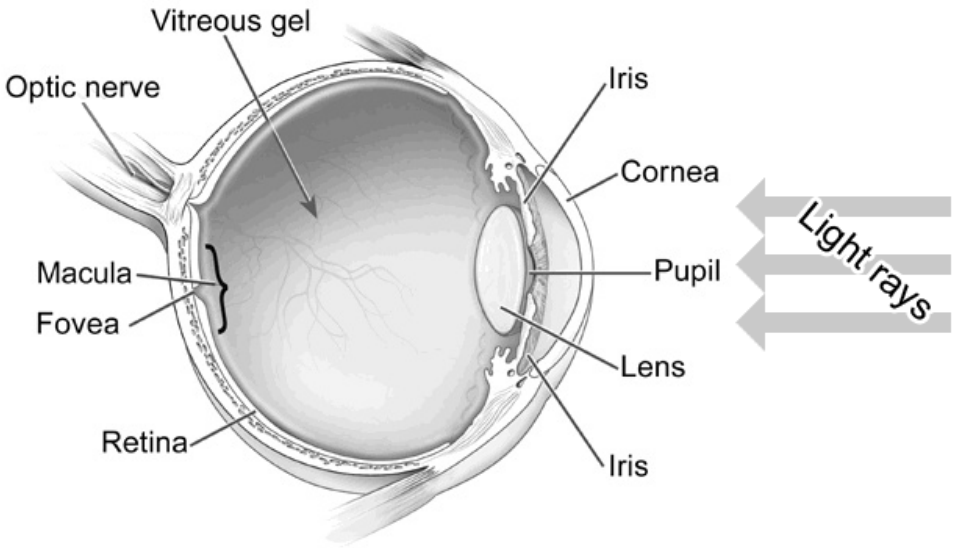

Adapted from National Eye Institute, https://nei.nih.gov/health/eyediagram

B

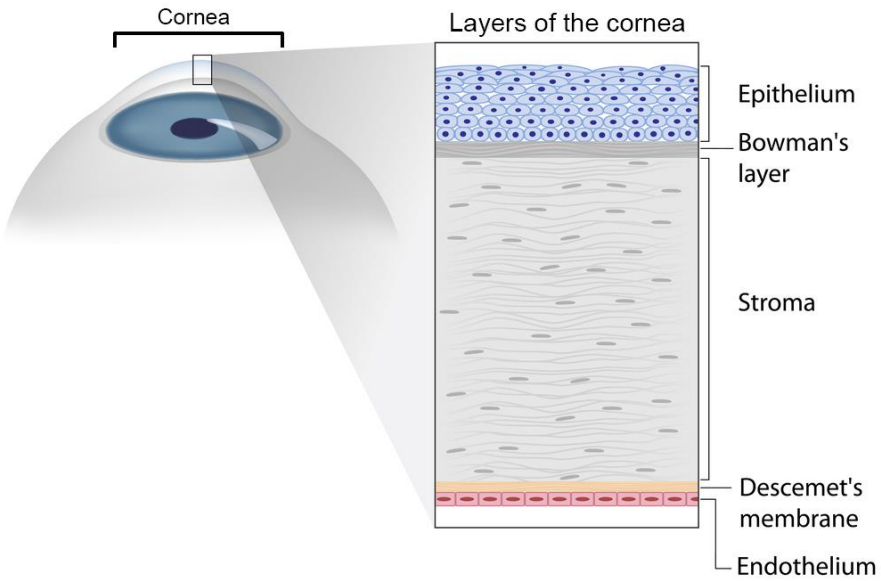

Adapted from Optometric Professional Network, http://www.eyedoctornetwork.org/cornea.htm

Figure 1-1: The eye and cornea.
A: Diagram of the eye. **B:** Diagram of the cornea.

vessels in the conjunctiva. The Bowman's layer covers the region between the corneal epithelium and stroma, and is composed of different matrix proteins: collagen IV, laminin, sulfated proteoglycans, and perlecan (Trinkaus-Randall, 2000). This layer's function is similar to the basement membrane and only present in primates (Wilson and Hong, 2000). The corneal stroma accounts for 50-80% of the cornea's total thickness and consists of collagens I and V, which are maintained by sparse neural crest-derived keratocytes and heterogeneous dendritic cells. The stroma's avascularity, organization of uniform collagen fibers, and presence of small leucine repeating proteoglycans contribute to its transparency. Any compromise in the stromal network of matrix molecules can affect its clarity (Jakus, 1961). The Descemet's membrane defines the boundary between the stroma and endothelium, and its composition is similar to the Bowman's layer plus fibronectin. The corneal endothelium is a cellular monolayer that outlines the posterior cornea and is one of the few avascular endothelium layers in the body. Its primary function is to regulate hydration and fluid flow of the stroma (Baum et al., 1984).

There are also two other cell types in the cornea: nerves and immune cells. Derived from the trigeminal nerve, corneal sensory nerves innervate the multiple layers of the cornea. They lie parallel to stromal collagen fibers in unmyelinated bundles and extend their free nerve endings through the epithelial basement membrane into basal and apical epithelium (Müller et al., 1996; 2003) (Fig. 1-2). The high density of nerve endings results in high sensitivity of the corneal epithelial surface to other environmental changes. During infection or injury, heterogeneous dendritic cells in the stroma are induced to infiltrate the conjunctiva (Hamrah et al., 2003).

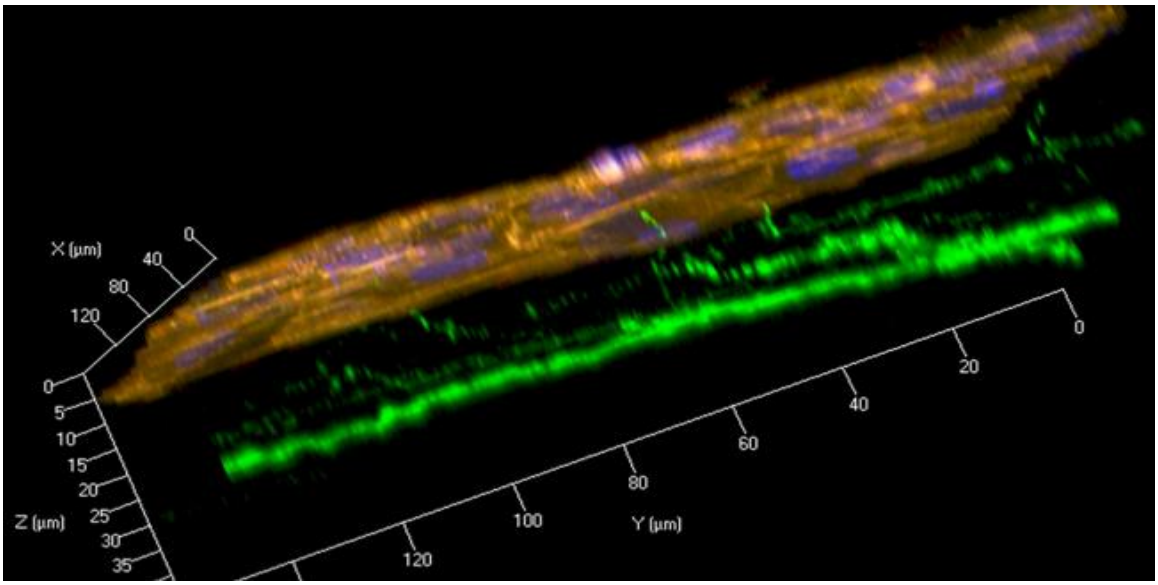

Figure 1-2: Immunofluorescence image of the innervation of the corneal epithelium. THY-1+ nerves were labeled with GFP (green) and the tissue was counterstained with rhodamine (red, for f-actin) and DAPI (blue, for nuclei).

The corneal epithelium turnover

The corneal epithelium provides essential barrier function and clarity to the cornea. These epithelial cells do not undergo apoptosis, and instead are sloughed off from the apical surface. This continuous turnover of cells results in complete replacement of the epithelium every 7-10 days (Hanna et al., 1961). Stem cells in the limbal region of the cornea form a thin ring of slow-dividing cells around the corneal periphery and contribute to the repopulation of the corneal epithelium during turnover (Daniels et al., 2001; Cotsarelis et al., 1989; Schermer et al., 1986). On the other hand, their proliferation is not directly involved in the wound healing process (Chen and Tseng, 1990; Cotsarelis et al., 1989; Hanna et al., 1961; Lavker et al., 1991)

In the turnover process, basal cells lose their adhesion to the basement membrane via hemidesmosomes, and the expression of receptor proteins such as integrins is altered. This process converts the basal cells into “wing” cells, which migrate apically, flatten, and transition into apical cells. The apical cells form a impermeable barrier with tight junction complexes that prevent the cornea from being stimulated by factors in tears such as growth factors (Klyce, 1972; Zieske et al., 2000). This “quiet” homeostasis in the apical epithelium allows the cornea to maintain normal thickness. These apical cells last a few days before being sloughed off into the tear fluid from the shear forces in blinking (Hanna et al., 1961). Any compromise in this process can lead to improper corneal epithelium maintenance and wound healing.

Clinical relevance of corneal injury

As the most-anterior structure of the eye, the cornea is constantly exposed to the environment, which makes it susceptible to damage from scratching, infections, and dystrophy. Therefore the process of epithelial wound healing is commonplace and critical for the maintenance of the cornea. Disruption of tight junctions can result in damage or loss of the corneal epithelium and induce cell migration (Hutcheon et al., 2007; Suzuki, 2003). Cell migration is a collective process, where cells retain a "sheet-like" structure of one or several cell layers that migrates as a unit until they come in contact with the opposing migrating cell sheet from the opposite side of the wound. As these epithelial sheets unite and wound closure is established, the cells re-establish the multilayered epithelium via proliferation and restoration of corneal cell junctions (Fig. 1-3). Unlike individual cell migration present in fibroblasts, this collective cell migration allows for a coordinated, rapid wound healing process. Simple abrasion wounds, where the Bowman's layer and basement membrane of the epithelium are not impaired, generally close within 24-48 hours depending on its size and are fully restored within 7-10 days after injury (Hanna, 1966; Minns et al., 2016).

Wound healing can be impaired in many different eye pathologies, including corneal infection and ulceration, herpes simplex infection, limbal stem cell deficiency, ocular surface diseases (i.e. dry eye syndrome and Meibomian gland dysfunction), recurrent corneal erosions, and both types of diabetes mellitus (hereafter shortened to "diabetes"). In particular, type II diabetes has increasingly become a huge financial burden on the U.S. healthcare system (Zimmet et al. 2001). Diabetic patients frequently

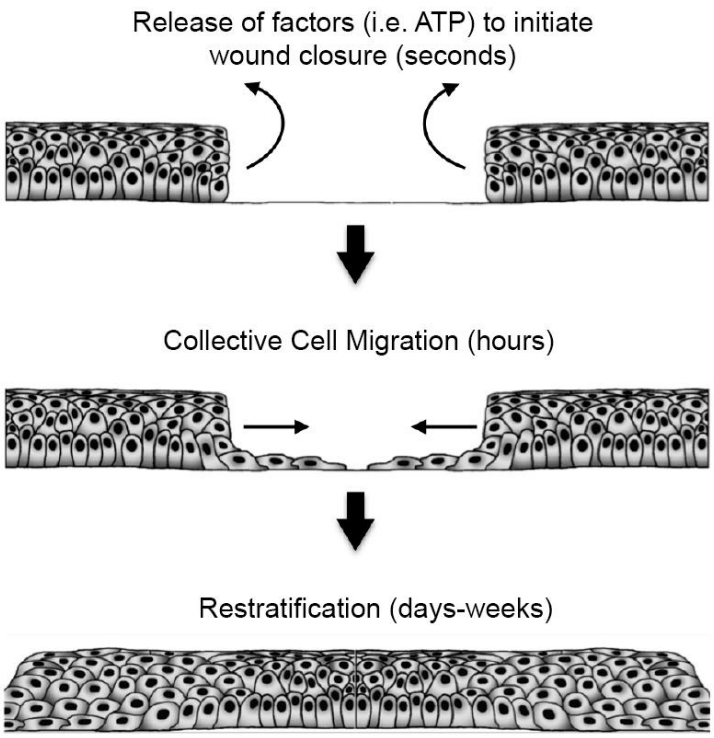

Figure 1-3: Timeline and diagram of wound healing in the corneal epithelium.

develop corneal erosions due to defects in epithelial wounding healing, an incomplete epithelial barrier, and exposed epithelial nerves. Many also report neuropathy and loss of sensation over time (Friend and Thoft, 1984; Friend et al., 1982; Schultz et al., 1981). Even in type II diabetes mouse models, the complex network of corneal nerve endings is observed to be unorganized and degraded compared to their wild-type counterparts (Kneer et al., 2018) (Fig. 1-4). According to the World Health Organization, corneal blindness from disease and injury is the fourth most common cause of preventable blindness (Whitcher et al. 2001). Treatments for this condition include corneal transplantation or grafting, but those options are not readily available worldwide.

1-2: Nucleotides, purinergic receptors, and Ca^{2+} signaling

Nucleotides and their effects as signaling molecules

One of the most immediate and ubiquitous responses in epithelial wound healing is the release of nucleotides, such as ATP. Once released into the extracellular milieu, ATP and other triphosphate nucleotides can be degraded into their diphosphate, monophosphate, and base nucleosides (Fig. 1-5). For instance, extracellular ATP can be dephosphorylated by ectonucleotidases to ADP, AMP, or adenosine. Not only are nucleotides sources of energy for cells, but they also have been extensively studied in context of molecular signaling.

In particular, extracellular ATP can elicit a number of responses in different cell types. It acts as a neurotransmitter responsible for non-adrenergic inhibition in intestinal smooth muscle cells (Burnstock et al., 1970). During inflammation, ATP acts as a danger

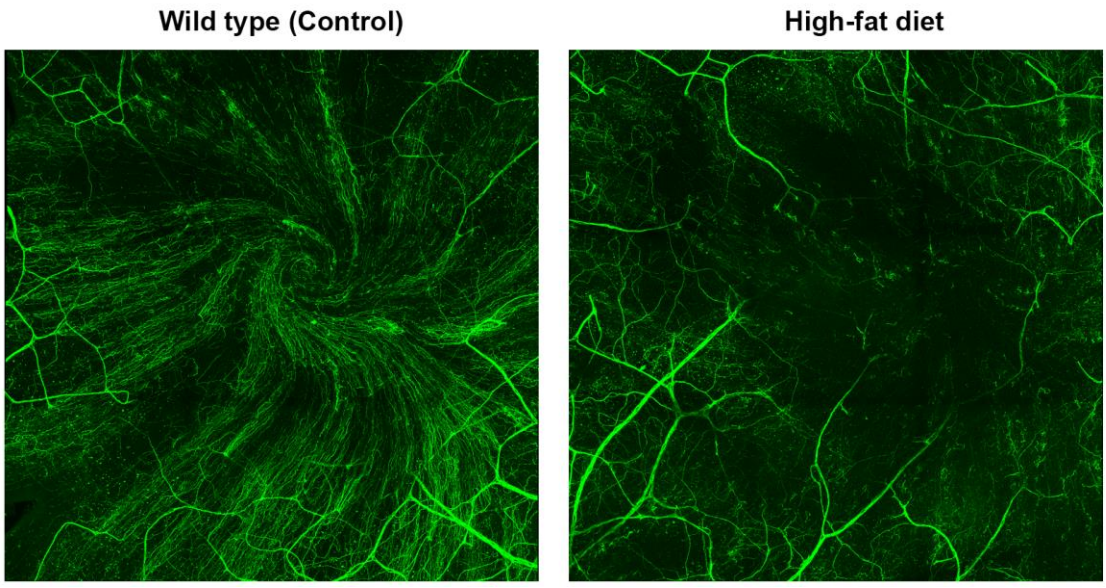

Adapted from Kneer et al., 2018

Figure 1-4: Difference in corneal innervation in wild type and high-fat diet mice. The control and high-fat diet mouse corneas were stained for Tuj1 (green) and imaged en face from the apical surface of the cornea.

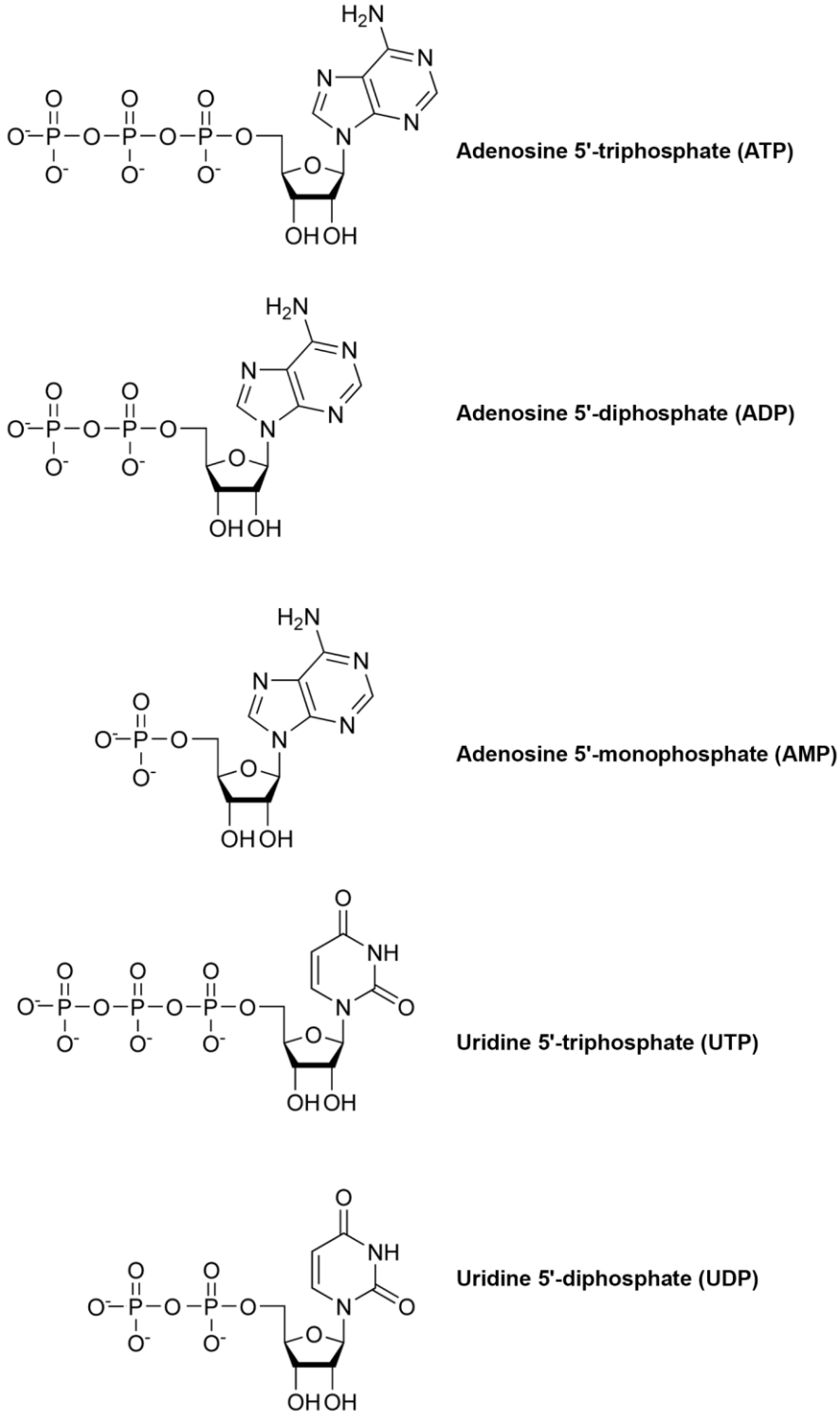

Figure 1-5: Chemical structures of nucleoside phosphates.

signal to induce the inflammatory response via activation of inflammasome complexes, T cell activation and maturation, and neutrophil chemotaxis (Baricordi et al., 1996; Chen et al., 2006; Junger, 2011; Schenk et al., 2008; Yip et al., 2009). ATP can also affect the phosphorylation of a number of proteins, including epidermal growth factor receptor (EGFR), Src, extracellular-signal-regulated protein kinase (ERK), β4 integrin, and paxillin (Boucher et al., 2007; Kehasse et al., 2013; Minns et al., 2016). Other studies demonstrated that ATP can affect motility of human lung cancer cells and epithelial cell migration after injury, including the corneal epithelium (Takai et al., 2014; Klepeis et al., 2004; Yin et al., 2007). In conclusion, ATP's diverse roles in cell motility and migration demonstrate its importance in context of corneal epithelial wound healing.

The purinergic receptor family

Purinergic receptors are the family of receptors that are characterized to be activated by nucleotides or nucleosides (Abbracchio and Burnstock, 1998). There are two classes of purinergic receptors P1 and P2, both of which have different subtypes (Fig. 1-6). The P1 class of purinergic receptors are only activated by adenosine and do not play any role in the corneal wound healing response (Yang et al., 2004). The P2 class of purinoreceptors consists of a large family of transmembrane receptors that is split into two main subtypes, P2X and P2Y receptors (Fig. 1-6). P2X purinergic receptors are ligand-gated trimeric ion channels that gate Ca^{2+} and other cations from the extracellular space. P2Y purinergic receptors are G protein-coupled receptors (GPCR) that mediate downstream signaling through increasing intracellular Ca^{2+} via cytosolic inositol (1,4,5)

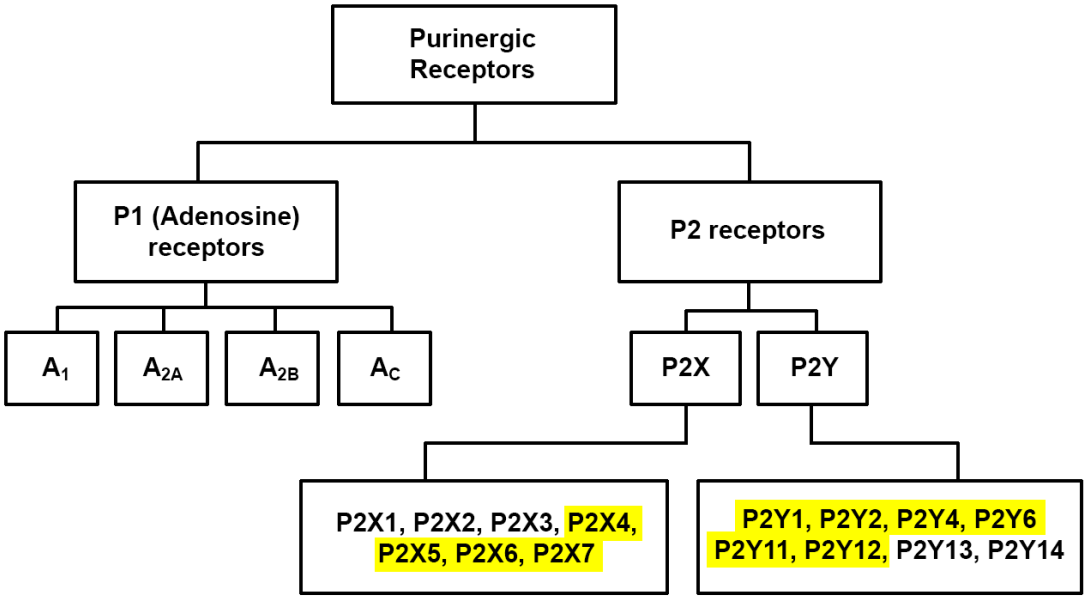

Figure 1-6: Diagram of the purinergic receptor family.
Purinergic receptors highlighted in yellow are known to be expressed in the corneal epithelium.

triphosphate (IP_3)-mediated signaling. Both subtypes are known to mediate cell migration, proliferation, and inflammation (Abbrachio and Burnstock 1998).

P2X purinergic receptors

P2X purinergic receptors are nucleotide-stimulated trimeric cation channels. There are seven members in this receptor subtype, named P2X1-7. The corneal epithelium has been shown to express P2X4-7, but not P2X1-3 (Mankus et al., 2011). Each of the monomers in the P2X purinergic receptor contains the following: a short N-terminus that lies in the cytoplasm, an ectodomain that is both N-glycosylated and crosslinked by disulfide bonds, and a cytoplasmic C-terminus connected by two short transmembrane regions (North, 2002). These monomers trimerize via interactions between the ectodomains and transmembrane domains (Becker et al., 2008; North, 2002). All the P2X receptor types can form heterotrimers, some of the more common ones being P2X2/3, P2X1/5, P2X4/6, P2X1/4, and P2X2/5 (Compan et al., 2012; Nicke et al., 2005; North, 2002). They can also form homotrimers except for P2X6 (Barrera et al., 2005; North, 2002; Ormond et al., 2006). The resulting trimer then acts as a gate that only opens in response to extracellular ATP to allow the passive influx Ca^{2+} and other cations down the concentration gradient (Virginio et al., 1997; Volonté et al., 2006) (Fig. 1-7A). Given that each subunit has at least one identified ATP-binding domain via x-ray crystallography, this means all P2X receptors have more than one ATP-binding site (North, 2002).

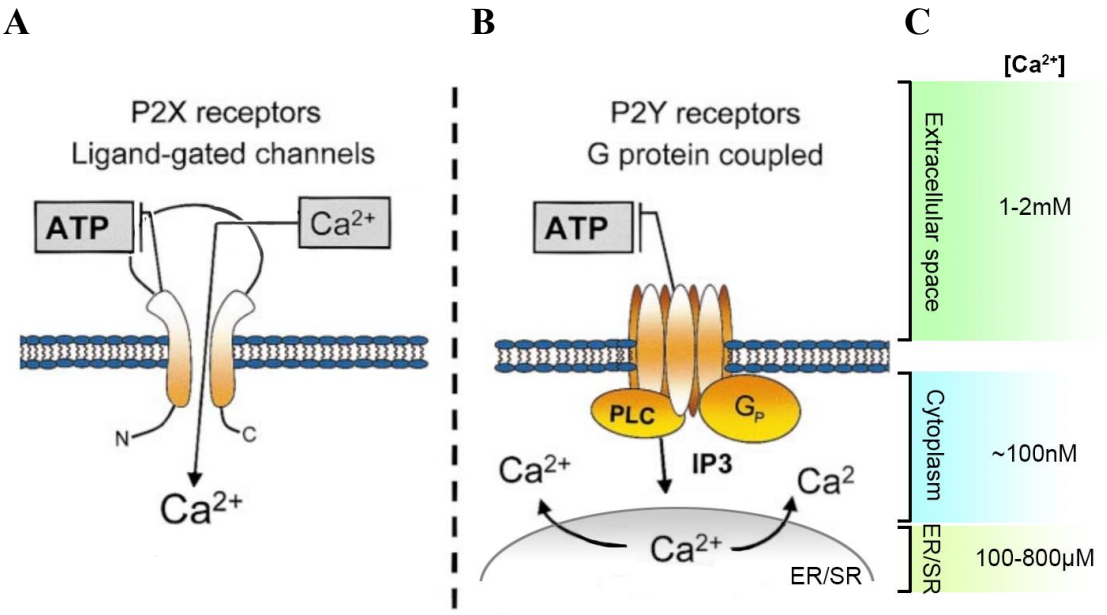

Adapted from Inscho, 2001

Figure 1-7: P2 receptors and the Ca^{2+} concentrations across extracellular and intracellular spaces.
A: Diagram of the P2X receptor **B:** Diagram of the P2Y receptor **C:** Ca^{2+} concentration ranges in the extracellular space, cytoplasm, and the lumen of the endoplasmic/sarcoplasmic reticulum (ER/SR)

P2Y purinergic receptors

P2Y purinergic receptors are nucleotide-stimulated G protein-coupled receptors (GPCR). There are eight members in this receptor subtype, named P2Y1, P2Y2, P2Y4, P2Y6, and P2Y11-14. The corneal epithelium was shown to express P2Y1-2, P2Y4, P2Y6, and P2Y11-12 (Mankus et al., 2011). All P2Y purinergic receptors signal through the universal GPCR pathway: on activation, bound Gα proteins release Gβγ dimers, which in turn activate phospholipase C (PLC); the activated PLC then cleaves phosphatidylinositol (4,5)-bisphosphate (PIP_2) into diacylglycerol (DAG) and cytosolic inositol (1,4,5) trisphosphate (IP_3); finally DAG activates enzymes such as protein kinase C (PKC), and IP_3 stimulates IP_3 receptors (IP_3R) that open channels in the endoplasmic and sarcoplasmic reticulum (ER/SR) to let Ca^{2+} into the cytoplasm (Clapham, 2007) (Fig. 1-7B).

The role and maintenance of the Ca^{2+} gradient

Ca^{2+} can act as a secondary messenger for multiple pathways, including those involved with P2X and P2Y purinergic receptors. The rapid intracellular influx of Ca^{2+} is only possible through the maintenance of the Ca^{2+} concentrations both in the intracellular and extracellular spaces (Fig. 1-7C). Normally the Ca^{2+} concentration in the cytoplasm is around 100 nM, which is significantly lower than those in the endoplasmic or sarcoplasmic reticulum (ER/SR), which usually range from 100 to 800 μM. The extracellular milieu has an even higher Ca^{2+} concentration ranging from 1-2 mM (Clapham, 2007). All the different Ca^{2+} concentrations are maintained through pumping

Ca^{2+} against the concentration gradient through active transport. To maintain a high ER/SR Ca^{2+} concentration, the smooth endoplasmic reticulum calcium ATPase (SERCA) pumps transport Ca^{2+} from the extracellular space and into the ER and SR lumens. To maintain the low cytoplasmic Ca^{2+} concentration, plasma membrane Ca^{2+} ATPase (PMCA) and Ca^{2+}/Na^{+} exchanger (NCX) pumps transport the Ca^{2+} from the cytoplasm to the extracellular space (Philipson et al., 1993; Reuter, 1991). Due to these systems in play, Ca^{2+} is a very potent signaling molecule.

Biological effects of intercellular Ca^{2+}mobilizations

Within milliseconds to seconds after injury, extracellular ATP binds to purinoreceptors and triggers an increase in intracellular Ca^{2+} in cells. This initial response can stimulate adjacent neighboring cells to result in large-scale mobilizations, such as waves and other intercellular Ca^{2+} oscillations. These Ca^{2+} mobilizations were first observed in vitro and were later proven to be physiologically relevant in in vivo models (Cornell-Bell et al., 1990; Hirase et al., 2004; Hoogland et al., 2009; Robb-Gaspers and Thomas, 1995; Sanderson et al., 1990; Weissman et al., 2004). These intercellular Ca^{2+}mobilizations synchronize cells into responding to stimuli in a more coordinated manner, which is essential in many different multicellular functions.

In wound healing, Ca^{2+} mobilizations play a role in transducing coordinated mechanical signals into chemical signals and alter signaling pathways (Adinolfi 2013; Boucher et al., 2007; Burnstock 2009; Kehasse et al., 2013; Yin et al., 2007). This

response is mimicked in unwounded cultures that are exposed to medium collected from injured cells (Boucher et al., 2007). Previous studies have shown that an initial transient response occurred with injury and proposed that it mediated downstream signaling events by altering phosphorylation of focal adhesion and adaptor proteins in a phosphoproteomic study (Kehasse et al., 2013; Klepeis et al., 2001). For example, P2Y2 receptor-mediated increase in intracellular Ca^{2+} plays a critical role in phosphorylation of proteins at specific residues such as Y118 of paxillin and Y1068 of EGFR (Boucher et al., 2010; Kehasse et al., 2013). These events or mobilizations were hypothesized to guide cell migration in zebrafish and modulate changes in IP_3-mediated Ca^{2+} release from an oscillatory to a tonic mode (Chen et al., 2017; Courjaret et al., 2017). In addition, they were detected during status epilepticus where Ca^{2+} waves continue for extended time periods (Deshpande et al., 2016). Furthermore in astrocytes and glial cells, intercellular Ca^{2+} changes were shown to regulate neuronal synaptic transmissions (Scemes and Giaume, 2006). Other investigators proposed that short flickers of Ca^{2+} may mediate the directionality of cell migration (Wei et al., 2009). The diverse roles Ca^{2+}mobilizations demonstrate how vital they are in multicellular tissues.

The P2X7 and P2Y2 receptors in wound healing

While there are several different P2 receptors that are expressed in the epithelial cornea, only two purinergic receptors within this family were found to participate in the wound healing response: P2X7 and P2Y2. Previously, our lab had performed a series of

siRNA knockdown and inhibition studies for P2X and P2Y receptor classes and demonstrated that only P2X7 and P2Y2 receptors participated in initial Ca^{2+} response after injury (Boucher et al., 2010; Mankus et al., 2011; Mayo et al., 2008; Minns et al., 2016).

P2X7 was predominantly studied as a receptor involved in cell death and inflammation, but there is evidence that P2X7 also is involved in the cell response to injury and wound healing. During inflammatory response in the body, P2X7 induces activation of the NALP3 inflammasome through caspase-1, and it is required in processing and secreting IL-1β (Di Virgilio, 2007; Ferrari et al., 2006; Lister et al., 2007; Verhoef et al., 2003). Prolonged stimulation of P2X7 causes formation of large pores in the plasma membrane to form a "death complex" with pannexin-1 to induce apoptosis (Iglesias et al., 2008; Locovei et al., 2007; Smart et al., 2003). In the corneal epithelium, however, the P2X7 purinergic receptor is an important mediator in normal wound healing (Mankus et al., 2011; Mayo et al., 2008; Minns et al., 2016). P2X7 mRNA expression is significantly elevated (6-7 fold) in diabetic corneas, and the corneal epithelium of a murine pre-diabetic model displayed a similar elevated mRNA (Mankus et al., 2011; Kneer et al., 2018). Furthermore, there is a change in localization of P2X7 where P2X7 exhibited a planar polarity after injury and was prominent at the leading edge (Minns et al., 2016; Kneer et al., 2018). The polarity was abrogated in the pre-diabetic model (Kneer et al., 2018). P2X7 is also unique from the other P2X family receptors in its synthetic agonist and antagonist profile (Fig. 1-8; 1-9).

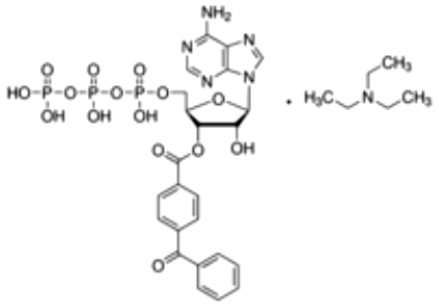

BzATP

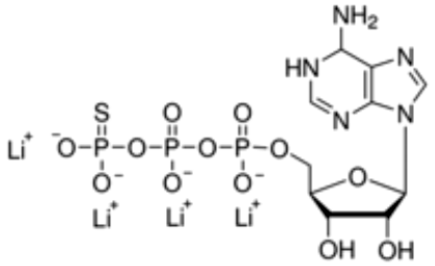

ATPγS

Figure 1-8: Chemical structures of agonists to P2X7.

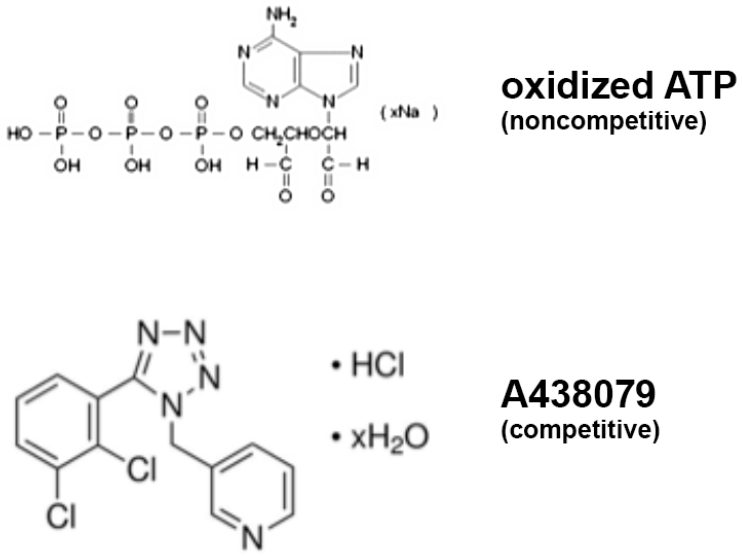

Figure 1-9: Chemical structures of specific antagonists to P2X7.

Similarly, the P2Y2 purinergic receptor is another key factor in wound healing in the corneal epithelium. The receptor itself has diverse functions across different cell types, one of its roles being phosphorylating downstream proteins such as epidermal growth factor receptor (EGFR) and paxillin to induce cell migration (Boucher et al., 2010; Kehasse et al., 2013; Ratchford et al., 2010; Wang et al., 2005). Knocking down P2Y2 in corneal epithelial cells resulted in a decrease in Ca^{2+} response, wound healing and phosphorylation of paxillin (Y118) and EGFR (Y1068), but not EGFR (Y1173) (Boucher et al., 2010; Kehasse et al., 2013). In contrast knocking down the P2Y4 receptor did not significantly reduce the injury-induced response, and its expression was not sensitive to changes in cell density (Boucher et al., 2010). While P2Y2 and P2Y6 purinergic receptors were seen to be involved in the Ca^{2+} mobilizations in neuronal and glial cells respectively, there has been no evidence of their involvement in the Ca^{2+} mobilizations in the cornea (Calvert et al., 2009). In addition, only the P2Y2 receptor increased in expression after injury (Kehasse et al., 2013). While its agonist profile is shared with the P2Y4 purinergic receptor, P2Y2 does have one specific antagonist that is commercially available (Fig. 1-10; 1-11).

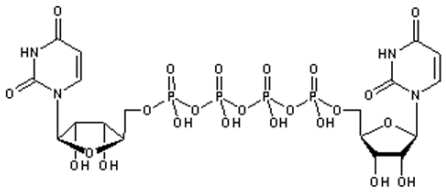

diquafosol tetrasodium

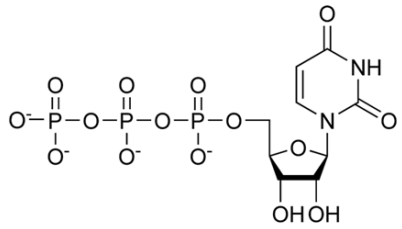

UTP

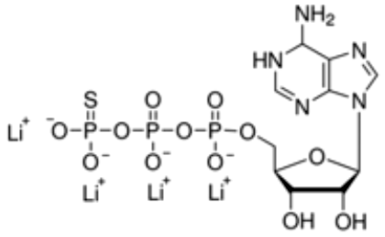

ATPγS

Figure 1-10: Chemical structures of agonists to P2Y2.

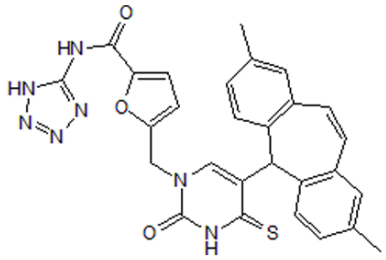

Figure 1-11: Chemical structure of a specific antagonist to P2Y2.

1-3: Cell-cell junctions in Ca^{2+} signaling

There are two possible methods for Ca^{2+} mobilizations to travel between cells: through gap junctions or through paracrine signaling. Gap junctions are formed by two connexons, comprised of 6 connexin subunits, that link cytoplasms of two adjacent cells (Fig. 1-12A). This linkage requires direct cell-cell contact. Currently, the connexin family consists of 21 genes in the human genome and 20 genes in the mouse genome, 19 of these grouped as orthologue pairs (Söhl and Willecke 2004). In the corneal epithelium three connexin proteins are expressed: Connexin-32 (Cx32), Connexin-43 (Cx43), and Connexin-50 (Cx50) (Klepeis et al., 2001; Oswald et al., 2012). When one cell has an increase in intracellular Ca^{2+}, the excess Ca^{2+} diffuses to the adjacent cell's cytoplasm via the gap junctions. Depending on the tissue and cell type, the mechanism of the gap junction-mediated Ca^{2+} propagation is activated either through the IP_3 pathway or the changed Ca^{2+} concentration during mobilization (D'Andrea and Vittur, 1997; Jørgensen et al., 1997; Grandolfo et al., 1998; Sanderson et al., 1994; Sneyd et al., 1998; Ullah et al., 2006; Quist et al., 2000).

Meanwhile, paracrine signaling involves neighboring cells to be in the general vicinity of one another and does not require direct cell-cell contact. Previously, these were assumed to be mediated by gap junctions, but now are proven to be caused by hemichannels (Cotrina et al., 1998). These channels consist of a single pannexon, which are comprised of 6 pannexin subunits (Fig. 1-12B). The pannexin protein family consists of three members: pannexin-1, pannexin-2, and pannexin-3. Only pannexin-1 has been shown to be expressed in the corneal epithelium (Cui et al., 2016; Mayo et al., 2008).

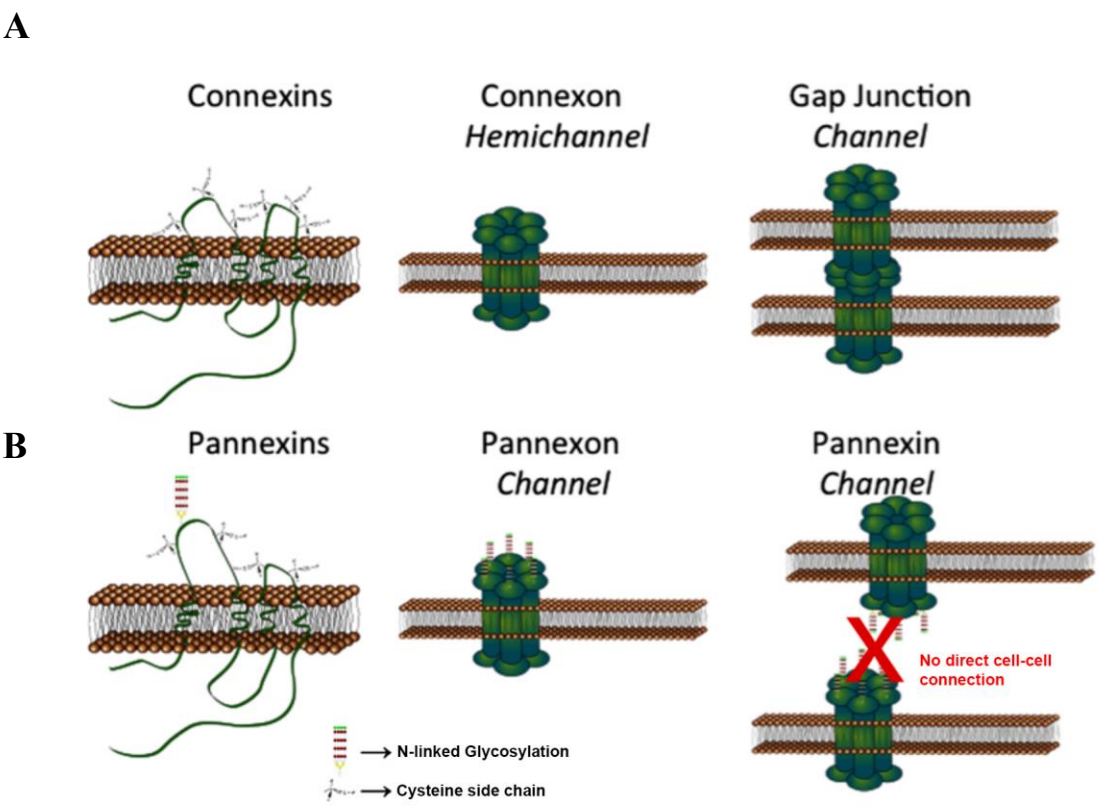

Adapted from Giaume et al., 2013

Figure 1-12: Schematic of connexin gap junctions and pannexin channels.
A: Structure of the connexin protein subunit, the hexameric connexon hemichannel, and the dimerized gap junction. **B:** Structure of the pannexin protein, the hexameric pannexon channel, and two adjacent pannexin channel. Due to the N-linked glycosylation they do not establish a direct cell-cell connection like the gap junctions.

Mimetic peptides have been developed to inhibit these pannexin channels, such as 10Panx for pannexin-1. Upon increase in intracellular Ca^{2+} in one cell, it induces release of agonist (i.e ATP) to the extracellular milieu. Then the agonists stimulate neighboring cells, which results in those cells undergoing Ca^{2+} mobilization and more agonists being released extracellularly to further propagate the original signal. Studies have demonstrated the importance of ATP's role in paracrine Ca^{2+} mobilization propagation in different cell types. For example in neutrophils and dendritic cells, ATP participates in chemotaxis during inflammation and cell migration during injury respectively (Junger 2008; Chen et al., 2015; Sumi et al., 2014; Sáez et al., 2017).

In the corneal epithelium, Ca^{2+} waves that appeared immediately after injury were found to be mediated by ATP. We demonstrated that Ca^{2+} mobilization waves travel through paracrine signaling and not gap junctions since the signal was able to propagate past a cell-free region (Klepeis et al., 2001; Weinger et al., 2005).

1-4: Quantitative cell analysis

Ca^{2+} signaling in the corneal epithelium is quantifiable through computer algorithms. The short activation window of these Ca^{2+} mobilizations allow for us to run many sample replicates in a short period of time. To visualize the Ca^{2+} mobilizations, we pre-incubate cells with a Ca^{2+}-sensitive dye that chelates Ca^{2+} and induces fluorescence detected by live-cell imaging with confocal microscopy (see Methods) (Fig. 1-13). In the corneal epithelium, the Ca^{2+} mobilization patterns can vary: clustered, concentrated at the leading edge after injury, or seemingly random (Bootman et al., 2001; Derricks et al.,

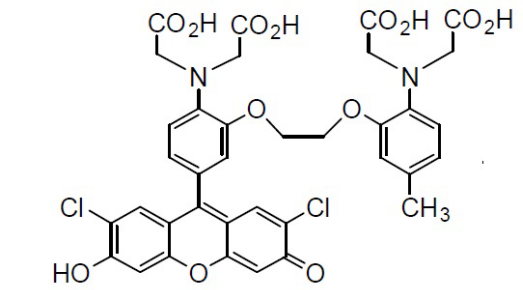

Fluo-3 AM

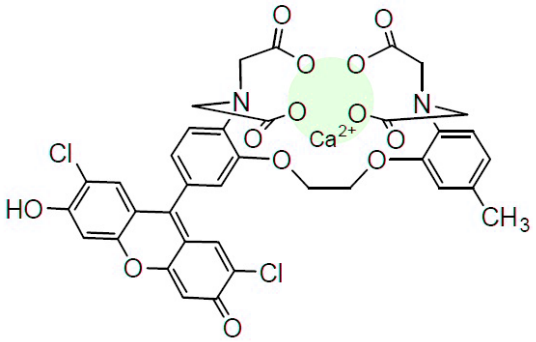

Fluo-3 AM, complex with Ca^{2+}

Figure 1-13: Structure of chelating Ca^{2+}-sensitive dye (Fluo-3 AM).
The native structure and the altered, fluorescent conformation of Fluo-3 AM dye when complexed with Ca^{2+}.

2015; Klepeis et al., 2001; Weinger et al., 2005). Quantifying and characterizing the behavior of these the Ca^{2+} mobilizations will be crucial in understanding its role in wound healing and other downstream pathways.

There are two main ways to quantify Ca^{2+} mobilizations over time: measuring the average fluorescence of an entire image field or measuring fluorescence level changes in individual cells through regions of interest (ROIs) (Cornell-Bell et al., 1990; Bootman et al., 2001). To determine the average fluorescence of an entire image field, the entire fluorescence of the image is normalized to the background fluorescence at baseline. However, this only offers limited information, since the averaging can potentially miss the individual Ca^{2+} mobilization events that may be crucial in specific cell-cell communication pathways. The ROI selection method is more precise in that individual cell fluorescence can be analyzed with the same normalization method, but there can be inherent bias in picking which cells to analyze, particularly if one wants to do a study of representative cells in a image field that may contain 200-300 cells in a 20x field. This bias can potentially be reduced with an algorithm that automatically detects individual cells for ROI and correct them for background. In different cell systems, computer programs have been used successfully to analyze Ca^{2+} signals to understand cell behavior (Awal et al., 2018; Bootman et al., 2001; Derricks et al., 2015; Weinger et al., 2005).

1-5: Specific Aims

The objectives of my research were to study the behavior and mechanism of sustained Ca^{2+} mobilizations mediated by purinergic receptors P2X7 and P2Y2 in the

corneal epithelium after injury. The major goal of the study was to establish a method to identify and characterize the degree of cell-cell communication that occurs through sustained Ca^{2+} mobilizations after injury in both in vitro and ex vivo models.

The specific aims were: 1) to characterize the role of the sustained Ca^{2+} mobilizations in cell migration and corneal wound healing, 2) to identify the Ca^{2+} mobilization profiles of purinergic receptors P2X7 and P2Y2 in context of agonist activation and wounding, and 3) to determine how the sustained Ca^{2+} mobilizations are propagated in corneal epithelial cells.

CHAPTER TWO: MATERIALS AND METHODS

2-1: Materials

Reagents, nucleotides, inhibitors

ATP, 2,3-O-(4-benzoylbenzoyl)-ATP (BzATP), and UTP were all purchased from Sigma-Aldrich (St. Louis, MO). A luciferase-based ATP Determination Kit was purchased from Invitrogen (Carlsbad, CA). A438079 hydrochloride, AR-C 118925XX, 10Panx Inhibitory peptide, and scramble control peptide were purchased from Tocris Biosciences (Minneapolis, MN). Fluo-3AM fluorescent dye, and Rhodamine-phalloidin were purchased from Invitrogen (Carlsbad, CA). CellMask™ Deep Red Plasma membrane stain was purchased from ThermoFisher (Waltham, MA) and SiR-Actin Spirochrome probe was purchased from Cytoskeleton Inc. (Denver, CO). VectaSHIELD with DAPI was purchased from Vector Labs (Burlingame, CA).

Antibodies

Pannexin-1 polyclonal rabbit antibodies were purchased from Alomone (Jerusalem, Israel). Connexin-43 (Cx43) polyclonal rabbit antibodies were purchased from Santa Cruz Biotechnology (Santa Cruz, CA). Rac1 monoclonal mouse antibodies were purchased from BD Biosciences (San Jose, CA). Secondary antibodies (Alexa Fluor-conjugated secondary antibody) were purchased from Invitrogen (Carlsbad, CA).

2-1: Materials

Cell culture

Human corneal limbal epithelial (HCLE) cells were a gift from Dr. Gipson (Schepens Eye Research Institute/Mass. Eye and Ear, Boston, MA) (Gipson et al., 2003). The HCLE cell line was verified at Johns Hopkins DNA Services (Baltimore, MD). Cells were maintained in Keratinocyte Serum-Free Media (KSFM) and growth supplements (25 μg/mL bovine pituitary extract, 0.02 nM EGF, and 0.3 mM $CaCl_2$). Cells were passaged when 70-80% confluent and plated on either glass bottom dishes (MatTek Corporation, Ashland, MA) for live cell imaging, scratch wound assays, and immunofluorescence, or on cell culture-treated plastic petri dishes for Western blot analysis for about 72 hours prior to experimentation at a density of 150 cells/mm^2. Approximately 16-24 hours before experimentation, the media were changed to unsupplemented KSFM, as previously described (Minns et al., 2016).

Organ and explant culture, tissue preparation

The research protocol conformed to the standards of the Association for Research in Vision and Ophthalmology for the Use of Animals in Ophthalmic Care and Vision Research and the Boston University IACUC. C57BL/6J mice were obtained at 8 and 15 weeks of age from Jackson Laboratory (The Jackson Laboratory; Bar Harbor, ME). The mice were euthanized by CO_2. For organ culture, the corneal injury was made by delineating a 1.5mm-diameter region in the center of the cornea with a trephine before using it to scratch-wound the epithelium by abrasion. Corneas were dissected leaving an

intact scleral rim and placed on agar molds and incubated in Dulbecco's modified Eagle's medium (DMEM) at 37 °C and 5% CO_2 as described (Lee et al., 2014; Minns et al., 2016). For live cell imaging, wounding was performed after the cornea was positioned on the microscope stage. For cornea explants, corneal-scleral rims from anonymized donors were obtained through BMC courtesy of Dr. Hyunjoo Lee.

Immunohistochemistry and confocal microscopy

Cells or corneas were fixed in freshly prepared 4% paraformaldehyde in PBS for 20 minutes at room temperature (for cells) or overnight at 4°C (for corneas). Immunofluorescent staining was performed (Minns et al., 2016). Briefly, cells or tissue were permeabilized with 0.1% v/v Triton X-100 in PBS for 2-5 minutes and blocked with 4% BSA in PBS for one hour. Cells or tissue were incubated in primary antibody solutions overnight at 4°C. Alexa Fluor-conjugated secondary antibodies (Invitrogen, Carlsbad, CA) were used at a dilution of 1:100 in blocking solution for 1 hour at room temperature. Rhodamine-conjugated phalloidin (Invitrogen, 1:50) was used to visualize F-actin. Cells or tissue were mounted using VectaSHIELD with DAPI (Vector Labs, Burlingame, CA). Images were taken on a Zeiss LSM 700 (Zeiss, Thornwood, NY) confocal microscope. Images were analyzed using ZEN (Zeiss, Thornwood, NY) or FIJI/ImageJ (NIH, Bethesda, MD; http://imagej.nih.gov/ij/).

Setting up AIRYScan instrument for imaging

For ex vivo imaging of mouse corneas, we utilized the FAST module and AIRYScan on the Zeiss LSM 880 (Zeiss, Thornwood, NY). The AIRYScan is designed to increase the resolution and overall image quality compared to traditional confocal microscopy, which we deemed was necessary for imaging corneal tissue. After setting up the imaging acquisition similar to the regular confocal, the appropriate emission filter for each fluorophore on the "ChA" detector was selected (Fig. 2-1).

Live cell confocal imaging for Ca^{2+} mobilization studies

Ca^{2+} mobilization was performed on cells as previously described (Minns et al., 2016; Weinger et l., 2005). Briefly, cells were cultured to confluence on glass bottom dishes and pre-loaded with 5 μM Fluo-3 AM (Invitrogen, Carlsbad, CA), at a final concentration of 1% (v/v) DMSO and 0.02% (w/v) pluronic acid for 30 minutes at 37°C and 5% CO_2 (Minns et al., 2016). For ex vivo imaging of mouse corneas, the corneas

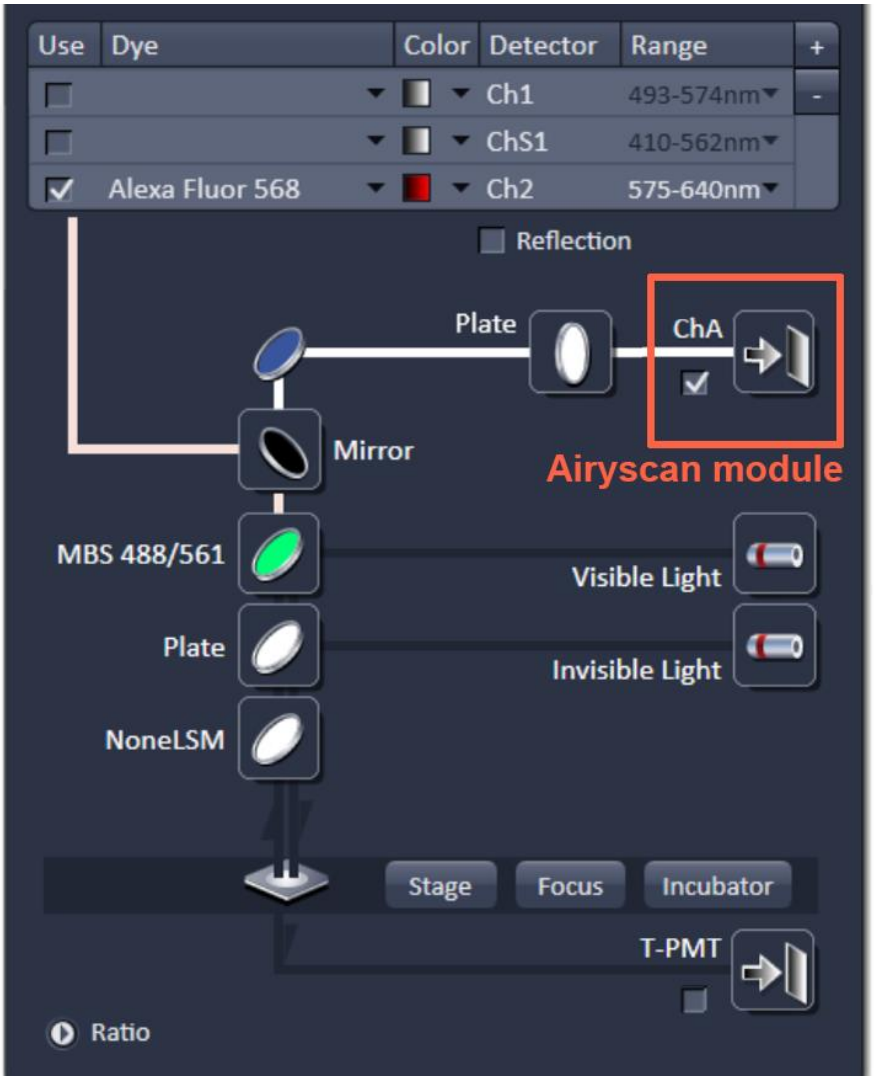

Figure 2-1: Zeiss LSM 880 interface to turn on the AIRYScan module
For AIRYScan the "ChA" detector (marked in orange box) needs to be checked after setting up the LSM settings.

were mounted on glass and preincubated with 50 μM Fluo-3 AM or Fluo-4 AM to visualize calcium for 4 hours at 37°C and 5% CO_2. Due to the mouse cornea being a multi-cell layered tissue, we also preincubated the corneal epithelial cells with either CellMask™ Deep Red Plasma membrane stain to visualize cell membrane for 1 hour at 37°C and 5% CO_2 or SiR-Actin Spirochrome probe (Cytoskeleton Inc., Denver, CO) to visualize F-actin for 4 hours at 37°C and 5% CO_2. Both the CellMask™ and Sir-Actin stain were used at the concentration recommended by manufacturer. To examine changes in Ca^{2+} mobilization on cells, images were collected every 3 seconds on a Zeiss Axiovert LSM 880 confocal microscope for a period of time up to 2 hours after either agonist stimulation or injury. To determine Ca^{2+} mobilization in live corneas, the FAST module and AIRYScan were used. Baseline and post-wound frames were captured as above, at indicated times, as noted above.

Live cell confocal imaging cell shape changes and migration

Cells were pre-loaded with CellMask™ Deep Red Plasma membrane stain at the concentration recommended by manufacturer for 5 minutes at 37°C and 5% CO_2. For live imaging of actin filaments, cells were pre-loaded with 1 μM of SiR-Actin Spirochrome probe for 30 minutes at 37°C and 5% CO_2. For overnight studies, images were collected every 5 minutes on a Zeiss Axiovert LSM 880 confocal microscope for a period of time up to 6 hours after injury. For short-term studies, images were taken every 5 seconds on a Zeiss Axiovert LSM 880 confocal microscope for a period of time up to 2 hours after

injury. Images were taken using either a 40x oil or 63x oil objective. The pinhole size was kept at 1 Airy Unit across all images. Images were obtained using Zen Black Edition software (Zeiss, Thornwood, NY) and analyzed further using FIJI/Image J (NIH, Bethesda, CA). Analyses for all the described image studies were performed using FIJI/ImageJ (NIH, Bethesda, MD; http://imagej.nih.gov/ij/) along with MATLAB programs described below.

ATP release assay

To determine ATP released after injury, HCLE cells were plated on culture-treated plastic and grown to confluence. Growth supplements were removed from media 24 hours prior to wounding. Cells were scratch wounded with a comb made from plastic gel-loading tips. After injury, media was collected and centrifuged at 663 x g and clarified media was collected and stored on ice. To determine ATP concentration, a luciferase-based ATP Determination Kit was used (Invitrogen, Carlsbad, CA). Samples were vortexed and 5 μL aliquots were plated on a white-bottomed 96-well plate (Corning). A reaction buffer containing 0.5 mM D-luciferin, 1.25 μg/mL firefly luciferase, 25 mM Trycine buffer, pH 7.8, 5 mM $MgSO_4$, 100 μM EDTA, and 1 mM DTT was prepared immediately before analysis and protected from light. To determine ATP levels, luciferase-generated luminescence was detected using a BioTek Synergy HT plate reader with injector (BioTek, Winooski, VT). A standard curve of ATP was made in the growth factor-depleted media used for cells. To ensure equal time for each reaction,

95 μL of reaction buffer was injected into a well and allowed to incubate for 4 seconds before luminescence was read. ATP levels were calculated from raw luminescence values using the standard curve.

Rac1 activation and western blot analysis

After stimulation or injury, epithelial cells were washed with cold PBS supplemented with 1 mM $MgCl_2$ and 0.5 mM $CaCl_2$ and lysis buffer (2.5 mM HEPES, 150 mM NaCl, 1% NP-40, 10 mM $MgCl_2$, 1 mM EDTA, 2% glycerol, 1 mM benzamidine, 0.5 mM PMSF, 1 ug/mL aprotinin, 1 ug/mL leupeptin). The lysates were centrifuged for 5 mins at 16,000 rcf. Protein concentration was determined using the BCA assay and normalized to 1.5 mg/mL (Bio-Rad, Hercules, CA). Lysates were incubated with either GST alone or GST-PAK-CRIB (cdc42 (p21) binding domain) fusion protein bound to glutathione-coupled sepharose beads at 4 °C for 1 hr. The beads and the proteins bound to the fusion protein were washed with cold lysis buffer, and the eluted bound Rac1 was analyzed by immunoblot analysis using a monoclonal mouse antibody against Rac1. Samples were resolved on SDS-polyacrylamide gels and transferred to nitrocellulose membranes. The membranes were incubated with either anti-Rac1 monoclonal (BD Biosciences, 1:1,000), or anti-actin (Sigma-Aldrich, 1:1,000,000) primary antibodies. Immunoreactive bands were visualized using SuperSignal West Femto Maximum Sensitivity Substrate Reagents (Thermo Scientific), and band

quantifications were performed using FIJI/ImageJ (NIH, Bethesda, MD; http://imagej.nih.gov/ij/).

Cell shape changes and migration

To examine cell migration and alterations in cell shape, HCLE cells were pre-loaded with either CellMask™ Deep Red Plasma membrane stain as described above or 1 μM of SiR-Actin Spirochrome probe (Cytoskeleton Inc., Denver, CO) for 10 minutes at 37°C and 5% CO_2, for imaging of F-actin. Both long- and short-term studies were performed. For long-term studies, images were collected immediately after injury and every 5 minutes for 6 hours on a Zeiss Axiovert LSM 880 confocal microscope. For short-term studies, images were taken immediately after injury and every 5 seconds for up to 2 hours on a Zeiss Axiovert LSM 880 confocal microscope. Analyses for all the described image studies were performed using FIJI/ImageJ (NIH, Bethesda, MD; http://imagej.nih.gov/ij/) along with MATLAB programs (MATLAB, MathWorks, Inc.) written for the analysis described below.

Grid-based Modeling of Ca^{2+} mobilizations

A customized video processing technique was developed to analyze spatiotemporal communication between groups of cells (Matlab, MathWorks, Inc.). Cell communication videos were collected from each experiment and exported in TIF format. Each image frame within the video was divided into a grid of smaller blocks of equal size

with each grid area being approximately equal to 1-2 cells. Each block was also assigned a number for identification. For each block within an image frame, background noise was minimized, and the average intensity was computed. The grid defining the block-level division remained fixed over the entire set of frames within the video, which allowed us to quantify inter-block communication and track synchronicity and behavior of a group of adjacent cells over time. To examine block-level communication over time under different experimental scenarios, we examined relationships between different blocks to determine if the signaling remained in phase or fell out of phase. We compared the intensity changes between each grid regions and generated a comprehensive heat map to display the relationships between each of the blocks. The average correlation values of the image studies were also generated based on the inter-block correlations values for each agonist condition.

Cell-based Modeling of Ca^{2+} mobilizations

In contrast to the grid-based method, the cell-based method analyzed the spatiotemporal communication between groups of cells. Videos were collected from each experiment and exported in TIF or AVI format. Two different custom MATLAB scripts (MATLAB, MathWorks, Inc.) were employed to analyze the measured Ca^{2+} responses based on individual cells or a population of cells, the former analysis technique described previously (Derricks et al., 2015). Cell positions were marked either manually or automatically via a computer program that calculated the centroid coordinates of each

cell. For the automated cell position tracking, X and Y centroid location of each cell would be recorded for every registered fluorescent area from the reference frame. The starting frame to detect these events is chosen manually, in which a frame is chosen after the initial Ca^{2+} transient response diminishes after the wounding/agonist event, and before the resurgence of Ca^{2+} signals. A cell was considered activated when it exhibited a rapid change in intensity due to the influx of Ca^{2+} into the cell. Signaling events within each trace were identified as being greater than a threshold of 50% of the average normalized fluorescent signal. A cluster was defined as a group of 2-3 adjacent cells where Ca^{2+} mobilizations occurred. With these criteria, the percent of activated cells and the number of clusters was measured over time.

Event probability calculation for Ca^{2+} mobilizations

To examine cell-cell communication we developed a script to identify Ca^{2+} events and generate an event kymograph and calculate the probability of neighboring cells having a correlated Ca^{2+} event. We defined "event probability" as the probability that a Ca^{2+} event in any particular cell would trigger a correlated event in any of its neighboring cells. Neighboring cells were defined as cells within <35 μm of each other. The neighboring cells that displayed events within 10 frames (approximately 30 sec) of each other were defined as correlated events. Cell positions were marked by either an automated computer program or manual detection as described previously. The detected

Ca^{2+} events were identified as presenting a fluorescence signal of at least 50% of the average normalized fluorescent signal.

Statistical analysis

Values are obtained by taking the mean plus and minus standard error of the mean of at least three independent experiments. Statistical significance was determined by unpaired, one-tailed Student's t-test or two-way ANOVA with appropriate post hoc tests using GraphPad Prism 5 (GraphPad Software, San Diego, CA) and R studio (RStudio, Inc., Boston, MA).

CHAPTER THREE: CHARACTERIZATION OF THE CALCIUM MOBILIZATION RESPONSE IN EPITHELIAL CELLS

3-1: Introduction

The goal of this study was to investigate the role of Ca^{2+} mobilizations in collective cell migration of corneal epithelial cells after agonist stimulation or scratch-wounding, based on past studies of the role of purinergic receptors. We hypothesized that these sustained Ca^{2+} mobilizations are responsible for cell-cell communication necessary for collective migration. The sustained Ca^{2+} mobilizations were present also after stimulation with either BzATP or UTP, and the responses were dose dependent for both agonists. The specificity was further demonstrated using competitive inhibitors of P2Y2 and P2X7, AR-C 118925XX and A438079 respectively. These sustained mobilizations are correlated with changes in cellular morphology and motility, which were prominent in cells at the leading edge during cell migration after wounding. Our results demonstrate that the sustained Ca^{2+} mobilizations mediated by purinoreceptors and pannexins are a vital component in regulating the long-term response to injury.

3-2: Results

Sustained Ca^{2+} mobilizations after injury are concentrated at the wound margin

We examined the Ca^{2+} mobilization within HCLE cells by live-cell imaging before and after wounding. Single-frame images of the Ca^{2+} mobilization before and after

(Baseline, 0, 5, and 120 mins) a scratch wound are shown (Fig. 3-1). Immediately after wounding, there is a large mobilization of Ca^{2+} that is transient and has been described (Klepeis et al., 2001) (Fig. 3-1, 0 mins). Then after the initial large Ca^{2+} mobilization, there were smaller Ca^{2+} mobilization events that were concentrated at the 1-2 cell rows closest to the wound edge, which we call the "leading edge" (Fig. 3-1, 5 mins and 120 mins). To examine the response we outlined the cells along the leading edge of the wound, thereby depicting the regions of interest (Fig. 3-2A).

From this data, we generated a kymograph (Fig. 3-2B), representing each of the individual leading edge cells (in brackets) and the changes in fluorescence intensity over time (Fig. 3-2B). At t=0 (wounding), the initial Ca^{2+} wave was observed, as indicated by the high intensity of Ca^{2+} (intensity scale) and this is followed by Ca^{2+} mobilizations that are sustained for up to two hours (Fig. 3-2B). We speculated that regions of neighboring cells at the leading edge displayed a synchronicity, indicating that the transfer of information between cells may be involved in wound healing. The cells back from the leading edge, denoted by being at least two cells distal from the wound, were less active compared to the cells at the leading edge of the wound (Fig. 3-3). Further quantitative analysis of these Ca^{2+} mobilizations were performed via MATLAB (See Chapter 4).

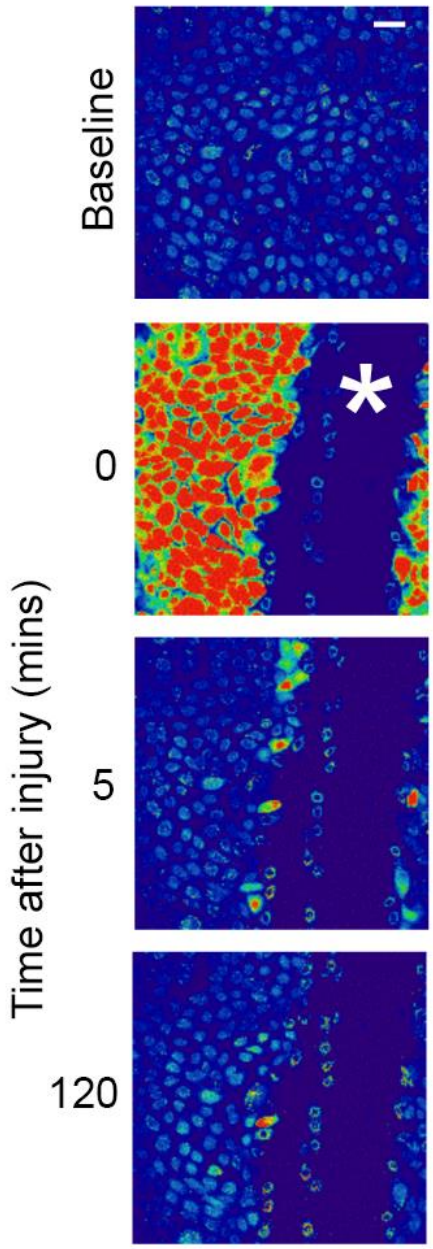

Figure 3-1: The timeline of the Ca^{2+} mobilization events after scratch-wounding. Cells were preincubated in 5 μM Fluo3-AM (Physics LUT) for 30 minutes and imaged on the Zeiss Axiovert LSM 700 confocal laser scanning microscope. Scale bar = 60 μm.

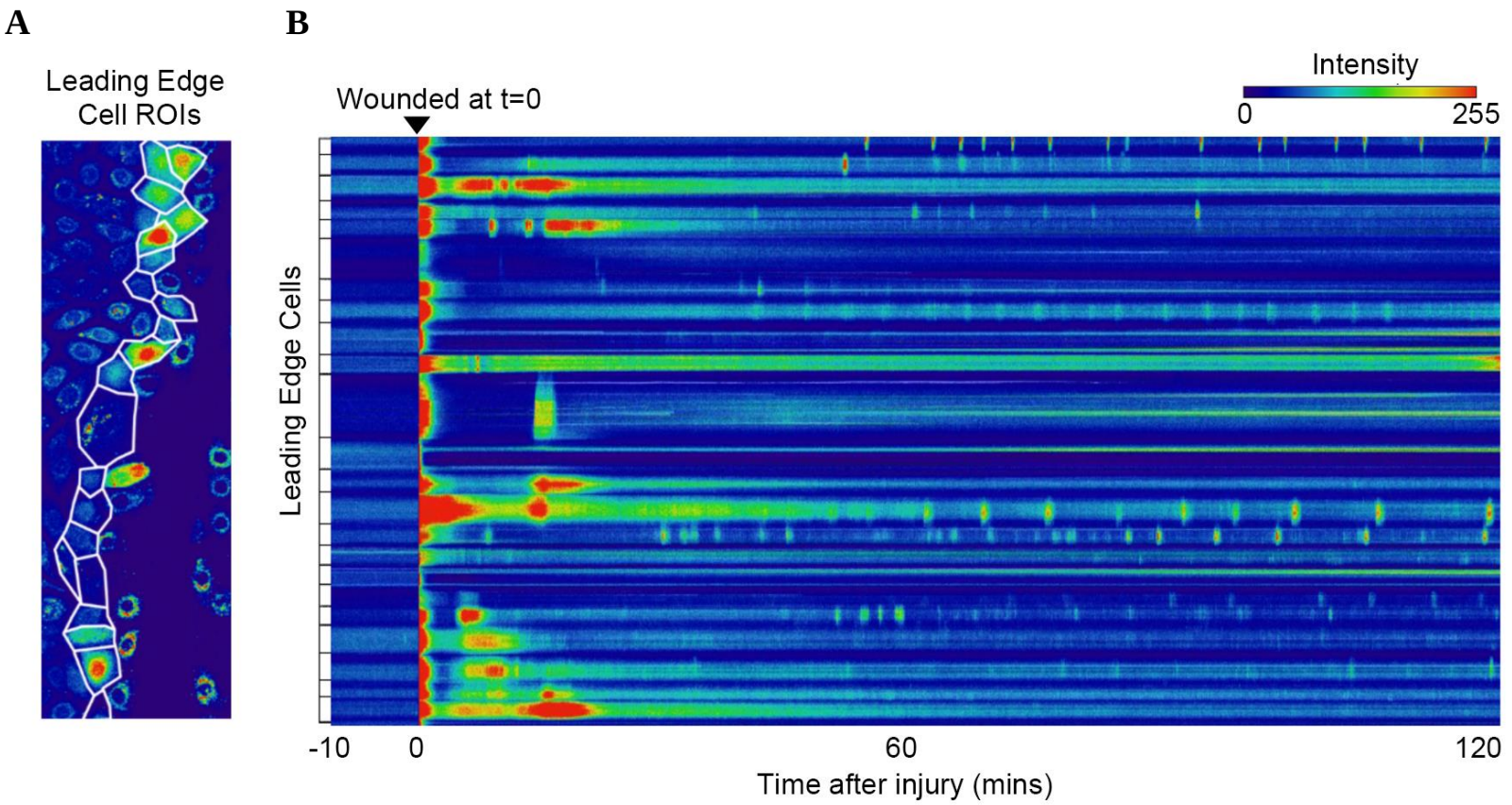

Figure 3-2: ROIs and kymographs of the leading edge cells.
A: The leading edge cells were outlined in white to get their regions of interest (ROIs). **B:** Based on ROIs, kymographs of the cells closest to the wound edge were generated to observe fluorescent intensity changes over time (Physics LUT, with intensity scale). The brackets on the Leading Edge Cells axis represents a single cell ROI, and each cell's activity is recorded as seen by the columns from the bracket. Cells were preincubated in 5μM Fluo3-AM for 30 minutes and imaged on the Zeiss Axiovert LSM 880 confocal laser scanning microscope (n=7).

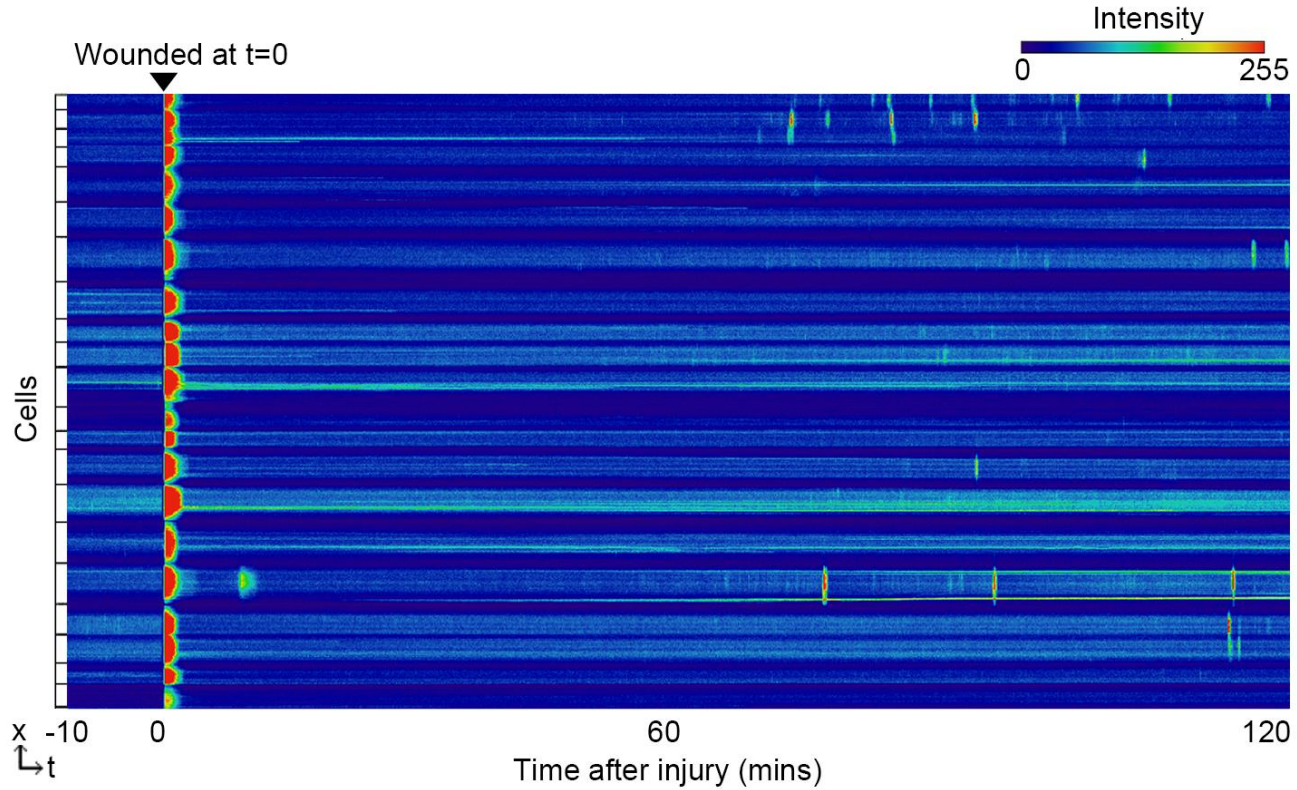

Figure 3-3: Kymograph of the cells away from the leading edge.
Cells that were further away and not part of the leading had their ROIs traced to generate a kymograph to observe fluorescent intensity changes over time (Physics LUT, with intensity scale). Cells were preincubated in 5µM Fluo3-AM for 30 minutes and imaged on the Zeiss Axiovert LSM 880 confocal laser scanning microscope. (n=7).

ATP release mediates the sustained Ca^{2+} mobilizations

In addition to live-cell imaging of the Ca^{2+} mobilization, ATP concentration in the media from HCLE cells (control and wounded) was examined by luciferase-based ATP determination assay. The concentration of ATP in wounded media was significantly greater than control for at least three hours (Fig. 3-4). Moreover, it was six-fold higher in the wounded sample than the unwounded control after 60 minutes (Fig. 3-4). This continuous presence of extracellular ATP after injury could be responsible for maintaining the sustained Ca^{2+} mobilizations.

To assess the role of ATP, we compared the response of unwounded cells to ATP, ATP + apyrase, or EGF and measured the normalized intensity value of fluorescence. Previously we had demonstrated the effect of ATP and the effect of the ectonucleotidase, apyrase, on the initial mobilization (Klepeis et al., 2001; Boucher et al., 2007). In these experiments we demonstrated the effect of apyrase on sustained mobilizations (Fig. 3-5) by adding apyrase after the initial Ca^{2+} wave. The addition quenched the subsequent Ca^{2+} mobilizations (Fig. 3-5, blue line), indicating that the sustained Ca^{2+} mobilizations were also dependent upon the presence of nucleotides. Together the data signify that the mobilizations and downstream signals depend upon extracellular ATP (Fig. 3-5).

EGF does not induce sustained Ca^{2+} mobilizations

Previously, we showed that there was a minor response to EGF and that the EGFR inhibitor, AG1478, suppressed the EGF-induced Ca^{2+} response, but not the

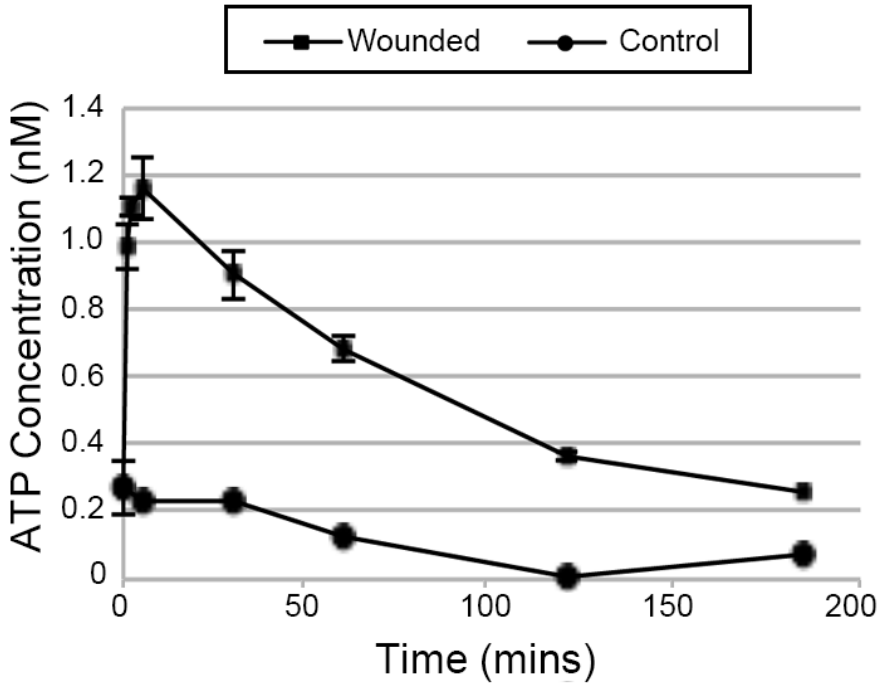

Figure 3-4: Mean extracellular ATP concentration after injury.
The mean extracellular ATP concentration over time after injury was compared to unwounded control. Error bars represent SEM (n=3).

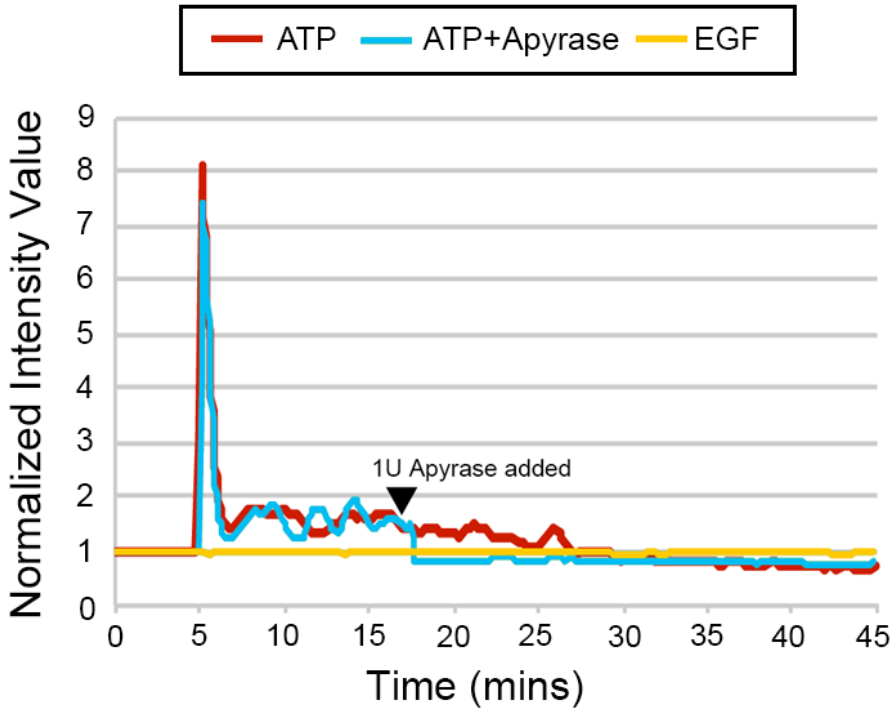

Figure 3-5: Changes in Ca^{2+} response with ATP + apyrase and EGF.
Representative fluorescence over time after treatment with ATP, ATP with apyrase, and EGF. The black arrowhead marks the time when apyrase was added (n=4).

ATP-induced response (Klepeis et al., 2001). We also reported that EGFR became phosphorylated on tyrosine residues after injury, and P2Y2 played a role in EGFR cross-activation during cell migration (Boucher et al., 2007; Kehasse et al., 2013). Therefore, we asked if EGF could induce the sustained Ca^{2+} mobilizations; but did not detect mobilizations above background levels (Fig. 3-5). These findings support the hypothesis that the sustained Ca^{2+} mobilizations are specific to extracellular ATP, indicating that purinoreceptors may play a major role in cell-cell communication.

Sustained Ca^{2+} mobilizations are mediated through P2X7 and P2Y2 receptors

Through a series of siRNA knockdown and inhibition experiments, we demonstrated that the P2Y2 and P2X7 receptors are major role players in the initial Ca^{2+} response after injury (Boucher et al., 2010; Mankus et al., 2011; Minns et al., 2016). While the cornea expresses a number of P2 purinergic receptors, the latter two receptors have a prominent role in Ca^{2+} mobilization after wounding and cell migration, and their expression changes after injury (Klepeis et al., 2004; Boucher et al., 2010; Kehasse et al., 2013; Minns et al., 2016; Kneer et al., 2018). Given these reports and our observation of sustained extracellular ATP-mediated Ca^{2+} mobilization (Fig. 3-2), we hypothesized that P2X7 and P2Y2 are involved in the sustained Ca^{2+} mobilizations, prompting the development of quantitative methods to examine events of cell communication during the sustained mobilizations. To determine quantitative changes in cell-cell communication, all cells must be inhibited and since siRNA knockdowns were only 60% efficient, we

used competitive inhibitors A438079 (for P2X7) and AR-C 118925XX (P2Y2) to achieve a uniform inhibition. The epithelial cells were preincubated with competitive inhibitors to purinergic receptors, wounded, and imaged over time. When cells were incubated with either A438079 (competitive inhibitor to P2X7) (green line) or AR-C 118925XX (competitive inhibitor for P2Y2 receptor) (orange line) and then wounded, the sustained responses were attenuated (Fig. 3-6). These results indicate that both P2X7 and P2Y2 are involved in Ca^{2+} mobilizations.

Sustained Ca^{2+} mobilizations exhibit a dose-dependent response for P2Y2 and P2X7

Out of the family of P2X and P2Y receptors expressed in the corneal epithelium, we chose to examine P2X7 and P2Y2, since their role in Ca^{2+} mobilization has been studied (Klepeis et al., 2004; Mankus et al., 2011; Weinger et al., 2005). Our goals were to examine whether selective activation of specific purinoreceptors led to distinct patterns of Ca^{2+} mobilization and to determine if these types of analyses could be used to define the contributions of specific receptors in wounded tissue. Cells were stimulated with agonists to receptors P2Y2 (UTP) and P2X7 (BzATP) with a range of concentrations (1 to 50 μM) and the average fluorescence was monitored over time (Fig. 3-7). The concentrations were adapted from receptor kinetics data of the initial wave (Weinger et al., 2005). At 50 μM for both agonists, the sustained mobilizations were rapid. Oscillatory patterns within local and large regions were detected. The intensity and duration of the responses were dose-dependent. The response to BzATP exhibited a

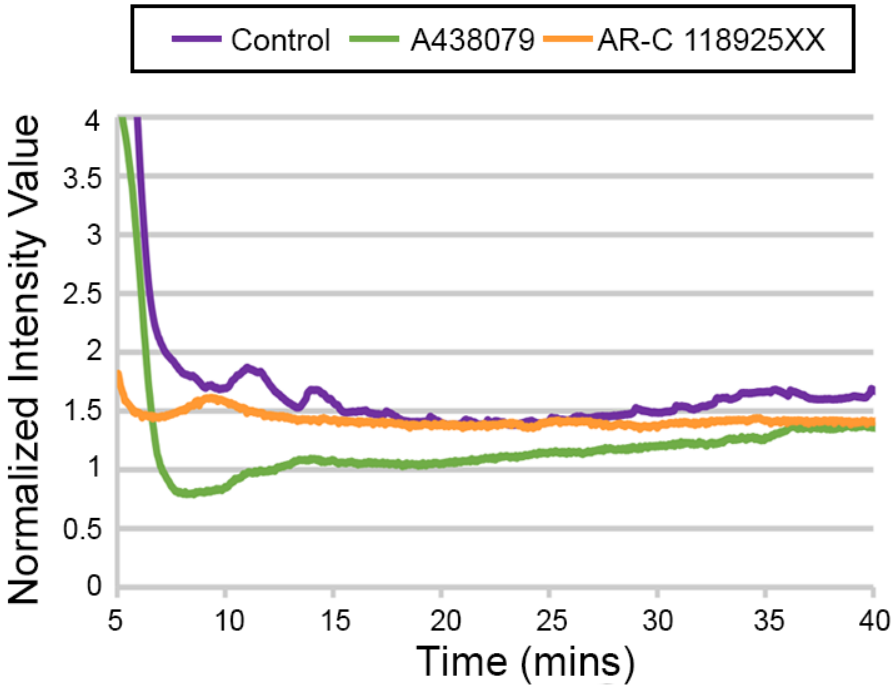

Figure 3-6: Changes in Ca^{2+} response with specific purinergic receptor inhibitors. Communication of cells closest to the wound edge after injury induced response is inhibited with A438079 (P2X7 competitive inhibitor) or AR-C 118925XX (P2Y2 competitive inhibitor) (n=4).

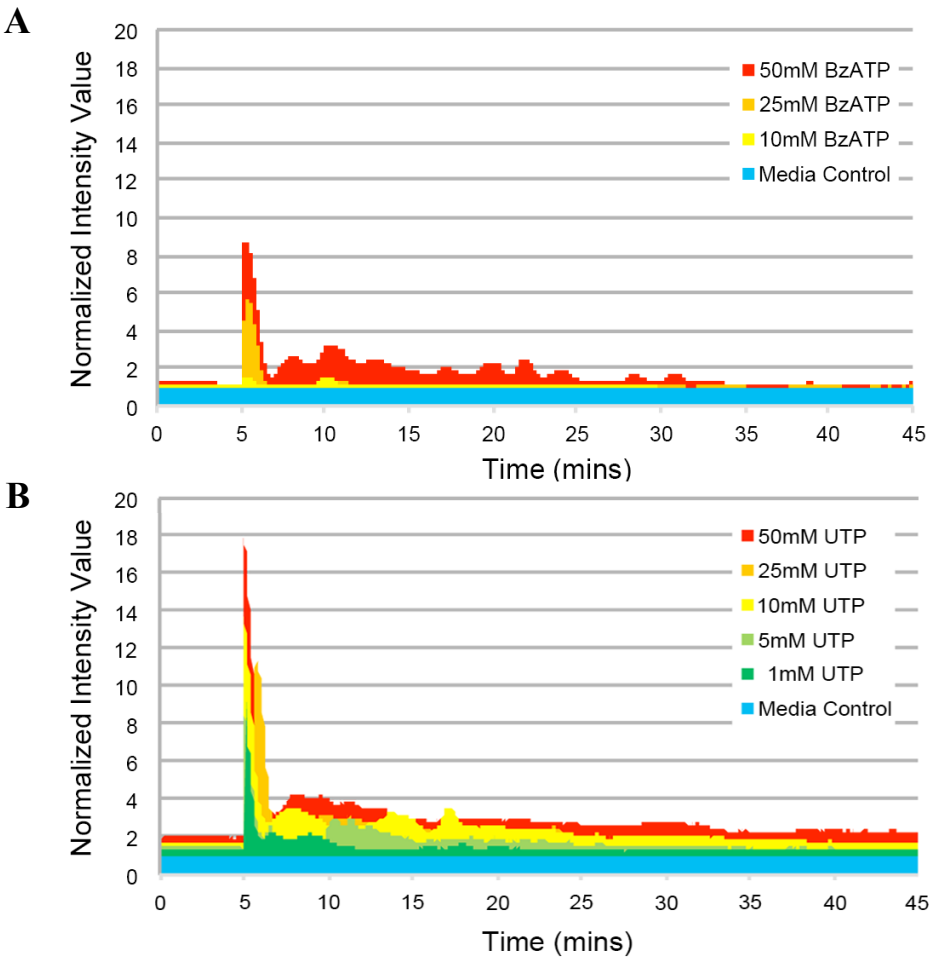

Figure 3-7: Agonist dose response curve for P2X7 and P2Y2.
Average intensity of the field was measured over the entire period of the imaging study, which lasted 45 minutes. (n=3). **A:** Dose oscillations curves for P2X7. The P2X7 receptor stimulation was with agonist BzATP. **B:** Dose oscillations curves for P2Y2. The P2Y2 receptor was stimulated with agonist UTP.

4-fold decrease at equivalent concentration compared to the UTP response (Fig. 3-7A; 3-7B). For example at 1 μM, the BzATP response is similar to baseline activity (Fig. 3-7A) while the UTP response is still greater than baseline (Fig. 3-7B).

Activation of purinoreceptors promote cell migration after injury

To examine the role of the purinoreceptors on cell motility, cells were loaded with Fluo-3AM (cyan) and CellMask™ (Fire LUT), injured, and monitored over several hours (Fig. 3-8A). Cells either displaying sustained Ca^{2+} mobilizations or lack thereof were classified as "active" and "inactive" cells respectively. The two groups of cells were tracked with CellMask™ membrane dye, and the cell membrane traces were used to record motility and change in cell shape. Active cells exhibited constant change in cell shape over time and cell motility (Fig. 3-8B). Inactive cells, despite being in the same condition, did not undergo detectable change in cell morphology (Fig. 3-8B). Based on these observations, we hypothesized that sustained Ca^{2+} mobilization patterns and altered cellular morphology are necessary for cell motility and proper wound healing.

Previously we demonstrated that paxillinY118 is highly phosphorylated after injury and in response to ATP and UTP. Its phosphorylation is significantly decreased when the P2Y2 receptor is knocked down (Kehasse et al., 2013). Furthermore, inhibition of P2X7 with oxidized ATP (oxATP), a noncompetitive inhibitor, caused a reduction of the initial Ca^{2+} response and focal adhesion turnover after wounding (Minns et al., 2016). Activation of paxillin in turn activates Rac1, which is thought to induce cell motility via lamellipodial ruffling (Valles et al., 2004). To examine the mode of activation of the cell

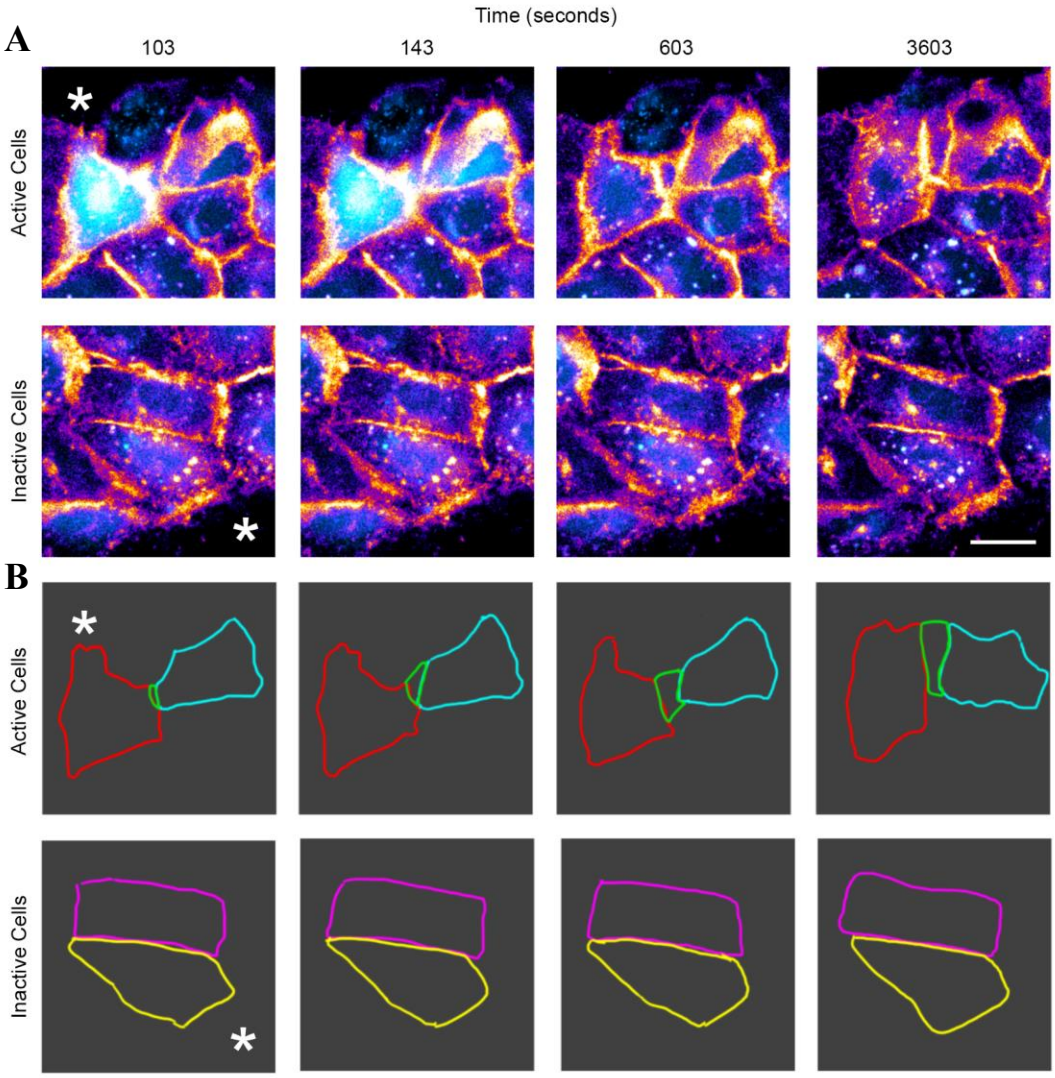

Figure 3-8: Ca^{2+} mobilizations between cells correlate with changes in cell shape. **A:** Live-cell imaging of the wound edge. Cells were incubated with CellMask membrane dye (Fire LUT) and Fluo-3AM (cyan) 10 minutes after injury to examine cell shape changes and Ca^{2+} mobilizations. The edge of the wound is marked with an asterisk. Scale bar = 34 μm. **B:** Cell traces were made for cells that exhibited active and inactive Ca^{2+} mobilization. When Ca^{2+} mobilizations are present between cells (Active), changes in cell morphology are detected. When Ca^{2+} mobilizations are absent (Inactive), there is no detectable change in cell morphology. (n=3 for both A and B).

motility, we confirmed that total Rac1 was present at the wound edge and then demonstrated Rac1 activation occurred after injury (Fig. 3-9). These results indicate that the purinergic receptors are involved in cell motility via Rac1.

Sustained Ca^{2+} mobilizations are detected in human cornea limbal explant tissue

Majority of the Ca^{2+} mobilizations has been performed on in vitro corneal cell line models (Klepeis et al., 2001; Weinger et al., 2005; Minns et al., 2016). To confirm these findings can be applied to animal and human tissue models, we examined whether purinergic receptor-induced Ca^{2+} response was present in human cornea limbal explants by culturing them in KSFM growth media before preincubating with Fluo-3AM (See Methods). When corneal epithelial cells were stimulated with ATP, Ca^{2+} mobilizations similar to the in vitro Ca^{2+} response were recorded (Fig. 3-10). We followed this up with imaging studies of ex vivo mouse corneas, which demonstrated that it would be feasible to apply Ca^{2+} image analyses for corneas with different pathologies and conditions (See Chapter 4).

3-3: Discussion

This study examined the role of the sustained Ca^{2+} mobilizations that were generated either after an epithelial injury or treatment with an agonist, and that lasted for a period of several hours. Experiments where apyrase, an ectonucleotidase, was added prior to the sustained Ca^{2+} mobilizations demonstrated that extracellular ATP was required (Fig. 3-5). Since this Ca^{2+} response required extracellular ATP, we examined the

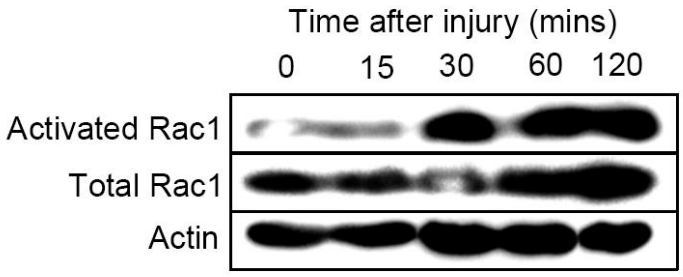

Figure 3-9: Rac1 activation assay with timepoints after scratch wounding. After scratch wounding, cells were lysed at indicated time points and pulldown was performed to collect phosphorylated Rac1 (activated) and total Rac1. The collected proteins were resolved by SDS-PAGE (12%) and immunoblotted for Rac1 (n=3).

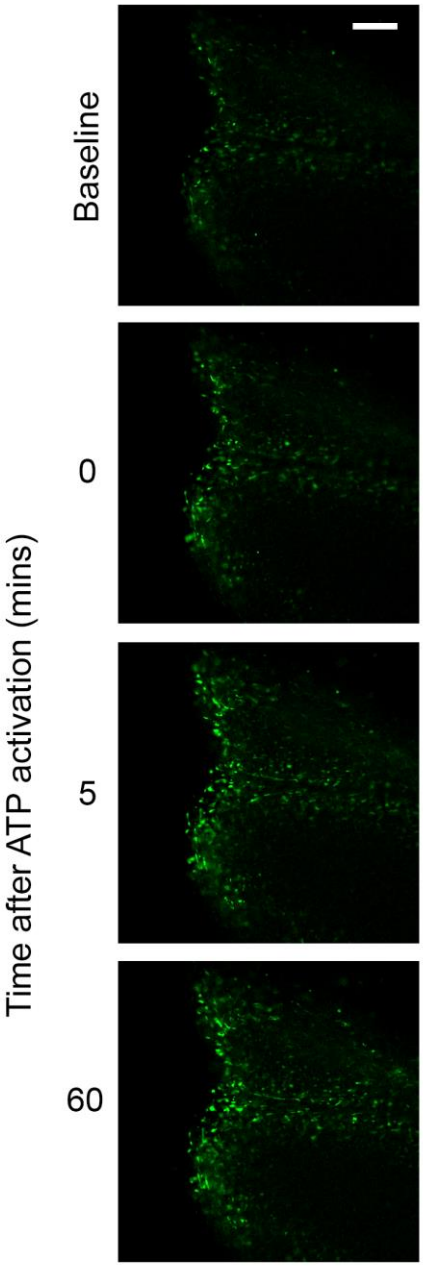

Figure 3-10: Snapshots of the Ca^{2+} mobilization events in human corneal explant tissue after activation with 25 µM ATP.
Cells were preincubated in 5 µM Fluo3-AM (Physics LUT) for 30 minutes and imaged on the Zeiss Axiovert LSM 880 confocal laser scanning microscope. Scale bar = 120 µm.

potential role of purinoreceptors in the sustained response as corneal epithelial cells express P2X7 and P2Y2 and both have been shown to play a role in cell migration (Kehasse et al., 2013; Minns et al., 2016). Responses to either BzATP or UTP, the specific agonists of P2X7 and P2Y2 respectively, were seen to be dose dependent, and the sustained injury-induced response was abrogated in the presence of competitive inhibitors to these receptors (Fig. 3-6; 3-7). While it is possible that the EGF receptor may mediate these features of cell-communication, it in of itself had a negligible effect (Fig. 3-5).

We provide evidence that the sustained Ca^{2+} mobilizations along the wound edge between cells are critical for the onset of cell motility. Mobilizations between cells near the wound edge were correlated with a change in cell shape when cells were co-stained with CellMask™ and Fluo-3AM (Fig. 3-8). Rac1 activity, which mediates actin turnover and cell migration, was elevated at 30 minutes after injury and maintained its high level at later timepoints (Fig. 3-9). Furthermore inhibition of either P2X7 or P2Y2 abrogated cell motility after injury, demonstrating the importance these two receptors in the process. This response could explain how injured cells coordinate themselves for collective migration to close the wound and is supported by studies demonstrating the transient localization of P2X7 at the wound edge (Minns et al., 2016).

Ca^{2+} mobilizations were also observed in human cornea limbal explant tissue, which demonstrates that our in vitro findings could be feasibly replicated or applied to ex vivo studies. Follow-up studies with ex vivo mouse corneas also proved that the purinergic Ca^{2+} mobilizations potentially can be analyzed qualitatively and quantitatively

(See Chapter 4). Furthermore if we can establish a system to analyze these sustained Ca^{2+} mobilizations, we can study communication between cells and provide insight into the mechanisms of wound repair in control and diseased conditions.

CHAPTER FOUR: QUANTITATIVE ANALYSIS OF CALCIUM RESPONSE TO DETERMINE CELL-CELL COMMUNICATION DURING WOUND HEALING

4-1: Introduction

To analyze the role of the P2Y2 and P2X7 receptors during the sustained response, we examined the Ca^{2+} mobilization patterns of the two receptors and established a profile for the response to each agonist. The agonist studies demonstrated that the sustained Ca^{2+} mobilizations traveled in groups of more than 3 cells at any given time (which we defined as a cluster) for both P2X7 and P2Y2 receptors. After observation of that behavior, we analyzed Ca^{2+} responses with MATLAB analysis scripts (see Methods) (Fig. 4-1). To analyze this phenomenon, grid- and cell-based MATLAB analysis of our Ca^{2+} imaging studies were performed. We also calculated the probability of cell-cell communication in neighboring cells, which we called "event probability." Our results demonstrated that epithelial cells have different patterns of cell-cell Ca^{2+} communication depending on the receptor activation through agonist activation or scratch-wounding.

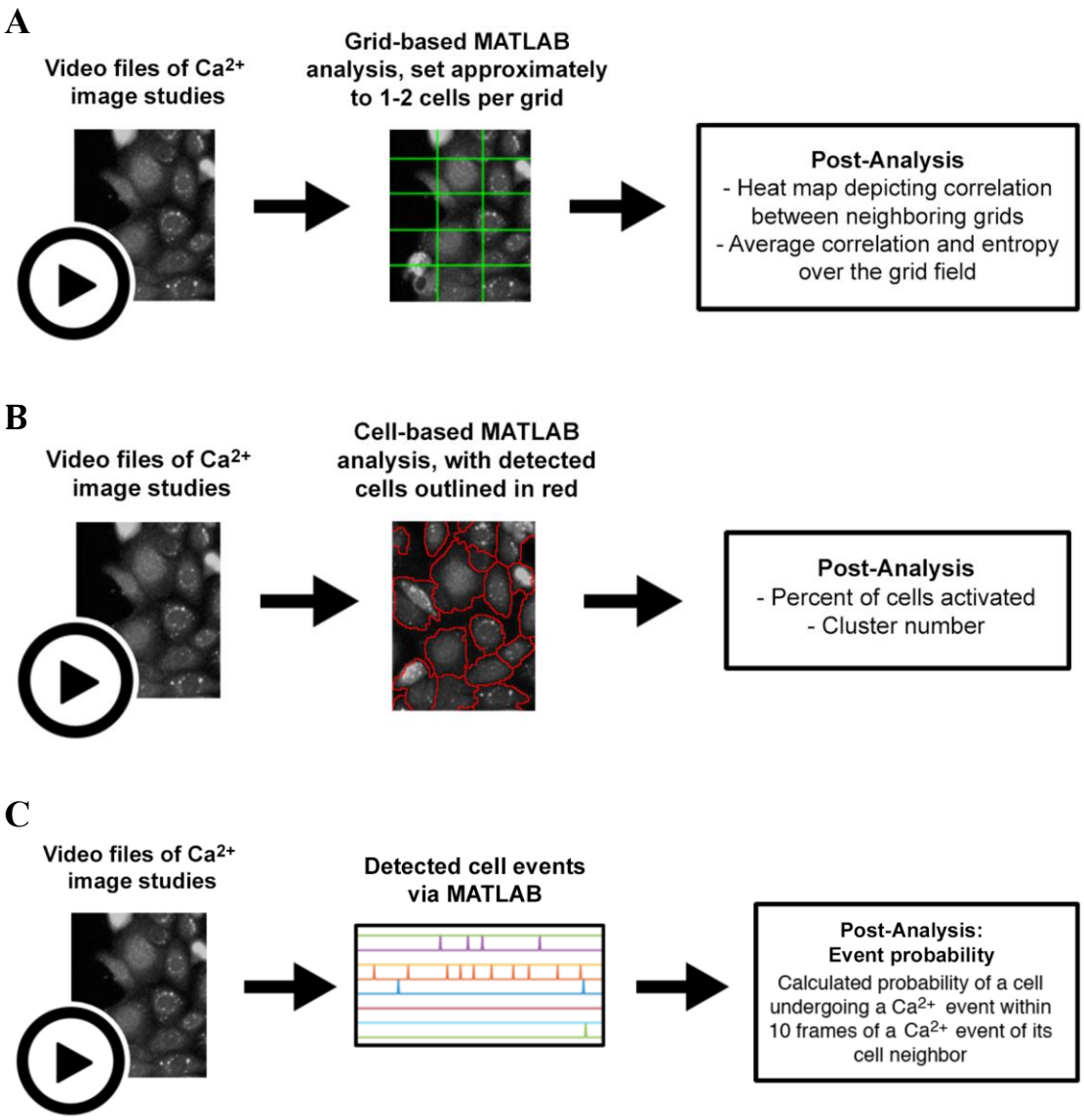

Figure 4-1: Schematic of the MATLAB approaches of the Ca^{2+} analysis.
A: Grid-based analysis. **B:** Cell/cluster-based analysis. **C:** Event probability analysis.

Grid-based Analysis

The grid-based analysis of Ca^{2+} imaging was created to make an unbiased automated method to determine the spatiotemporal correlation between areas defined by a set grid. This processing technique was made in MATLAB (Matlab, MathWorks, Inc.) through a collaboration with Dr. Vijaya B. Kolachalama in the Section of Computational Biomedicine in the Department of Medicine. The grid for each image study was set such that the block's size would be approximately equal to that of 1-2 cells, and each block was assigned a number for identification. For each block within an image frame, background noise was minimized, and the average intensity computed within that block. To examine block-level communication over time under different experimental scenarios, we examined relationships between different blocks to determine if the signaling remained in phase or fell out of phase. Since each block's intensity changes over time, it was compared with one another. Thus each inter-block correlation was examined in a comprehensive heat map to display the relationships between each of the blocks. The average correlation values of the image studies were generated based on the inter-block correlations values, which helped quantify how correlated all the blocks were in a given condition.

Cell-based Analysis

To analyze spatiotemporal communication between individual cells or groups of cells, videos from each experiment were exported in TIF or AVI format. Two different

custom MATLAB scripts were employed to analyze the Ca^{2+} responses based on cell population (individual cells or a population of cells). The individual cell analysis technique was previously described (Derricks et al., 2015). Unlike the grid-based method, cell positions were marked by either an automated computer program or manual detection. We defined the Ca^{2+} event as a rapid change in intensity due to the influx of Ca^{2+} into a cell during our image studies. Signaling events within each trace were identified as being greater than a threshold of 50% of the average normalized fluorescent signal. A cluster was defined as a group of 2-3 adjacent cells where Ca^{2+} mobilizations occurred, and the number of clusters was measured over time. Neighboring cells were identified as all cells within < 35 μm of one another. Ca^{2+} events and cell data were used to calculate percent of cells activated over time, and the detected cell clusters were used to determine number of cell clusters over time.

Event probability calculation

To quantify the cell-cell communication that we observed in the Ca^{2+} imaging studies, we used a script provided by the Christopher Gabel lab to calculate the event probability of cells under specific conditions. We defined "event probability" as the probability that a Ca^{2+} event in any particular cell would trigger a correlated event in any of its neighboring cells. Neighboring cells were defined as cells within < 35 μm of each other. The neighboring cells that displayed events within 10 frames (approximately 30 sec) of each other were defined as correlated events. The event probability was calculated

based on cell position, which was identified manually or automatically, and the number of detected Ca^{2+} events. The detected Ca^{2+} events, like cell-based analysis, were identified as presenting a fluorescence signal of at least 50% of the average normalized fluorescent signal. This technique provides a comprehensive way to compare the degree of Ca^{2+} mobilization between cells that occurs in different conditions.

4-2: Results

Grid-based characterization of the Ca^{2+} Response Patterns of P2X7 and P2Y2

We examined the Ca^{2+} mobilization patterns of P2Y2 and P2X7 receptors to analyze the role of the two receptors and demonstrated unique profiles for each agonist response specific to the receptors. These sustained Ca^{2+} mobilizations traveled in groups of 3 or more cells at any given time (defined as a cluster) for both P2X7 and P2Y2 receptors. One of the image processing techniques we applied was the grid-based MATLAB analysis, which is an automated video processing technique used to identify the cell clusters and track them over time (See Methods). Once each image frame within the video was divided into a grid of smaller blocks of equal size, metrics such as average correlation and entropy were computed using the block-level information followed by generation of heat maps (Fig. 4-1A). The correlation and entropy values represent the degree of cell involvement in the sustained oscillations and the randomness of the cell participation respectively. The heat map of the P2Y2 response demonstrated overall high-participation in sustained Ca^{2+} oscillations within and between regions. In contrast,

activation of P2X7 demonstrated overall low-participation between regions. However, it was a mixture of areas of relatively high correlation in clusters with regions of low correlation and low activity. This diversity in activity yielded a higher entropy for the BzATP response than for the UTP response, while their correlation values showed the opposite trend (Fig. 4-2). These results confirmed our hypothesis that the two receptors exhibited unique Ca^{2+} mobilization profiles. However, it did not allow us to analyze the changes in synchronicity between individual regions over time. To understand changes at the wound edge, this was critical.

To address this, we generated line graphs demonstrating mean fluorescence over time for high and low correlation regions in response to both UTP and BzATP. Representative regions are shown in Fig. 4-3A (for P2Y2) and 4-3B (for P2X7). The high correlation regions for both agonists exhibited synchronicity in their changes in fluorescence over time while the low correlations were asynchronous. The regions that displayed high correlation were generally adjacent to each other. To determine whether these regional correlations were distance-dependent, we plotted the regional correlation values over the Euclidean distance with respect to one chosen region for each agonist study and generated trend-lines for each experimental condition (Fig. 4-4). While the response to both UTP and BzATP exhibited decreased correlation over increased distance, the response to BzATP yielded a steeper negative slope compared to UTP (Fig. 4-4A; 4-4B). The response to ATP, the common nucleotide agonist that activates both P2X7 and P2Y2, had a slope between that of the responses generated by UTP and BzATP (Fig. 4-4C). The activities of these receptors demonstrate that Ca^{2+} signaling is

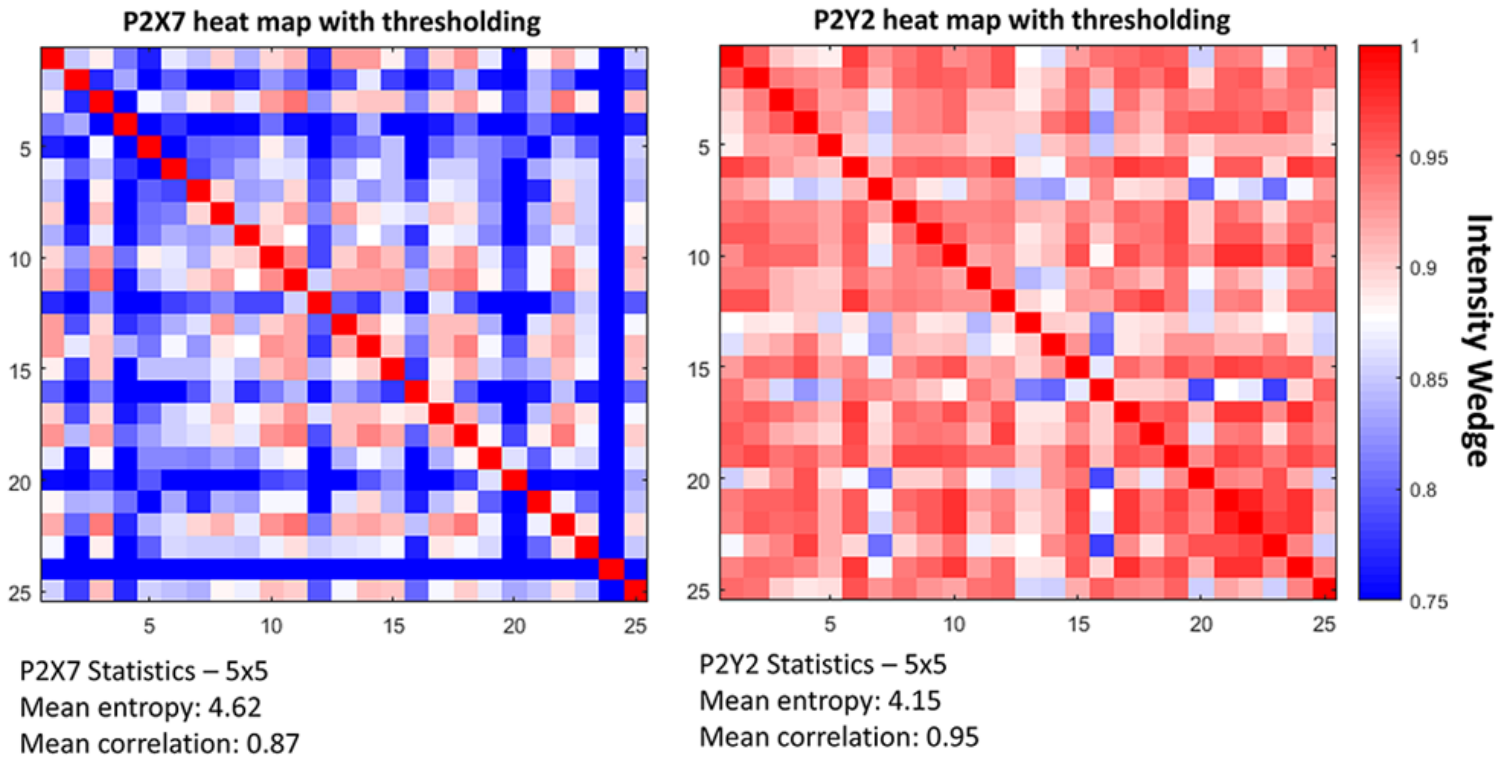

Figure 4-2: Heat maps and correlation/entropy values of the P2X7 and P2Y2 agonist response.
MATLAB-based image analyses of the sustained Ca2+ oscillations generate unique profiles for each purinoreceptor. The heat maps are representative of 3 independent imaging studies. Our ultimate goal is to use these purinergic receptor profiles to determine what role the receptors play in the wound healing response (n=3).

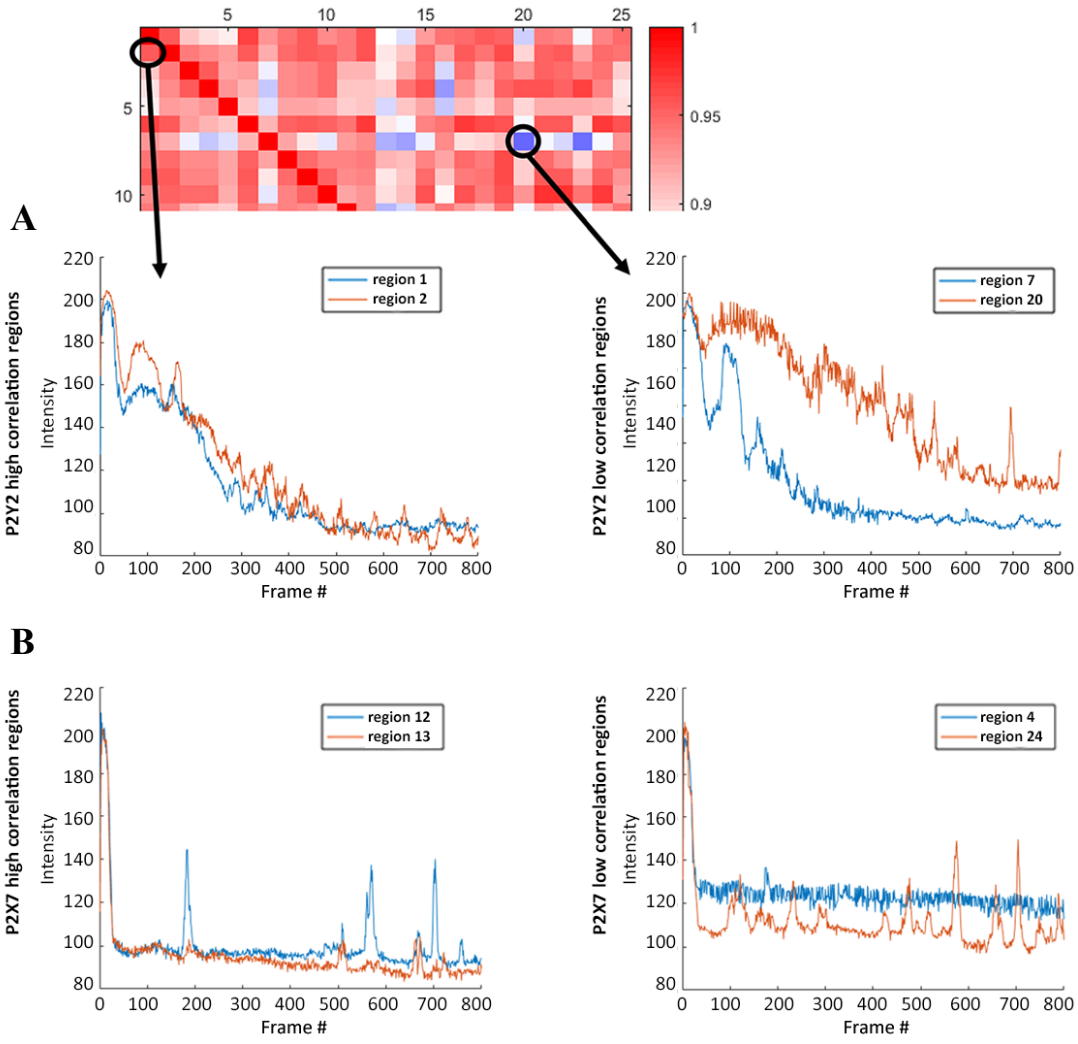

Figure 4-3: Fluorescence intensity over time for regions of high and low correlation. **A:** Based on the heatmap sections, representative fluorescence intensity over time (presented as frame #) is graphed for regions of high and low correlation for the P2Y2 (UTP) response. **B:** Representative fluorescence intensity over time is graphed for regions of high and low correlation for the P2X7 (BzATP) response (n=3).

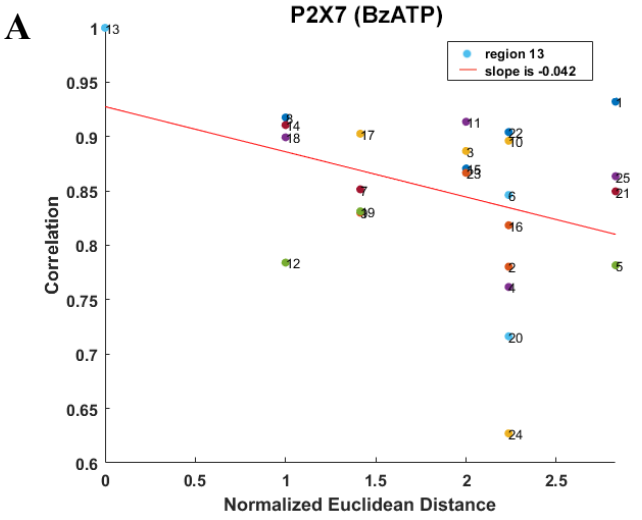
A
P2X7 (BzATP)
region 13
slope is -0.042
Correlation
Normalized Euclidean Distance

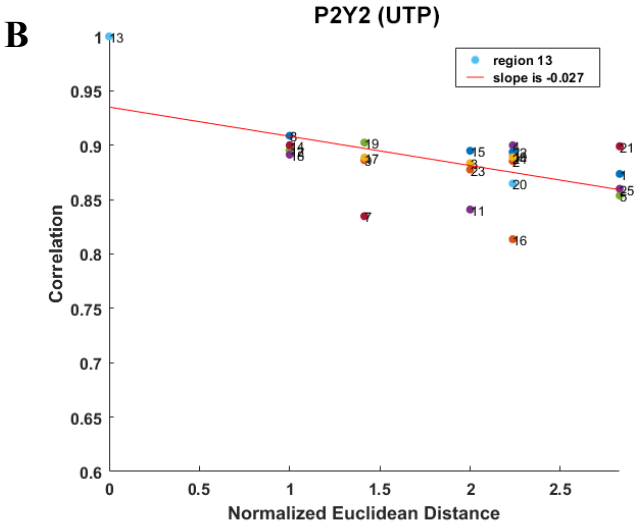
B
P2Y2 (UTP)
region 13
slope is -0.027
Correlation
Normalized Euclidean Distance

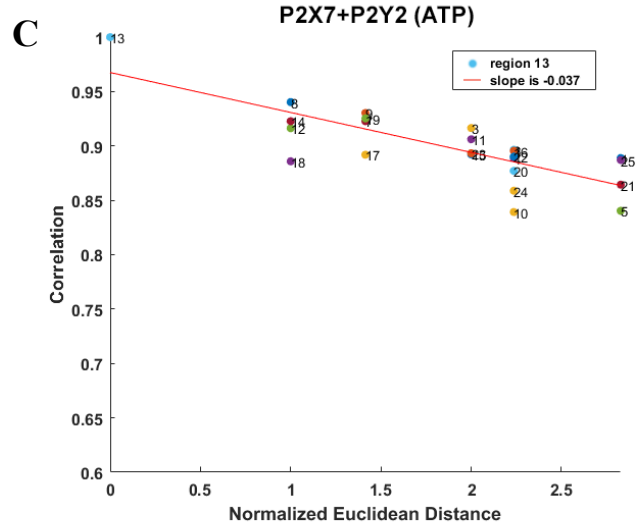
C
P2X7+P2Y2 (ATP)
region 13
slope is -0.037
Correlation
Normalized Euclidean Distance

Figure 4-4: Correlation of the grid-regions are distance dependent for both P2X7 and P2Y2.
Representative graphs of MATLAB-based correlation over normalized Euclidean distance for the agonist response to BzATP (agonist for P2X7), UTP (agonist for P2Y2) and ATP (general P2 agonist). The correlation trend-lines are drawn with respect to a chosen region (Region 13). **A:** Correlation over distance graph comparing region 13 with other regions (based on the 5x5 grid shown in Fig. 4-3) for the BzATP agonist response. **B:** Correlation over distance graph comparing region 13 with other regions (based on the 5x5 grid shown in Fig. 4-3) for the UTP agonist response. **C:** Correlation over distance graph comparing region 13 with other regions (based on the 5x5 grid shown in Fig. 4-3) for the ATP agonist response. These results demonstrate that the proximity of the cells that are displaying mobilization are crucial for the sustained propagation (n=3).

orchestrated between epithelial cells via purinoreceptors. The unique behavior may be responsible for recruiting the cells at the leading edge to undergo collective migration.

Cell-based characterization of the Ca^{2+} response patterns with agonist stimulation of purinergic receptors

Given the shortcomings of the grid-based method, we developed MATLAB analyses that to examine cell-cell communication. To analyze the role of the purinoreceptors in cell-cell communication, we examined the sustained Ca^{2+} mobilization patterns in HCLE cells after activation with the agonists, BzATP or UTP, for a minimum of 45 minutes. We analyzed the Ca^{2+} responses of these clusters with cell-based MATLAB analysis scripts (Fig. 4-1B) and demonstrated that each agonist elicited a unique profile (Derricks et al., 2015). The analysis revealed that the average percent of active cells and cluster number over time in response to BzATP was less than that detected in response to UTP (Fig. 4-5). This suggests that the UTP activates more cells to induce a Ca^{2+} response at any given time compared to BzATP.

Cell-based event probability calculation of the Ca^{2+} response patterns with agonist stimulation of purinergic receptors

To quantify the distinct sustained Ca^{2+} mobilization patterns in response to the agonists, kymographs were generated that displayed all of the cells with a known location of each cell. The graph displays activity approximately 10 mins after the immediate Ca^{2+} response (Fig. 4-6), and this was done to reduce the background noise that occurred due

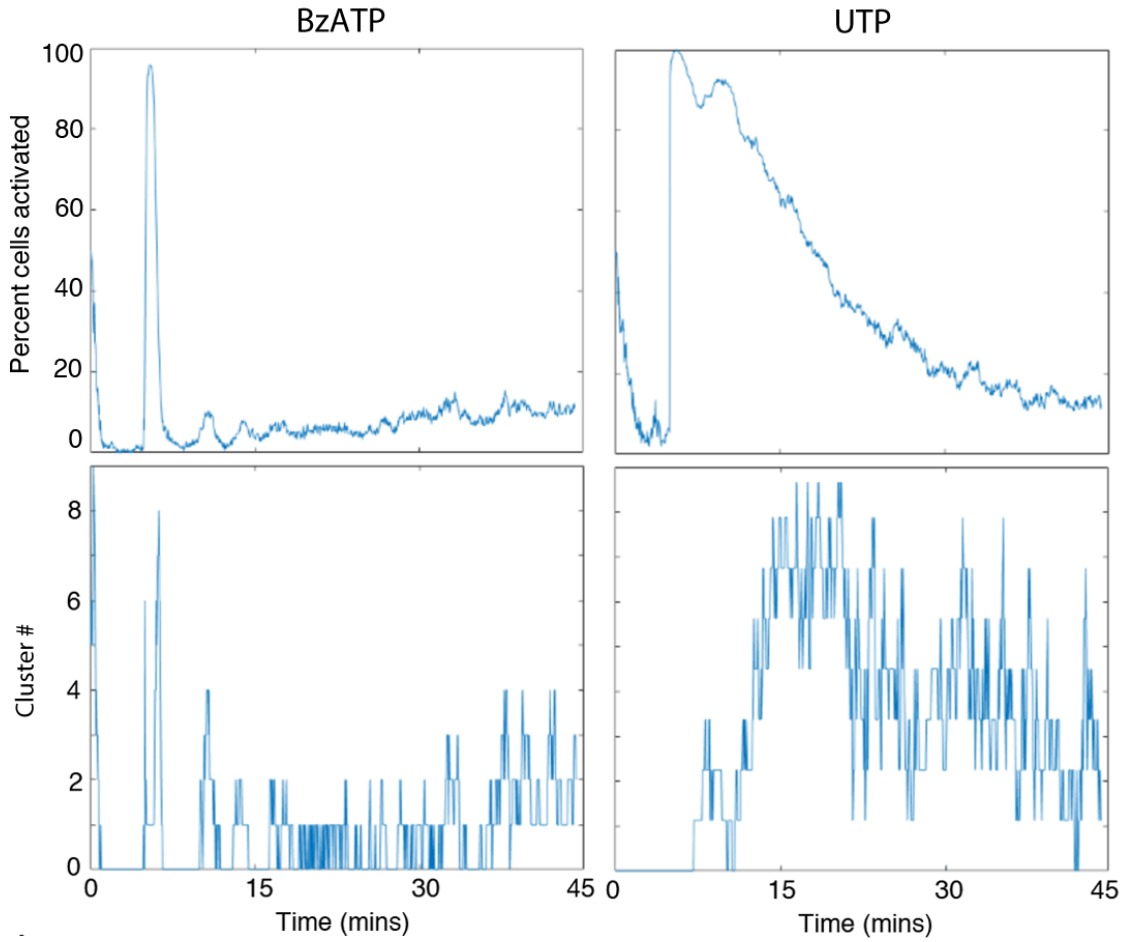

Figure 4-5: Cell-based analysis of the BzATP and UTP agonist response.
Representative graphs of percent cells activated over time and cluster number versus time for BzATP (for P2X7) and UTP (for P2Y2) agonist image studies (n=6).

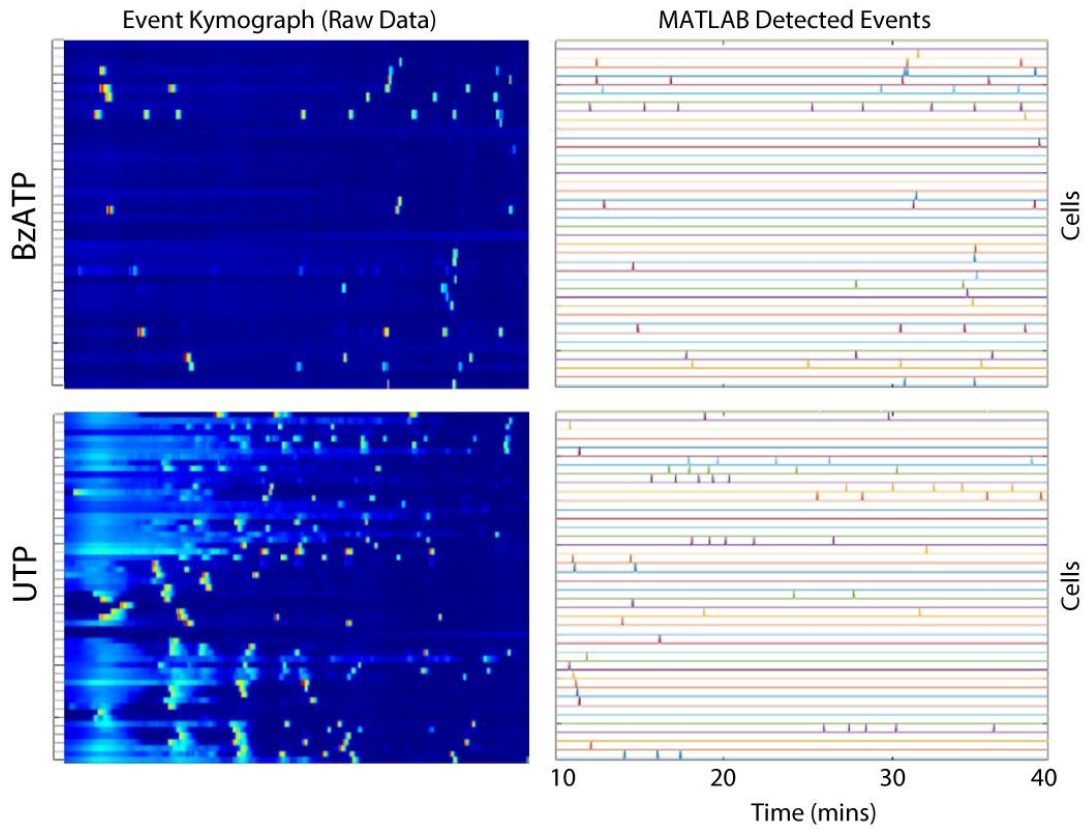

Figure 4-6: Kymograph and event detection graphs of the BzATP and UTP agonist response.

Representative kymographs and event charts of UTP and BzATP agonist image studies. To reduce the background noise from the high-intensity initial Ca^{2+} oscillations, mobilizations are analyzed 10 minutes after agonist stimulation (n=6).

to the high-intensity produced by the immediate Ca^{2+} response. The events that were detected were processed with another MATLAB-based script that calculated "event probability", which was defined as the probability of one cell displaying a Ca^{2+} event within 10 frames of a detected event of a neighboring cell (Fig. 4-1C).

While we demonstrated that BzATP elicited fewer total number of detected Ca^{2+} events compared to UTP, the average communication event probability for UTP was significantly lower than that for BzATP (Fig. 4-7). These results indicate that the sustained Ca^{2+} mobilization in response to BzATP, while less active overall compared to UTP, exhibits a more coordinated pattern of cell-cell communication. Similar experiments performed with specific P2X7 or P2Y2 inhibitors revealed that the Ca^{2+} event probabilities decreased compared to their respective agonist controls (Fig. 4-7). Together these indicate that the receptors most likely to be responsible for cell-cell communication are P2Y2 and P2X7.

Cell-based event probability calculation of the Ca^{2+} response patterns in wounded conditions

While analyzing the event probability for HCLE cells stimulated by an agonist revealed a distinct response, our goal was to determine the profile of the sustained Ca^{2+} mobilization pattern after injury. Based on our initial observations that the immediate Ca^{2+} response was generated in cells closest to the wound, the cells in wounded culture were categorized into two groups: the first two rows of cells closest to the wound were

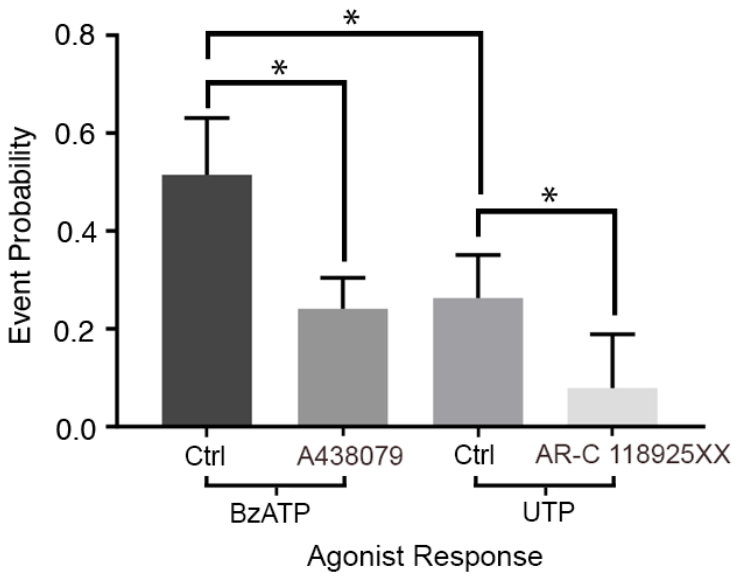

Figure 4-7: Event probability values for each agonist and their specific competitive inhibitors.
The competitive inhibitors used were A438079 (for P2X7), AR-C 118925XX (for P2Y2). Data are means ± SEM and were analyzed with a Tukey's multiple comparisons test (*$p<0.05$ for each of the indicated comparisons, n=4).

defined as the leading edge (LE) and the cells in rows further away were defined as back from leading edge (BFLE) (Fig. 4-8). The event kymographs and the resulting detected events demonstrated that the LE cells had a larger number of cells exhibiting Ca^{2+} activity compared to BFLE cells (Fig. 4-9). When the potential for cell-cell communication was quantified, the average event probability between LE cells was significantly higher (**$p<0.01$) than that of BFLE cells (Fig. 4-10). When the LE wounded cell event probability values were compared to the agonist induced events, they were statistically similar to those stimulated with BzATP (Fig. 4-11). These results imply that the P2X7 receptor may play a role in the healing response of LE cells to coordinate the collective migration process in wound closing.

Cell-based event probability calculation of the Ca^{2+} response patterns in wounded conditions with specific purinergic inhibitors

To further test the role of P2X7 and P2Y2 in cell-cell communication during wound healing, we calculated the event probability of the LE cells when preincubated with either A438079 or AR-C 118925XX. While the A438079 wounded group had a significantly reduced (***$p<0.001$) event probability compared to control, the AR-C 118925XX wounded group had no detectable event probability (Fig. 4-12). While the AR-C 118925XX treated wound did have visible Ca^{2+} events, they did not occur between neighboring cells, which is required to calculate the event probability values. Given that both receptors are activated by the ATP released from wounded epithelial cells, these

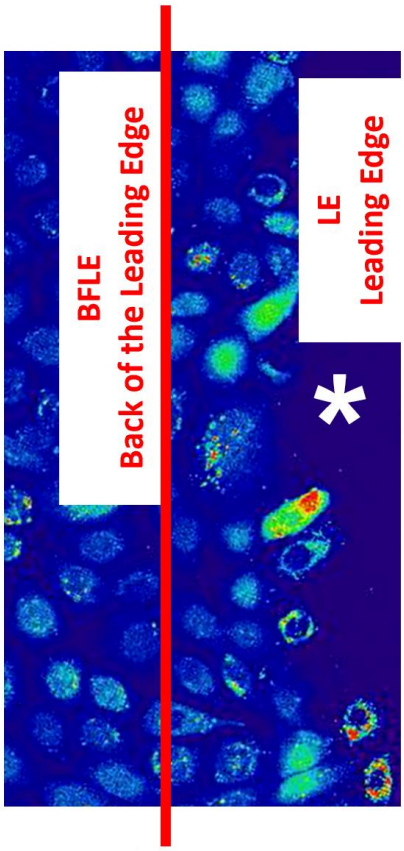

Figure 4-8: Diagram of the LE and BFLE groups in wounded condition.
The first two rows of cells closest to the wound were defined as the leading edge (LE) and the cells in rows further away were defined as back from leading edge (BFLE). The wound is marked with a white asterisk.

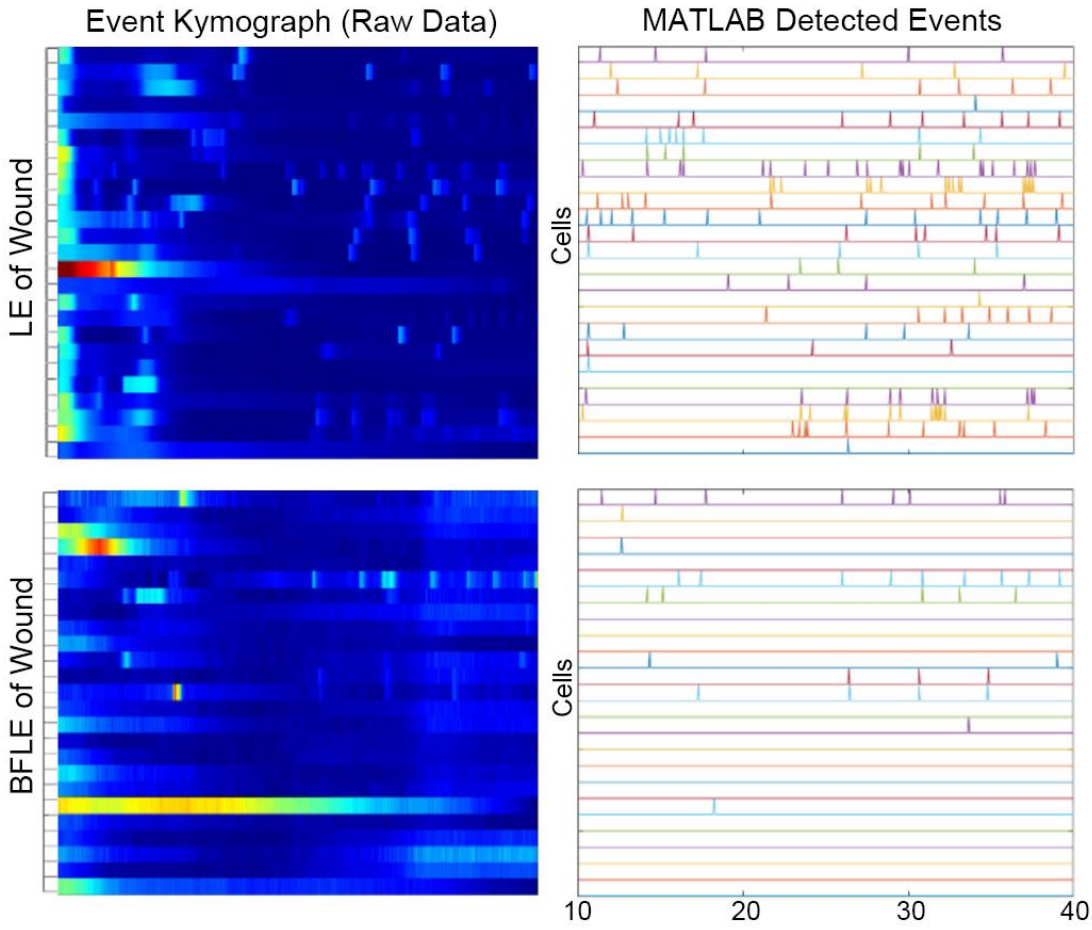

Figure 4-9: Kymograph and event detection graphs of the LE and BFLE cells after wounding.

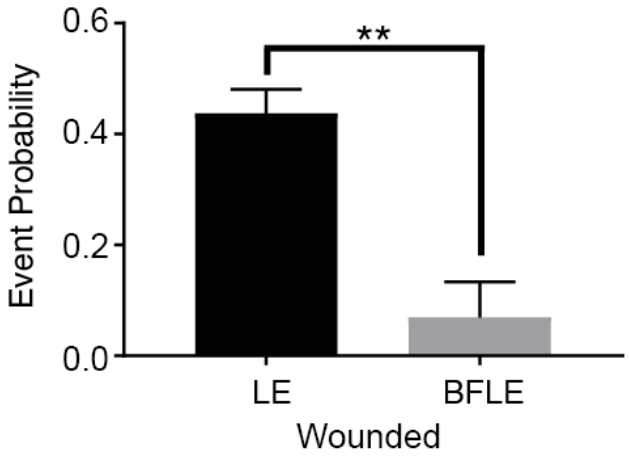

Figure 4-10: Mean event probability values for LE and BFLE cells after wounding. Data are mean ± SEM and were analyzed with a two-tailed unpaired t-test (**p<0.002, n=3).

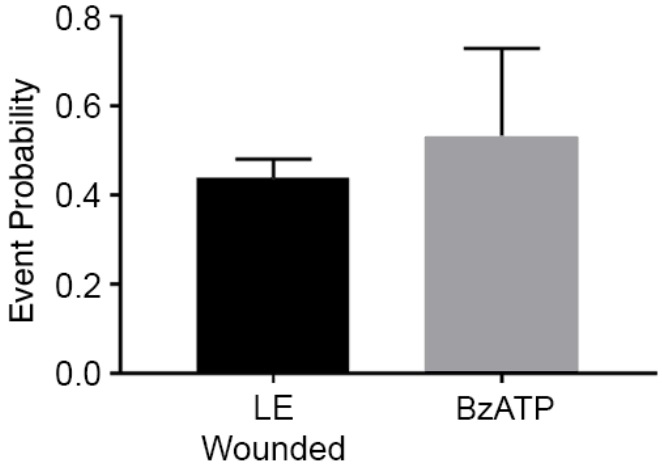

Figure 4-11: Mean event probability values for the LE wound and BzATP agonist response.
Data are mean ± SEM and were analyzed with a two-tailed unpaired t-test (ns, n=3).

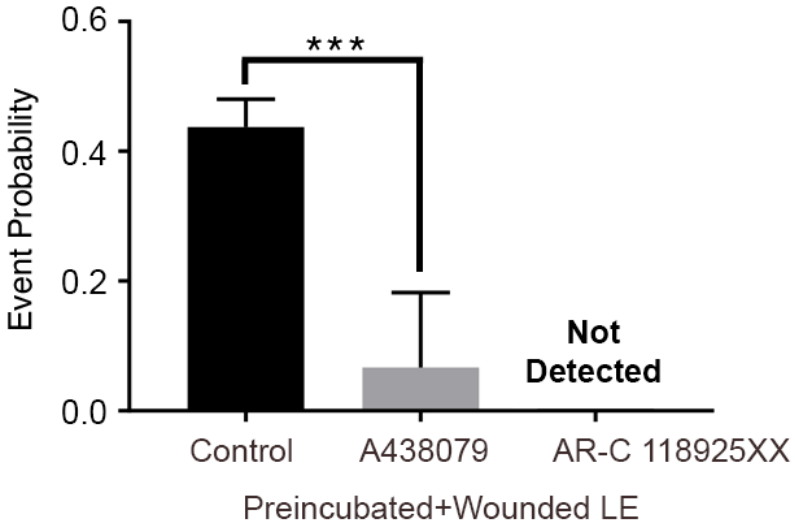

Figure 4-12: Mean event probability values for the LE cells with specific competitive inhibitors.
Cells were preincubated in the presence or absence of A438079 or AR-C 118925XX before scratch-wounding. Data are mean ± SEM and were analyzed with a one-way ANOVA with the Tukey's multiple comparisons test (***$p<0.001$, n=4).

differing results imply that Ca^{2+} signaling is orchestrated via cooperation between P2X7 and P2Y2.

Sustained Ca^{2+} mobilizations are detected in ex vivo models of the cornea

Previously, work on Ca^{2+} mobilizations has been performed primarily on in vitro corneal models (Klepeis et al., 2001; Weinger et al., 2005; Minns et al., 2016). The next logical step was to confirm the presence of the sustained mobilizations in animal models. Therefore, we examined if the purinergic receptor-induced Ca^{2+} response was present in the mouse cornea by establishing an organ culture live-imaging protocol by preincubating the eyes in Fluo-3AM and CellMask™ or SiR Actin (See Methods). Use of the CellMask™ or SiR Actin (red) enabled us to image specific layers of cells. When corneal epithelial cells were stimulated with ATP, images were not recorded for the first 10 minutes as described previously because of the noise generated by the initial transient wave. The basal cells exhibited sustained Ca^{2+} mobilizations (Fig. 4-13) and these events were examined using MATLAB analyses to generate the event kymograph and detected events were employed (Fig. 4-14). The results demonstrate that it is feasible in the future to apply our image analyses on corneas with different pathologies and conditions.

4-3: Discussion

Both P2X7 and P2Y2 and both have been shown to play a role in cell migration and wound healing (Kehasse et al., 2013; Minns et al., 2016). Given that these two

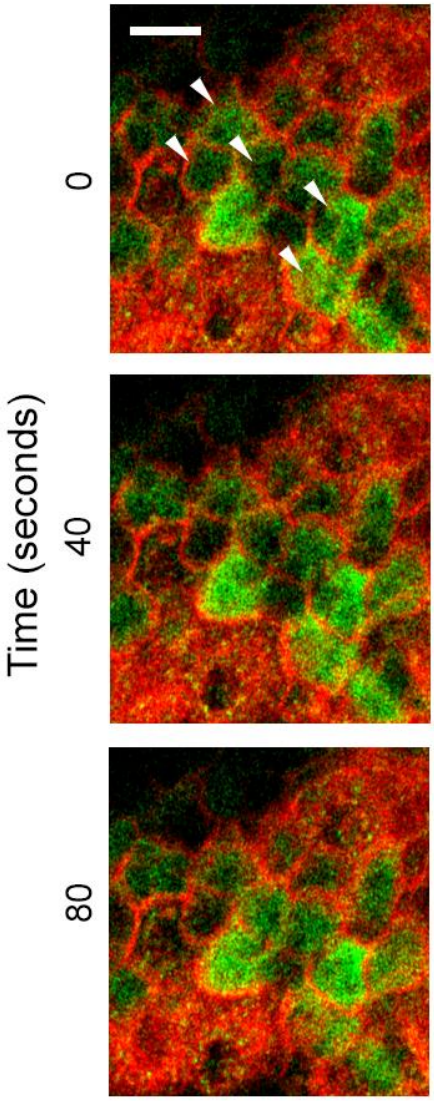

Figure 4-13: Ca^{2+} mobilizations are present in the mouse corneal epithelium
Similar to in vitro experiments, images are not recorded until 10 minutes after the addition of 100 uM ATP. Ca^{2+} events are highlighted in white arrowheads. Scale bar = 15 µm. (n=2).

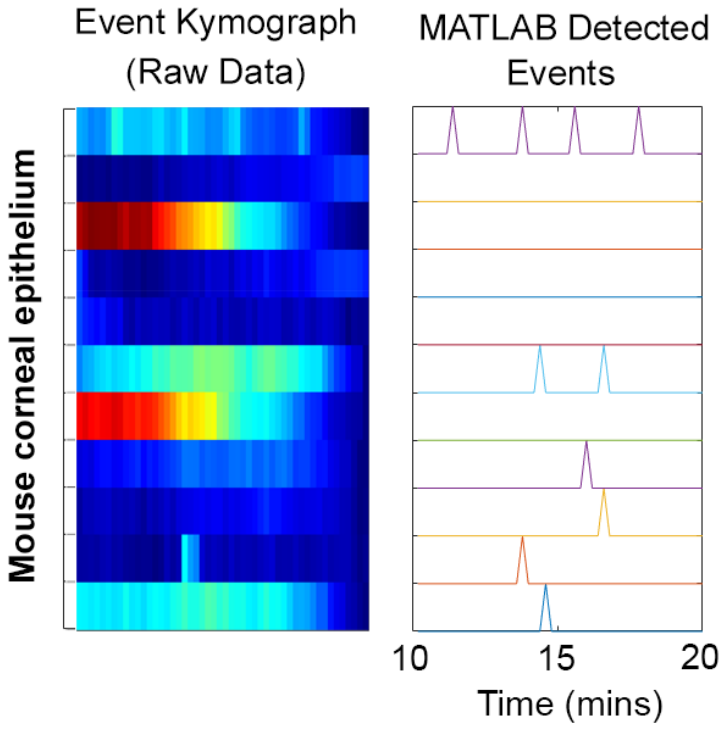

Figure 4-14: Representative kymograph and event chart of the mouse corneal epithelium Ca^{2+} mobilizations after stimulation with ATP.

receptors induce sustained Ca^{2+} mobilizations, analyzing the Ca^{2+} mobilization behavior of these cells is critical. To quantify the response, we developed image processing techniques in MATLAB to monitor the cells and examine their interactions through the following: correlation of assigned regions, percent of active cells, cluster number, and probability event values. These tools were developed to analyze the response to agonist stimulation and then applied to the wound response. For example a qualitative assessment of the response to the agonist UTP indicated that the majority of the cells appeared to be in an "on or off state", while in response to BzATP there were regions of high activity and regions of low activity.

For the grid-based analysis, the automated tools were developed to analyze the response to agonist stimulation and then extend to examine the wound response. Heat maps generated from the grid-based correlation program verified the observation of the UTP response and demonstrated that there was a higher overall continuous Ca^{2+} mobilization, with a higher average correlation and lower entropy. Metrics such as entropy denote statistical measures of randomness that can be and are used to characterize the texture of an image (Gonzalez et al., 2003). In contrast, in response to BzATP the heat maps reflected the distance traveled by depicting an overall low-participation between the regions while regions of high activity had a high correlation. However, these analyses lacked a dynamic quality showing changes in synchronicity between individual regions over time. Line graphs of regions of high and low correlation regions were generated in response to both UTP and BzATP, demonstrating that high correlation regions for both agonists exhibited synchronicity in their changes in

fluorescence over time while the low correlation were asynchronous. We then asked if regional correlations were distance-dependent. To address this, we plotted the correlation values over the Euclidean distance with respect to one chosen region for each agonist study and generated trend-lines. While both the UTP and BzATP responses showed decreased correlation over increased distance, the BzATP responses exhibited steeper negative slopes compared to UTP. These indicate that there are unique responses and we will use that information in the future to dissect out how the two receptors interact in the wound response. These will be performed in association with either non-competitive or competitive inhibitors since focal adhesion turnover is reduced upon inactivation of P2X7 (Minns et al., 2016).

Through the cell-based and cluster-based analyses, we verified that the Ca^{2+} response to BzATP elicited a lower percent of active cells and cluster number compared to UTP. However, the sustained Ca^{2+} mobilization in response to BzATP, while less active overall compared to UTP, exhibited a more coordinated pattern of cell-cell communication as demonstrated by higher event probabilities. Additional experiments performed with competitive inhibitors of P2X7 or P2Y2 revealed that the Ca^{2+} event probabilities decreased compared to their respective agonist controls. These indicated that the receptor most likely responsible for cell-cell communication was P2X7.

Interestingly, the event probability values of LE cells were similar to those when cells were stimulated with BzATP, suggesting that the P2X7 receptor may be involved in the wound healing response induced by the LE cells. This response could explain how injured cells coordinate themselves for collective migration to close the wound and is

supported by studies demonstrating the transient localization of P2X7 at the wound edge (Minns et al., 2016). The coordinated activity in the Ca^{2+} response to BzATP may be explained in part by the fact that the P2X7 receptor is a channel that allows for ATP transport in and out of cells, resulting in a positive feedback by allowing the cells at the leading edge to function as mechanically coupled yet electrochemically isolated units (Takai et al., 2014). Preliminary experiments revealed that thapsigargin, an inhibitor of IP_3 mediated Ca^{2+} release, diminished ruffling at the edge and these were associated with a change in Ca^{2+} mobilization (Lee et al., 2014).

CHAPTER FIVE: STUDY OF CELL-CELL JUNCTIONS AND ITS ROLE IN PROPAGATION OF CALCIUM MOBILIZATION RESPONSE

5-1: Introduction

Previously, our studies demonstrate the corneal epithelium uses Ca^{2+} mobilizations to coordinate collective cell migration. Given the importance of this cell-cell communication in this process, our studies focused on determining how the Ca^{2+} mobilizations are propagated. We hypothesized that they are propagated through either connexin gap junctions or pannexin channels. Our results show that pannexin-1 channels, not connexin gap junctions, are important in the propagation of cell-cell Ca^{2+} mobilizations after either agonist activation or scratch-wounding. Inhibition studies showed that both Ca^{2+} cell-cell communication and cell migration is attenuated when pannexin channels are inhibited. Furthermore, the localization of pannexin-1 is concentrated along the leading edge of the wound for both cell and tissue culture. Our results demonstrate pannexin channels are crucial players in Ca^{2+} mobilization and cell migration in corneal epithelial cells.

5-2: Results

In order to determine how sustained Ca^{2+} mobilizations are transmitted from cell-cell, we examined both connexin gap junctions and pannexin channels as methods of cellular communication.

The localization of connexin gap junctions are cell density dependent, but its inhibition does not prevent Ca^{2+} mobilizations

In our past studies, we demonstrated that the initial Ca^{2+} mobilizations do not travel through gap junctions (Klepeis et al., 2001; Weinger et al., 2005). However it is unknown whether this was also true for the sustained Ca^{2+} mobilizations that occur after the initial response. We investigated whether the transmission of the sustained mobilizations depended on connexin gap junctions, specifically connexin 43 (Cx43). Immunohistochemistry studies demonstrated that Cx43 was present as punctate staining along the cellular membrane in HCLE cells seeded at high density, but at low density the staining pattern was sparser (Fig. 5-1). Based on the density dependence of its localization, we hypothesized that there is a possibility the sustained Ca^{2+} mobilizations could go through gap junctions.

To test whether gap junctions were responsible for the transmission of sustained Ca^{2+} mobilizations, we preincubated the cells with alpha-glycyrrhetinic acid (α-GA), a connexin-specific inhibitor that disassembles junctions (Klepeis et al., 2001). Utilizing the cell-based MATLAB analysis scripts (see Chapter 4), we demonstrated that while α-GA dampens the % of activated cells, it does not alter the average cluster number (Fig. 5-2). Furthermore, there was no significant difference in the mean event probability values between the two groups (Fig. 5-3). These results indicate that propagation of events between cells does not occur via gap junctions but instead through some other means.

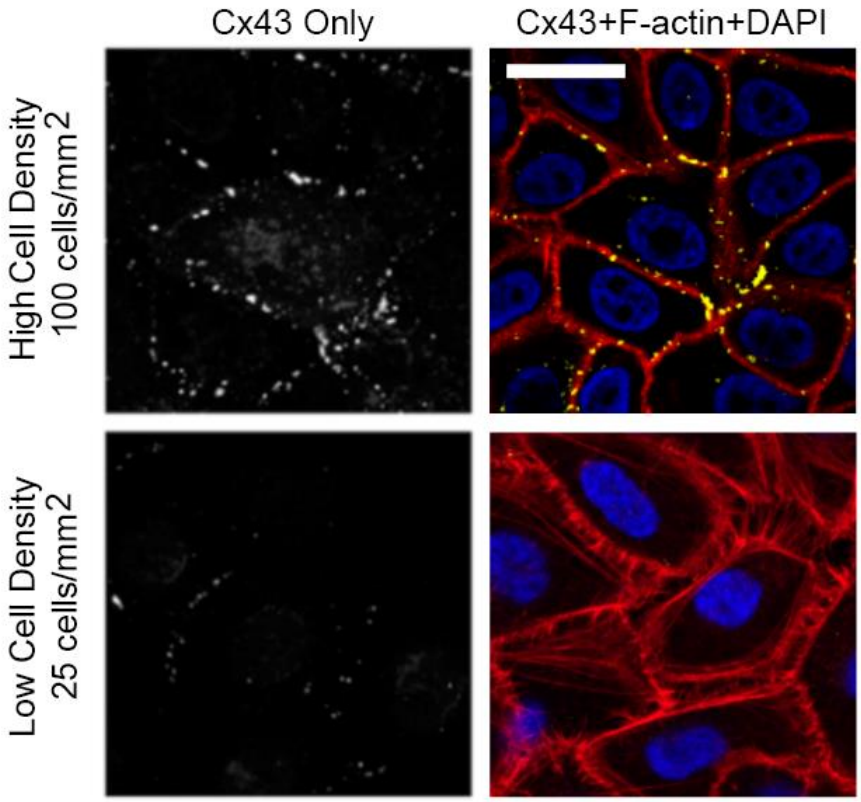

Figure 5-1: Localization of connexin gap junctions is cell density dependent.
Cells were stained for connexin -43 (Cx43, white in the Cx43 only image, yellow in the composite image) and counter-stained with rhodamine phalloidin (red) and DAPI (blue).

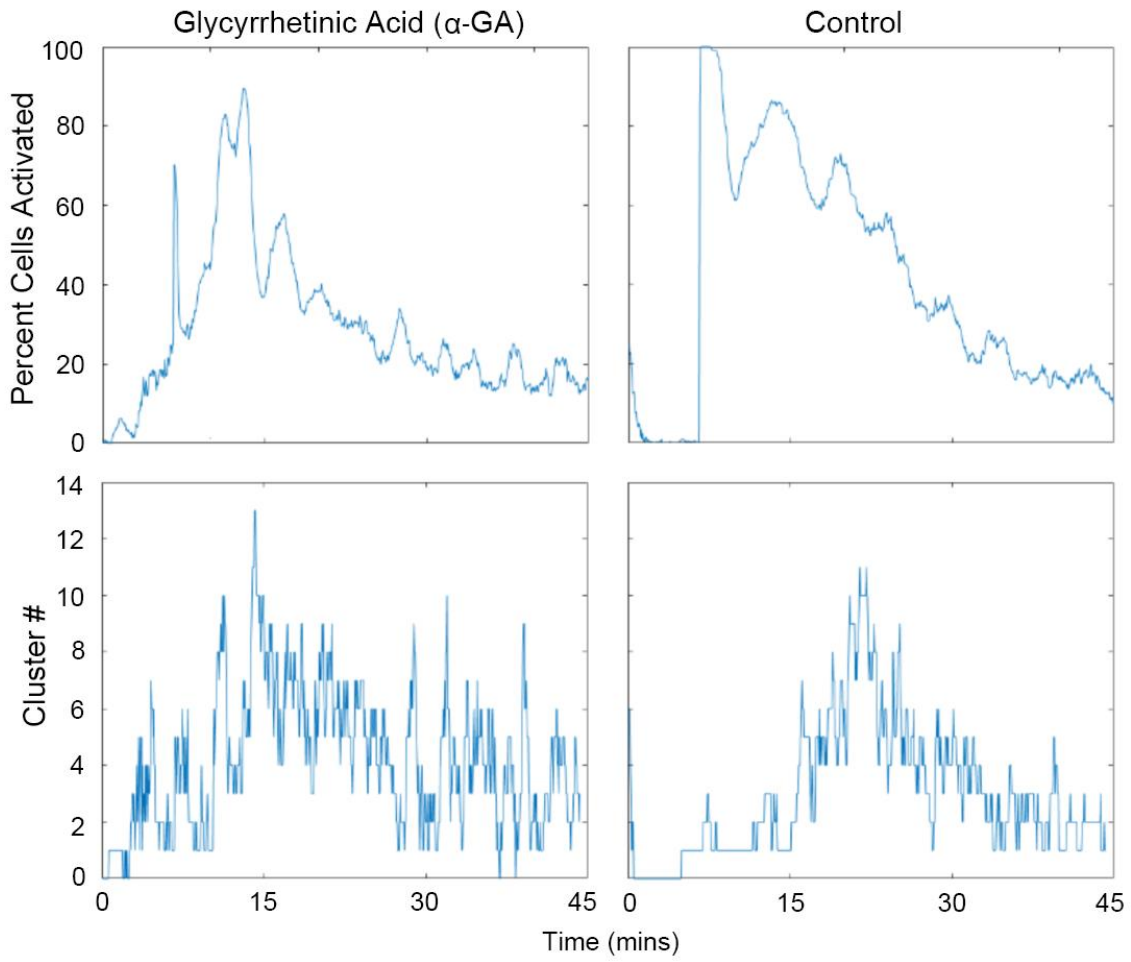

Figure 5-2: Cell-based analysis of the ATP response with a Cx43 inhibitor. The specific Cx43 inhibitor used was alpha-glycyrrhetinic acid (α-GA). Cells were preincubated with cells preincubated with 120 µM α-GA for 1 hour before ATP stimulation (n=4).

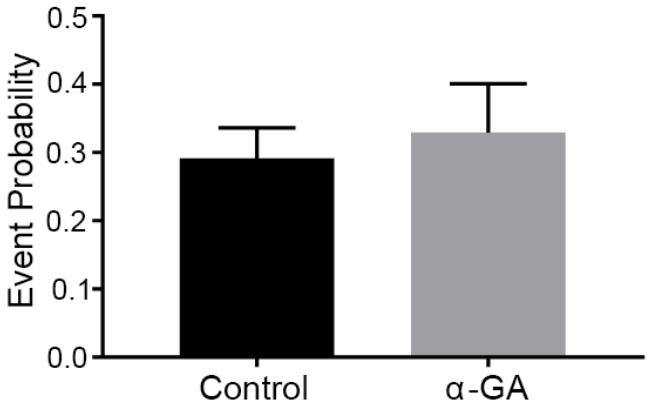

Figure 5-3: Mean event probability values for the control and α-GA treated cells
Data are mean ± SEM and were analyzed with a two-tailed unpaired t-test (ns, n=3).

Ca^{2+} mobilizations are altered upon inhibition of pannexin channels

Given that gap junctions were shown to not propagate both the initial and sustained Ca^{2+} mobilizations, we hypothesized that this process is mediated through paracrine signaling via pannexin channels. To test whether inhibiting pannexin would affect Ca^{2+} mobilizations, we used a pannexin-specific inhibitor 10Panx and the scramble Panx peptide control (Ctrl) (Romanov et al., 2012; Basova et al., 2017). When cells were preincubated with 10Panx and stimulated with BzATP, there was a significant decrease in the percent of activated cells and cluster number over time in the 10Panx group compared to Ctrl (Fig. 5-4). We also demonstrated that P2X7 interacted with pannexin-1 in corneal epithelial cells using in situ crosslinking studies (Fig. 5-5). Stimulation of cells using the agonists, BzATP (for P2X7) and UTP (for P2Y2), demonstrated that inhibition of pannexin channels abrogated the sustained Ca^{2+} mobilizations stimulated with BzATP. Furthermore, inhibition with 10Panx resulted in an event probability that was significantly decreased (**$p<0.009$) (Fig. 5-6). Cells stimulated with UTP did not have their event probability significantly affected by the inhibition of pannexin channels through 10Panx (Fig. 5-6). Together these data indicate the participation of pannexin channels in Ca^{2+} mobilization.

The localization of pannexin channels post-injury are concentrated at the wound edge

To understand the role of pannexin channels in wound healing, the localization of pannexin-1 (Fig. 5-7; yellow) was examined in control and wounded conditions in vitro

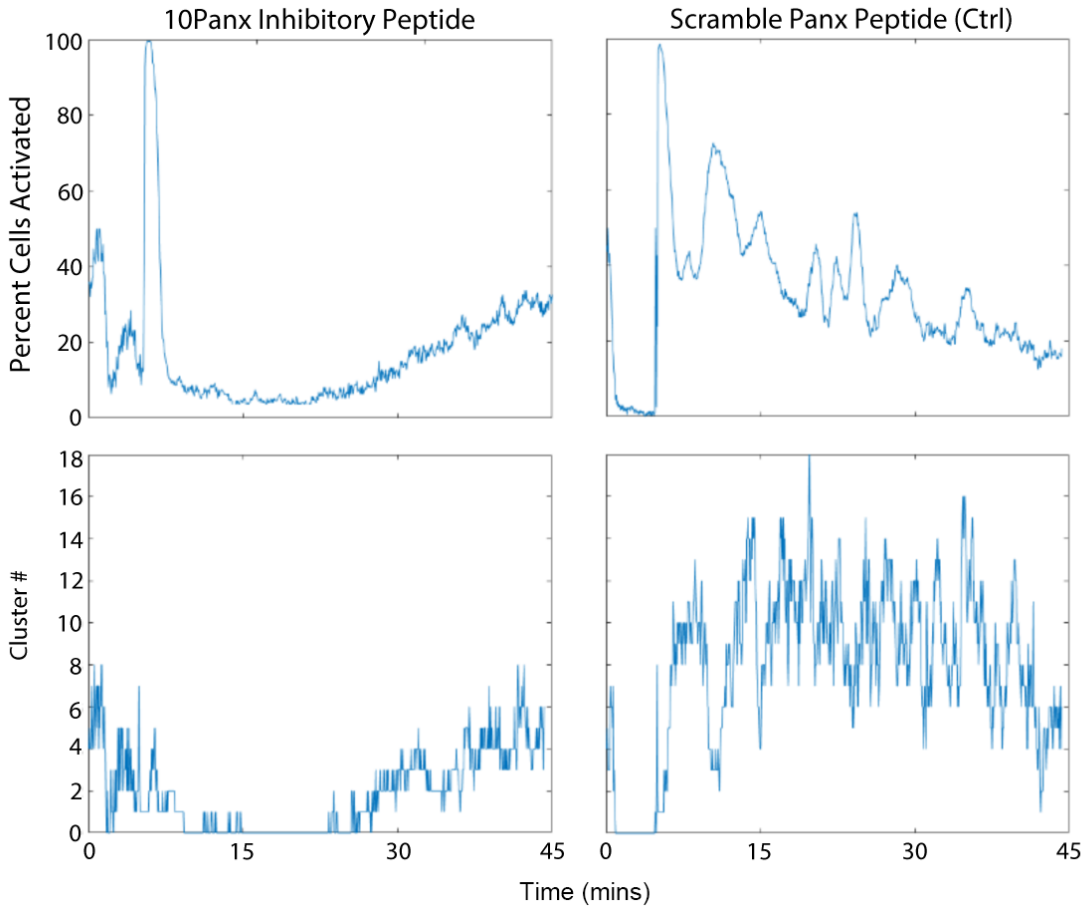

Figure 5-4: Cell-based analysis of the ATP response with a pannexin inhibitor. The specific pannexin-1 inhibitor used was 10Panx peptide, and the control was from the scramble 10Panx peptide. Cells were preincubated with cells preincubated with 100 μM 10Panx for 1 hour before ATP stimulation (n=4).

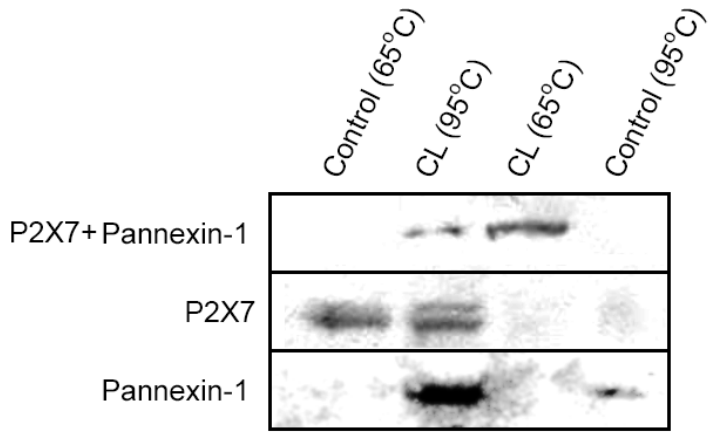

Figure 5-5: In situ crosslinking studies of P2X7 and pannexin-1 protein.
Cells were cultured until confluent, and cross-linking was performed with formaldehyde in situ, as previously described (Mankus et al., 2011). Each crosslinked experimental sample (labeled "CL") and its corresponding control were heated at two different temperature settings: 65ºC (to maintain crosslinks) and 95ºC (to disrupt crosslinks). Both CL lanes displayed the crosslinked P2X7+ pannexin-1 protein product, with the CL (95ºC) lane verifying the composition crosslinked protein product. (n=3).

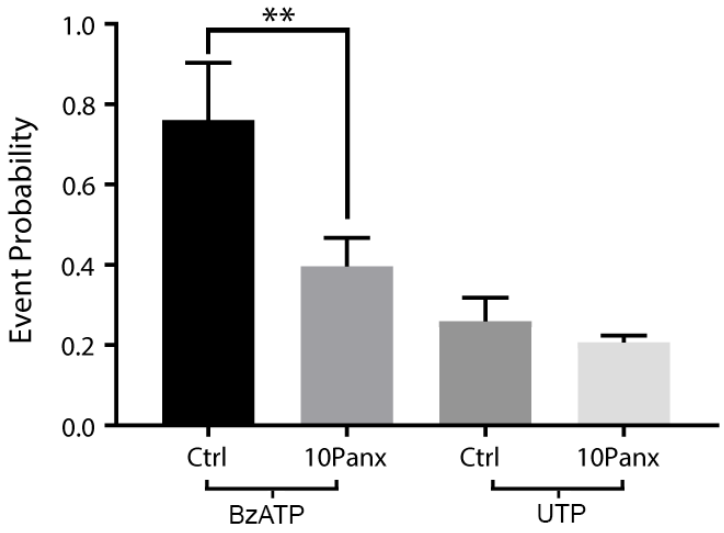

Figure 5-6: Mean event probability values of cells preincubated with either 10Panx or Scrambled Panx control group and activated with either BzATP or UTP.
Data are mean ± SEM and were analyzed with a two-tailed unpaired t-test. 10Panx significantly lowered cell-cell communication if cells were stimulated with P2X7 (**$p<0.009$), while communication was unaffected when stimulated with UTP (ns, n=4).

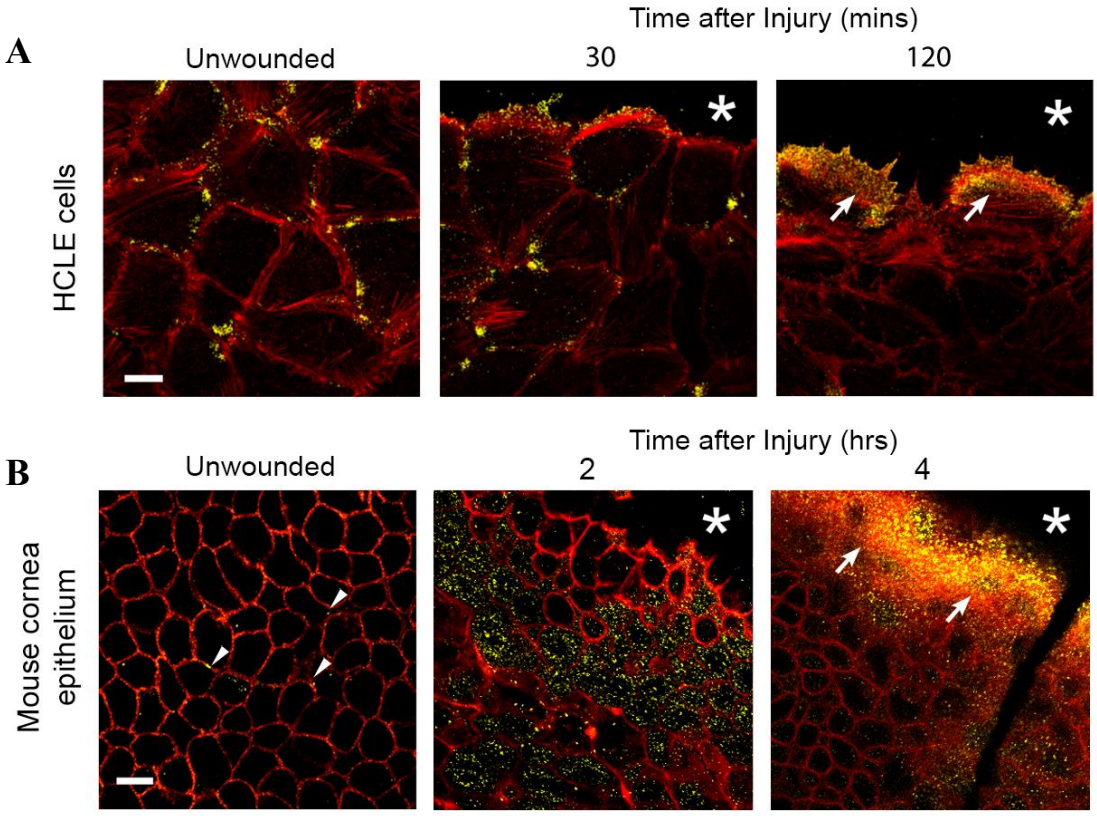

Figure 5-7: Immunofluorescence studies of pannexin-1 after wounding in cell culture and tissue show that pannexin channels concentrate at the wound edge. **A:** Representative confocal immunofluorescence images of cultured cells stained for pannexin-1 localization (yellow) and counterstained with rhodamine phalloidin (red). Scale bar = 23 µm. (n=3). **B:** Representative confocal immunofluorescence images of basal corneal epithelium stained for pannexin-1 (yellow) and counterstained for rhodamine phalloidin (red). Scale bar = 18.5 µm. (n=3). The asterisk for both (A) and (B) indicates the leading edge of migrating epithelium.

and in tissue. Pannexin-1 was localized at the intercellular space of confluent unwounded epithelial cells in culture and 30 minutes after wounding (Fig. 5-7A; * indicates wound), it was detected also at the leading edge of the wound. However, by two hours it was prominent along the wound (Fig. 5-7A; arrows). In corresponding unwounded mouse corneal tissue (Fig. 5-7B; arrowheads), pannexin-1 localization was similar to the confluent cells (Fig. 5-7B). Within two hours after wounding, pannexin-1 was punctate and present for several cells back from the leading edge of the wound, and by four hours the localization was prominent (Fig. 5-7B, arrows). This change in pannexin-1 localization may explain why the sustained Ca^{2+} mobilizations after injury were present predominantly in cells closest to the wound edge.

Inhibition of pannexin alters cell-cell communication and wound closure

Due to pannexin being more localized to the wound edge after injury, we hypothesized that pannexin inhibition would also affect the Ca^{2+} mobilization patterns and cell migration during wound healing. To study the effects of pannexin inhibition on cell-cell communication, epithelial cells were incubated in the presence or absence of inhibitory peptide 10Panx prior to scratch wounding, and the event probability analyses were applied to the videos and cells at the LE were analyzed. Cells treated with 10Panx had fewer detected Ca^{2+} events compared to Ctrl (Fig. 5-8), resulting in significantly lower average event probability values in the 10Panx-treated group (Fig. 5-9; $^{**}p<0.01$).

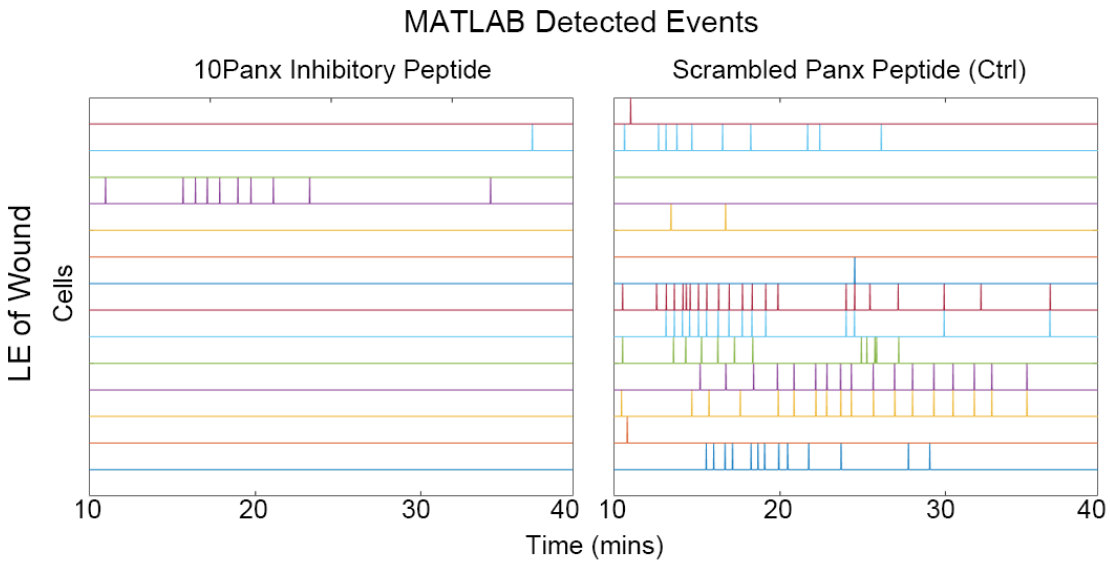

Figure 5-8: Ca^{2+} event graphs for LE cells preincubated with 10Panx or scrambled Panx control before scratch-wounding.
Ca^{2+} mobilizations are represented over time in event charts of LE cells 10 minutes after wounding (n=3).

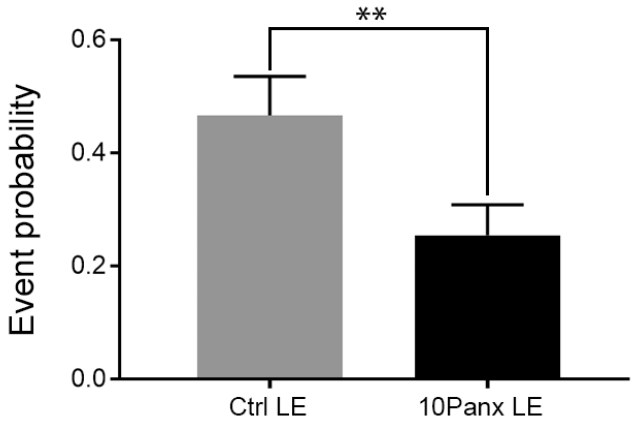

Figure 5-9: Mean event probability values for LE cells after wounding for both 10Panx-treated and control (Ctrl).
Ca^{2+} mobilizations are represented over time in event charts of LE cells 10 minutes after wounding (n=3). Data are mean ± SEM and were analyzed with a one-way ANOVA with the Tukey's multiple comparisons test (**p<0.01, n=3)

To study the effect of effects of pannexin inhibition on wound closure, we used long-term live cell imaging of cells preincubated with SiR actin Spirochrome to examine cell migration and wound closure in the presence of 10Panx and scrambled control peptide. The cell traces of the epithelial cells obtained from the migration videos demonstrated that 10Panx inhibited wound closure rate and altered cell migration (Fig. 5-10). The individual cells revealed different trajectories at the LE compared to those BFLE (Fig. 5-10C). As shown, the rate of closure was initially faster in the 10Panx group (red) but over time, the control group's wound closure rate increased while the inhibitor group stagnated, resulting in delayed wound closure for the 10Panx group (Fig. 5-10B; 5-11). The individual trajectories were analyzed and the data was organized and presented as two cell groups, LE and BFLE cells (Fig. 5-12). The LE cells in both groups generally moved in the direction of the wound (Fig. 5-12A), while the BFLE cells in the control wounds moved in the direction of the wound, the majority of the cells pretreated with 10Panx did not move in the forward direction and instead moved laterally (Fig. 5-12B). These findings support our hypothesis that pannexin channels are crucial players in sustained Ca^{2+} mobilization and cell migration in corneal epithelial cells.

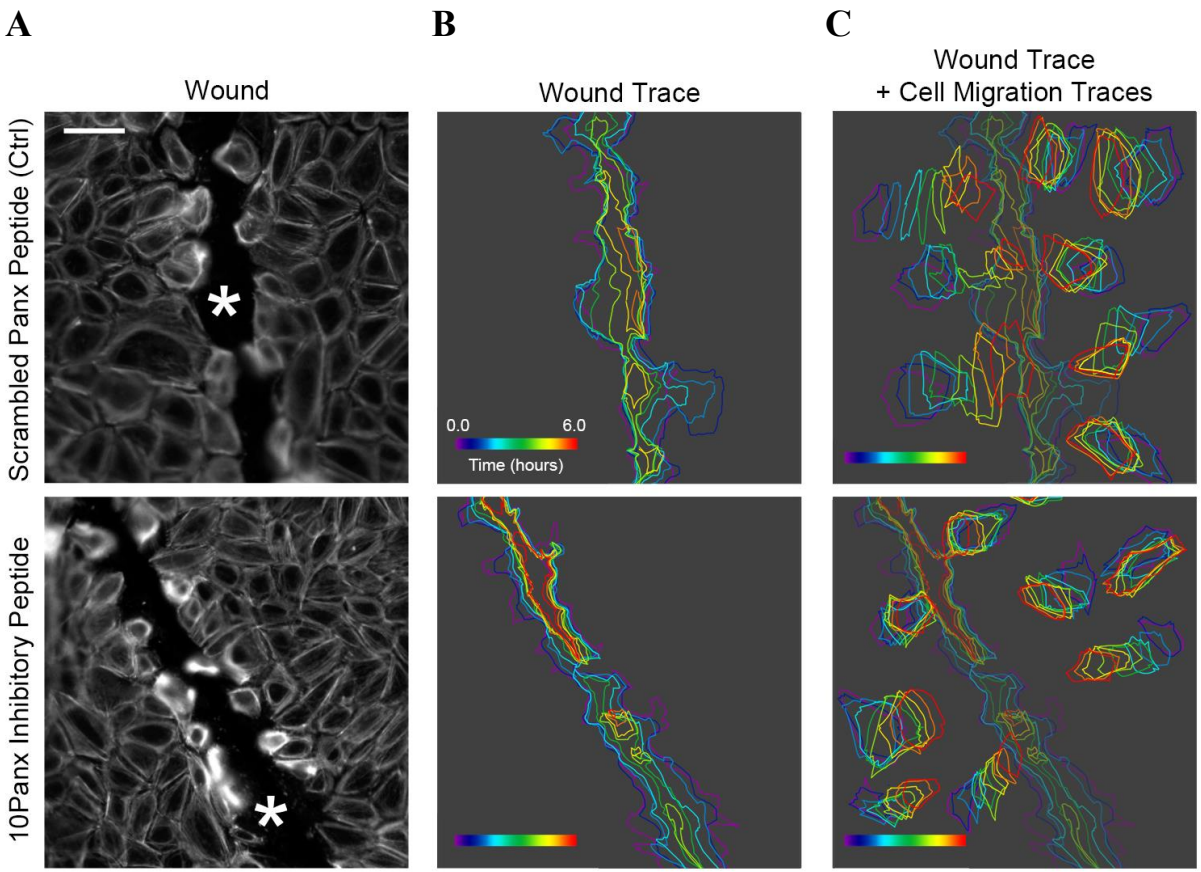

Figure 5-10: Inhibition of pannexin channels affect cell migration and wound healing.
A: Live-cell imaging of the wound edge of cells preincubated with SiR-Actin Spirochrome, a f-actin dye, (in grayscale) to determine cell migration over a 16 hour period (n=3). **B:** Traces of the wound area were drawn over time to observe the rate of wound closure for the experimental and control conditions. **C:** Traces of 8 random cells (representative) were drawn over time to observe the rate of cell migration for the experimental and control conditions. Colors reflect time and are indicated by time wedge. Scale bar = 66 μm.

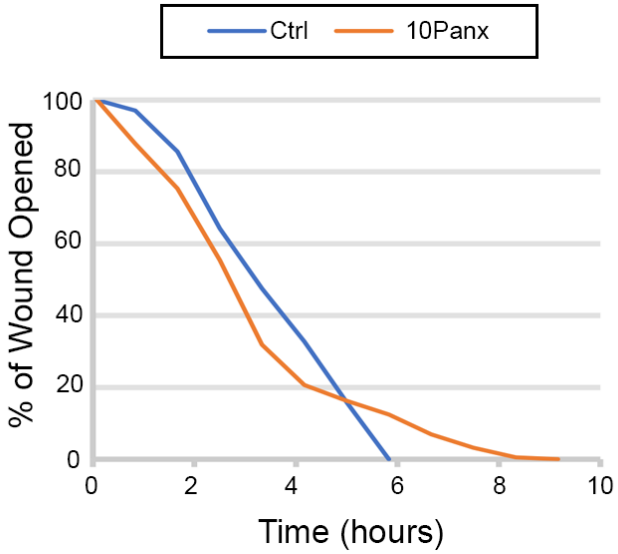

Figure 5-11: Inhibition of pannexin channels delays wound closure rate
Representative percent wound closure graph of cells preincubated with 10Panx and control over time (n=3).

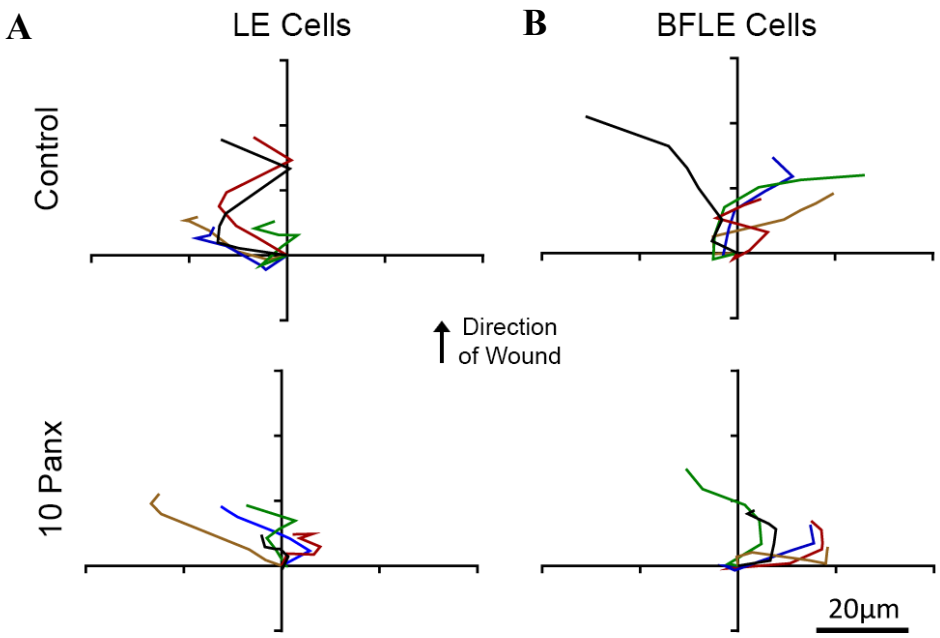

Figure 5-12: Inhibition of pannexin channels affects cell migration direction
Representative cell migration trajectory diagrams of LE and BFLE cells cells treated with 10Panx and Panx scrambled peptide control. Each line represents the migration path of a single cell plotted from a common origin. Scale bar = 20 µm. **A:** Representative cell migration trajectory of LE cells for both 10Panx and Control. **B:** Representative cell migration trajectory of BFLE cells for both 10Panx and Control.

5-3: Discussion

Our data demonstrate the importance of pannexin channels in the propagation of the sustained Ca^{2+} mobilizations in the corneal epithelium. Experiments performed in the presence of α-GA, a specific inhibitor of gap junctions, did not alter either the visual mobilizations or the kymograph representing mobilizations of neighboring cells. While these results indicate that gap junctions don't promote the sustained mobilizations, other channel proteins such as pannexin may be a more likely candidate (Romanov et al., 2012; Lu et al., 2017). Furthermore, in dendritic cells, pannexin-1 and P2X7 both play a role in cell migration during injury (Sáez et al., 2017). Using a specific pannexin channel inhibitor, 10Panx, we were able to demonstrate that both cell migration and the Ca^{2+} response is dampened. Specifically, the Ca^{2+} mobilization pattern of P2X7 was significantly decreased with inhibition with 10Panx compared to the control group while those of P2Y2 did not change. The same inhibition also altered the Ca^{2+} mobilization behavior of the LE cells after injury. These results, in addition to our immunoprecipitation studies showing the interaction between P2X7 and pannexin-1, suggest a model where P2X7 Ca^{2+} mobilization is propagated through pannexin channels.

CHAPTER SIX: DISCUSSION AND PERSPECTIVES ON FUTURE RESEARCH

6-1: Summary

While the importance of epithelial sheet migration is well recognized, there is a lack of understanding in the role of communication that occurs between cells after injury (Friedl and Mayor 2017). One way of examining how epithelial cells move is to evaluate the dynamic communication that occurs after injury and understand how it is coordinated and this can be examined by evaluating the role of Ca^{2+} signaling in orchestrating cell migration and wound repair.

In this study we identified and characterized the role of sustained Ca^{2+} mobilizations that occur after stimulation of the purinergic receptors P2Y2 and P2X7 following injury or with agonists. The signal response to the wound was concentrated along the wound edge and reduced in cells that are further away from the injury. Quantitative analyses were performed on the cell Ca^{2+} mobilizations and demonstrated a unique profile for the response to each agonist. Analysis of the wounded condition was performed and revealed a profile that was similar to P2X7 agonist stimulation. The presence of these Ca^{2+} mobilizations between cells correlated with changes in cell morphology and motility, which is prominent in cells at the leading edge during cell migration after wounding. A similar Ca^{2+} mobilization was detected in ex vivo organ culture models in response to stimulus. Further analysis of the long-term Ca^{2+} mobilizations revealed that they were not mediated by connexin gap junctions but rather by pannexin channels. Inhibition of pannexin abrogates the Ca^{2+} mobilization response

of the P2X7 receptor. Together, our results demonstrate that sustained Ca^{2+} mobilizations mediated by P2X7 and P2Y2 are a vital component in regulating the short- and long-term response to injury. This chapter will discuss the implications of these findings and questions for future research endeavors.

6-2: The role sustained Ca^{2+} mobilizations in injury

Sustained Ca^{2+} mobilization patterns of P2X7 and P2Y2

Out of all the P2 purinergic receptors that are expressed in the cornea, P2X7 and P2Y2 were seen to mediate the initial Ca^{2+} mobilization response and cell migration after wounding (Klepeis et al., 2004; Boucher et al., 2010; Kehasse et al., 2013; Minns et al., 2016; Kneer et al., 2018). Previous studies with inhibition and siRNA knockdown experiments for both P2X7 and P2Y2 receptors abrogated the initial Ca^{2+} response and had other downstream effects that altered wound healing, including tissue polarity and phosphorylation of focal adhesion proteins (Boucher et al., 2010; Kneer et al., 2018; Mankus et al., 2011; Mayo et al., 2008).

In Chapter 3, our data showed that P2X7 and P2Y2 are also involved in the more long-term sustained Ca^{2+} mobilizations that occurred after the initial response. Furthermore the Ca^{2+} mobilization profiles for P2X7 and P2Y2 were seen to be unique, and further characterized in Chapter 4. Sustained Ca^{2+} mobilizations are defined as long-term events since the response is maintained for periods of time up to two hours post-injury (Fig. 3-1). Our studies demonstrate a distinct difference in the cellular response

using agonists that stimulate the P2X7 receptor, an ion channel protein, or the P2Y2 receptor, a GPCR protein. In response to UTP (for P2Y2 response), the majority of the cells appeared to be "on", while in response to BzATP (for P2X7 response) there were regions of high activity and regions of low activity. While it is possible that the EGF receptor may mediate these features of cell-cell communication, it in of itself had a negligible effect (Fig. 3-5). The differences in communication, frequency and intensity of these Ca^{2+} mobilizations are similar to events found in development (Schneider et al., 2008). These similarities are not unexpected as wound repair or directed migration after an injury may have a number of stimuli that are present in developing systems.

In Chapter 4, we used quantitative analysis techniques to profile the Ca^{2+} mobilizations of P2X7 and P2Y2. As opposed to describing the activity qualitatively by describing the general localization pattern of the Ca^{2+}, we were able to identify each of the Ca^{2+} events and the participating cells or regions (Fig. 4-1). The two different methods used allowed us to distinguish the P2X7 and P2Y2 profiles quantitatively. Most importantly, this automatically detected data contributed to the calculation of event probability, which gives us insight into the degree of cell-cell communication the epithelial cells have after either agonist activation or injury (Fig. 4-1C). P2X7 specifically had higher cell-cell communication activity compared to P2Y2, suggesting it can play a larger role in the sustained Ca^{2+} mobilizations (Fig. 4-7). Pharmacological inhibition of either P2X7 or P2Y2 was shown to negatively affect event probability for both agonist and wounded experiments (Fig. 4-7, Fig. 4-12). We further demonstrated that this technique can be applied to tissue models, which gives us the potential to analyze Ca^{2+}

mobilizations in abnormal tissue pathologies (Fig. 4-13, Fig. 4-14). P2X7 localization and mRNA level were seen to be altered in pre-diabetic mouse models compared to the wild-type control (Kneer et al., 2018). Therefore, seeing how different pathologies, such as type II diabetes, affect Ca^{2+} mobilizations in tissue would be crucial in directly learning how injury signaling is delayed.

Nearly all of our studies were done with the HCLE cell line, and one of the limitations of this model is that the corneal epithelium is typically stratified except under injured conditions, where at the wound margin it is a single cell. While there are several stratified cultures systems available, the cells are either cultured over feeder layers or cultured in the presence of medium containing serum (Nakajima et al 2015). Since the stratified cells are already cultured in a wounded environment, it is unclear whether the Ca^{2+} mobilization effect would be the same when we create a physical wound in this system. While imaging the organ culture cornea is a great advancement and we were able to establish that the Ca^{2+}analysis can be applied for the model, there are many obstacles that had to be overcome including the use of plasma membrane dyes or SiR actin to determine which layer of cells were being captured. Furthermore any movement of the tissue can also result in distortion or change in hydration of the tissue. These limitations are being worked on and future work should be able to compare cell-cell communication in different diseased states.

Type II diabetes in particular is of high interest to us since the disease prevalence in the U.S. is increasing and burdening the healthcare system (Zimmet et al. 2001). In type II diabetes patients, there was an increase P2X7 mRNA in peripheral bone monocyte

cells compared to control patients (García-Hernández et al., 2011). However this increase did not change P2X7 activity, as measured by CD62L shedding and IL-1β secretion, or cytokine release (García-Hernández et al., 2011). These findings suggest the P2X7 signaling in diabetic patients does not contribute to inflammation. Instead P2X7 could be affecting the Ca^{2+}-mediated wound healing response. Learning why and how type II diabetes affects the mechanism of wound healing via Ca^{2+} mobilizations could potentially offer novel targets for treatment of these symptoms.

Connexins and pannexins: how cell junctions contribute to Ca^{2+} mobilization

As mentioned in Chapter 1, cell junctions provide direct or indirect communications between neighboring cells. In the case for the corneal epithelium, these cell junctions allow for cell-cell communication to coordinate collective cell migration for wound healing. Our data in Chapter 3 and 4 demonstrated that Ca^{2+} mobilizations mediate this process. However the mechanism in which this Ca^{2+} mobilization propagate from cell to cell has not been studied.

In Chapter 5, the two candidates we examined were connexin gap junctions and pannexin channels. Although the activity of the sustained Ca^{2+} mobilizations is cell density dependent, it does not require propagation through gap junctions (Fig. 5-1). When gap junctions were inhibited, the Ca^{2+} mobilizations or the cell-cell communication of neighboring cells were not altered (Fig. 5-2; 5-3). On the other hand, inhibiting pannexin-1 channels significantly suppressed the Ca^{2+} mobilization activity and the cell-

cell communication (Fig. 5-4; 5-6; 5-8; 5-9). Wound healing and cell migration was also affected with pannexin inhibition (Fig. 5-10; 5-11; 5-12). The localization of pannexin was also seen to change over time after injury in both in vitro cell culture and tissue (Fig. 5-7). Given that pannexin is concentrated at the LE cells, which are the main areas of Ca^{2+} mobilization, this suggests that pannexin is the main mediator of this cell-cell signaling. In the eye, pannexin has been shown to participate in extracellular ATP release for cell signaling (Lu et al., 2017; Romanov et al., 2012; Sáez et al., 2017). Furthermore, pannexin has been seen to be associated with P2X7 to contribute to cell migration during injury in dendritic cells (Sáez et al., 2017). Our crosslinking studies also demonstrate that the pannexin-1 channel and P2X7 in the corneal epithelium do interact directly (Fig. 5-5).

Studies looking at the dynamics of pannexin-1 localization over time would help us learn more about the Ca^{2+} mobilization during wound healing. This could be achieved directly with live-cell imaging with fluorescently-tagged pannexin proteins or indirectly with fluorescence recovery after photobleaching (FRAP). Preliminary FRAP studies showed that LE cells have a slower recovery rate compared to BFLE cells (Fig. 6-1). This behavior was significantly enhanced when pannexin channels were inhibited (Fig. 6-1). This finding may seem to conflict with the hypothesis that pannexin channels mediate cell-cell communication in the corneal epithelium, but pannexin channels mediate paracrine signaling through an ATP-forward mechanism and not through direct cell-cell transmission of Ca^{2+} as demonstrated in Chapter 5.

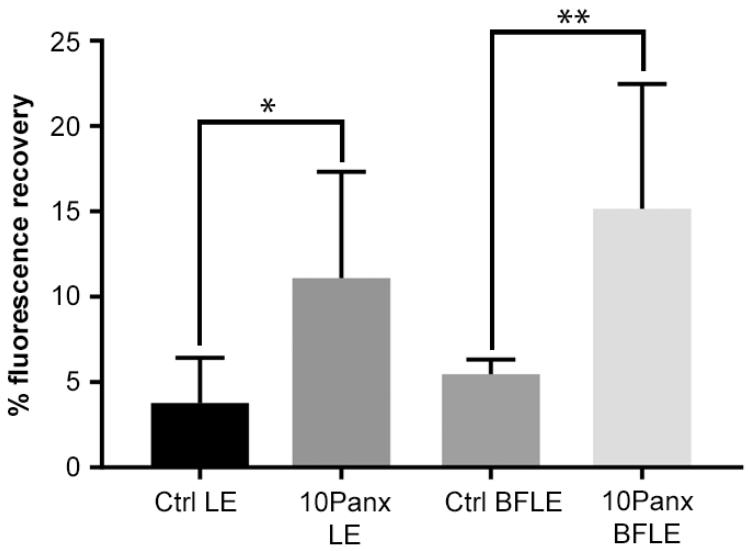

Figure 6-1: Event probability values for LE and BFLE cells treated with 10Panx
Data are mean ± SEM and were analyzed with a one-way ANOVA. 10Panx significantly raised cell-cell communication for both LE (*$p<0.05$) and BFLE cells (**$p<0.007$) (n=3)

The current model for wound healing in the corneal epithelium

Based on our data, the current proposed model for Ca^{2+} mobilization propagation is that localized release of ATP through pannexin channels activates purinergic receptors in neighboring epithelial cells (Fig. 6-2). In epithelial cells, ATP remained 6- to 7-fold higher after injury compared to the near constant basal levels of unwounded control cells (Fig. 3-4). This indicates there may be an overall greater release than degradation of ATP, suggesting it is secreted continually by migrating cells. This ATP release from the cells at the leading edge induces mobilization of Ca^{2+}, which associated with cell shape change and migration (Fig. 3-8). These observations are supported by the activation of Rac1 that occurs with injury (Fig. 3-9). Further studies looking at the state of Rac1 activity upon stimulation with P2X7 and P2Y2 agonists could offer insight into the mechanism in which the P2 purinergic receptors mediate cell migration after injury. Another question that we have yet to answer is whether P2X7 or P2Y2 work upstream or downstream with respect to each other. Both receptors increase intracellular Ca^{2+} and have different downstream effects. It would be interesting to see how their pathways overlap or interact with one other in the wound healing process.

6-3: Conclusion

Study of the communication between cells provides insight into the mechanisms of wound repair in control and diseased conditions. Overall, our epithelial injury model and the quantitative processing provides a valuable system to investigate how cells communicate in response to specific receptors. This model can be used to identify

therapeutic targets and test strategies in the cornea and in other tissues to modulate the collective cell migration in treating and preventing disease progression.

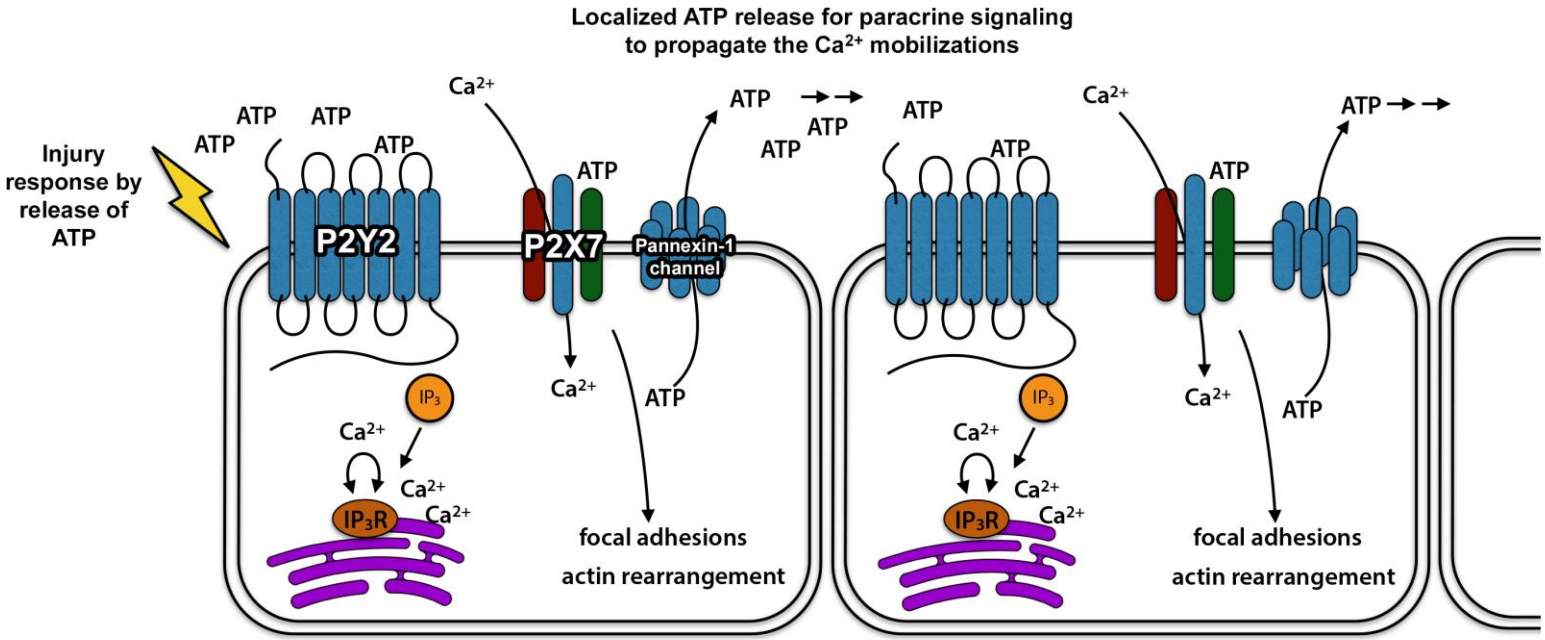

Figure 6-2: Proposed mechanism for the Ca^{2+} mobilization response after injury in epithelial cells.
ATP released into the extracellular space after injury activates both P2X7 and P2Y2 receptors, which induce an increase in cytoplasmic Ca^{2+} through either the P2X7 ion channels or through the activation of the IP_3 pathway via P2Y2. This causes further ATP release from pannexin-1 channels to propagate the injury signal via paracrine signaling.

BIBLIOGRAPHY

Abbracchio, M.P., and Burnstock, G. (1998). Purinergic Signaling: Pathophysiological Roles. Japanese Journal of Pharmacology 78, 113–145.

Adinolfi, E. (2013). New intriguing roles of ATP and its receptors in promoting tumor metastasis. Purinergic Signaling 9, 487–490.

Awal, M.R., Austin, D., Florman, J., Alkema, M., Gabel, C.V., and Connor, C.W. (2018). Breakdown of Neural Function under Isoflurane Anesthesia: In Vivo, Multineuronal Imaging in Caenorhabditis elegans. Anesthesiology 129, 733–743.

Baricordi, O.R., Ferrari, D., Melchiorri, L., Chiozzi, P., Hanau, S., Chiari, E., Rubini, M., and Di Virgilio, F. (1996). An ATP-activated channel is involved in mitogenic stimulation of human T lymphocytes. Blood 87, 682–690.

Barrera, N.P., Ormond, S.J., Henderson, R.M., Murrell-Lagnado, R.D., and Edwardson, J.M. (2005). Atomic force microscopy imaging demonstrates that P2X2 receptors are trimers but that P2X6 receptor subunits do not oligomerize. The Journal of Biological Chemistry 280, 10759–10765.

Barrios, J., Patel, K.R., Aven, L., Achey, R., Minns, M.S., Lee, Y., Trinkaus-Randall, V.E., and Ai, X. (2017). Early life allergen-induced mucus overproduction requires augmented neural stimulation of pulmonary neuroendocrine cell secretion. The FASEB Journal 31, 4117–4128.

Basova, L.V., Tang, X., Umasume, T., Gromova, A., Zyrianova, T., Shmushkovich, T., Wolfson, A., Hawley, D., Zoukhri, D., Shestopalov, V.I., et al. (2017). Manipulation of Panx1 Activity Increases the Engraftment of Transplanted Lacrimal Gland Epithelial Progenitor Cells. Investigative Ophthalmology & Visual Science 58, 5654–5665.

Baum, J.P., Maurice, D.M., and McCarey, B.E. (1984). The active and passive transport of water across the corneal endothelium. Experimental Eye Research 39, 335–342.

Becker, D., Woltersdorf, R., Boldt, W., Schmitz, S., Braam, U., Schmalzing, G., and Markwardt, F. (2008). The P2X7 carboxyl tail is a regulatory module of P2X7 receptor channel activity. The Journal of Biological Chemistry 283, 25725–25734.

Bootman, M.D., Collins, T.J., Peppiatt, C.M., Prothero, L.S., MacKenzie, L., De Smet, P., Travers, M., Tovey, S.C., Seo, J.T., Berridge, M.J., et al. (2001). Calcium signalling—an overview. Seminars in Cell & Developmental Biology 12, 3–10.

Boucher, I., Rich, C., Lee, A., Marcincin, M., and Trinkaus-Randall, V. (2010). The P2Y2 receptor mediates the epithelial injury response and cell migration. American Journal of Physiology-Cell Physiology 299, C411–C421.

Boucher, I., Yang, L., Mayo, C., Klepeis, V., and Trinkaus-Randall, V. (2007). Injury and nucleotides induce phosphorylation of epidermal growth factor receptor: MMP and HB-EGF dependent pathway. Experimental Eye Research 85, 130–141.

Boudreault, F., and Grygorczyk, R. (2004). Cell swelling-induced ATP release is tightly dependent on intracellular calcium elevations. The Journal of Physiology 561, 499–513.

Burnstock, G. (2009). Purinergic Mechanosensory Transduction and Visceral Pain, Purinergic Mechanosensory Transduction and Visceral Pain. Molecular Pain 5, 1744-8069-5–69.

Burnstock, G., Campbell, G., Satchell, D., and Smythe, A. (1970). Evidence that adenosine triphosphate or a related nucleotide is the transmitter substance released by non-adrenergic inhibitory nerves in the gut. British Journal of Pharmacology 40, 668–688.

Calvert, J.A., Atterbury-Thomas, A.E., Leon, C., Forsythe, I.D., Gachet, C., and Evans, R.J. (2004). Evidence for P2Y1, P2Y2, P2Y6 and atypical UTP-sensitive receptors coupled to rises in intracellular calcium in mouse cultured superior cervical ganglion neurons and glia. British Journal of Pharmacology 143, 525–532.

Chen, J., Xia, L., Bruchas, M.R., and Solnica-Krezel, L. (2017). Imaging early embryonic calcium activity with GCaMP6s transgenic zebrafish. Developmental Biology 430, 385–396.

Chen, Y., Bao, Y., Zhang, J., Woehrle, T., Sumi, Y., Ledderose, S., Li, X., Ledderose, C., and Junger, W.G. (2015). Inhibition of neutrophils by hypertonic saline involves pannexin-1, CD39, CD73, and other ectonucleotidases. Shock 44, 221–227.

Chen, J.J., and Tseng, S.C. (1990). Corneal epithelial wound healing in partial limbal deficiency. Investigative Ophthalmology & Visual Science 31, 1301–1314.

Chen, Y., Corriden, R., Inoue, Y., Yip, L., Hashiguchi, N., Zinkernagel, A., Nizet, V., Insel, P.A., and Junger, W.G. (2006). ATP release guides neutrophil chemotaxis via P2Y2 and A3 receptors. Science 314, 1792–1795.

Clapham, D.E. (2007). Calcium signaling. Cell 131, 1047–1058.

Compan, V., Ulmann, L., Stelmashenko, O., Chemin, J., Chaumont, S., and Rassendren, F. (2012). P2X2 and P2X5 Subunits Define a New Heteromeric Receptor with P2X7-Like Properties. Journal of Neuroscience 32, 4284–4296.

Cornell-Bell, A.H., Finkbeiner, S.M., Cooper, M.S., and Smith, S.J. (1990). Glutamate induces calcium waves in cultured astrocytes: long-range glial signaling. Science 247, 470–473.

Cotrina, M.L., Lin, J.H., Alves-Rodrigues, A., Liu, S., Li, J., Azmi-Ghadimi, H., Kang, J., Naus, C.C., and Nedergaard, M. (1998). Connexins regulate calcium signaling by controlling ATP release. Proceedings of the National Academy of Sciences of the United States of America 95, 15735–15740.

Cotsarelis, G., Cheng, S.Z., Dong, G., Sun, T.T., and Lavker, R.M. (1989). Existence of slow-cycling limbal epithelial basal cells that can be preferentially stimulated to proliferate: implications on epithelial stem cells. Cell 57, 201–209.

Courjaret, R., Dib, M., and Machaca, K. (2017). Store-Operated Ca^{2+} Entry in Oocytes Modulate the Dynamics of IP3 -Dependent Ca^{2+} Release from Oscillatory to Tonic. Journal of Cellular Physiology 232, 1095–1103.

Cui, H., Liu, Y., Qin, L., Wang, L., and Huang, Y. (2016). Increased membrane localization of pannexin1 in human corneal synaptosomes causes enhanced stimulated ATP release in chronic diabetes mellitus. Medicine (Baltimore) 95, e5084–e5084.

D'Andrea, P., and Vittur, F. (1997). Propagation of intercellular Ca^{2+} waves in mechanically stimulated articular chondrocytes. FEBS Letters 400, 58–64.

Daniels, J.T., Dart, J.K., Tuft, S.J., and Khaw, P.T. (2001). Corneal stem cells in review. Wound Repair and Regeneneration 9, 483–494.

Derricks, K.E., Trinkaus-Randall, V., and Nugent, M.A. (2015). Extracellular matrix stiffness modulates VEGF calcium signaling in endothelial cells: individual cell and population analysis. Integrative Biology 7, 1011–1025.

Deshpande, L.S., Blair, R.E., Phillips, K.F., and DeLorenzo, R.J. (2016). Role of the calcium plateau in neuronal injury and behavioral morbidities following organophosphate intoxication. Annals of the New York Academy of Sciences 1374, 176–183.

Di Virgilio, F. (2007). Liaisons dangereuses: P2X(7) and the inflammasome. Trends in Pharmacology Science 28, 465–472.

Ferrari, D., Pizzirani, C., Adinolfi, E., Lemoli, R.M., Curti, A., Idzko, M., Panther, E., and Di Virgilio, F. (2006). The P2X7 receptor: a key player in IL-1 processing and release. The Journal of Immunology 176, 3877–3883.

Friedl, P., and Mayor, R. (2017). Tuning Collective Cell Migration by Cell–Cell Junction Regulation. Cold Spring Harbor Perspectives in Biology 9, a029199.

Friend, J., and Thoft, R.A. (1984). The diabetic cornea. International Ophthalmology Clinics 24, 111–123.

Friend, J., Ishii, Y., and Thoft, R.A. (1982). Corneal epithelial changes in diabetic rats. Ophthalmic Research 14, 269–278.

García-Hernández, M.H., Portales-Cervantes, L., Cortez-Espinosa, N., Vargas-Morales, J.M., Fritche Salazar, J.F., Rivera-López, E., Rodríguez-Rivera, J.G., Quezada-Calvillo, R., and Portales-Pérez, D.P. (2011). Expression and function of P2X(7) receptor and CD39/Entpd1 in patients with type 2 diabetes and their association with biochemical parameters. Cellular Immunology 269, 135–143.

Gipson, I.K., Spurr-Michaud, S., Argüeso, P., Tisdale, A., Ng, T.F., and Russo, C.L. (2003). Mucin gene expression in immortalized human corneal-limbal and conjunctival epithelial cell lines. Investigative Ophthalmology & Visual Science 44, 2496–2506.

Grandolfo, M., Calabrese, A., and D'andrea, P. (1998). Mechanism of Mechanically Induced Intercellular Calcium Waves in Rabbit Articular Chondrocytes and in HIG-82 Synovial Cells. Journal of Bone and Mineral Research 13, 443–453.

Hamrah, P., Liu, Y., Zhang, Q., and Dana, M.R. (2003). The Corneal Stroma Is Endowed with a Significant Number of Resident Dendritic Cells. Investigative Ophthalmology & Visual Science 44, 581–589.

Hanna, C. (1966). Proliferation and migration of epithelial cells during corneal wound repair in the rabbit and the rat. American Journal of Ophthalmology 61, 55–63.

Hanna, C., Bicknell, D.S., and O'Brien, J.E. (1961). Cell turnover in the adult human eye. Archives of Ophthalmology 65, 695–698.

Hirase, H., Qian, L., Barthó, P., and Buzsáki, G. (2004). Calcium dynamics of cortical astrocytic networks in vivo. PLoS Biology 2, E96.

Hoogland, T.M., Kuhn, B., Göbel, W., Huang, W., Nakai, J., Helmchen, F., Flint, J., and Wang, S.S.-H. (2009). Radially expanding transglial calcium waves in the intact cerebellum. Proceedings of the National Academy of Sciences of the United States of America 106, 3496–3501.

Hutcheon, A.E.K., Sippel, K.C., and Zieske, J.D. (2007). Examination of the restoration of epithelial barrier function following superficial keratectomy. Experimental Eye Research 84, 32–38.

Iglesias, R., Locovei, S., Roque, A., Alberto, A.P., Dahl, G., Spray, D.C., and Scemes, E. (2008). P2X7 receptor-Pannexin1 complex: pharmacology and signaling. American Journal of Physiology: Cell Physiology 295, C752–C760.

Jakus, M. A. (1961) "Structure of the human cornea." The structure of the eye, 343-366.

Jørgensen, N.R., Geist, S.T., Civitelli, R., and Steinberg, T.H. (1997). ATP- and Gap Junction–dependent Intercellular Calcium Signaling in Osteoblastic Cells. The Journal of Cell Biology 139, 497–506.

Junger, W.G. (2008). Purinergic regulation of neutrophil chemotaxis. Cellular and Molecular Life Sciences 65, 2528–2540.

Junger, W.G. (2011). Immune cell regulation by autocrine purinergic signalling. Nature Reviews Immunology 11, 201–212.

Kehasse, A., Rich, C.B., Lee, A., McComb, M.E., Costello, C.E., and Trinkaus-Randall, V. (2013). Epithelial Wounds Induce Differential Phosphorylation Changes in Response to Purinergic and EGF Receptor Activation. The American Journal of Pathology 183, 1841–1852.

Klepeis, V.E., Cornell-Bell, A., and Trinkaus-Randall, V. (2001). Growth factors but not gap junctions play a role in injury-induced Ca^{2+} waves in epithelial cells. Journal of Cell Science 114, 4185–4195.

Klepeis, V.E., Weinger, I., Kaczmarek, E., and Trinkaus-Randall, V. (2004). P2Y receptors play a critical role in epithelial cell communication and migration. Journal of Cellular Biochemistry 93, 1115–1133.

Klyce, S.D. (1972). Electrical profiles in the corneal epithelium. The Journal of Physiology 226, 407–429.

Kneer, K., Green, M.B., Meyer, J., Rich, C.B., Minns, M.S., and Trinkaus-Randall, V. (2018). High fat diet induces pre-type 2 diabetes with regional changes in corneal sensory nerves and altered P2X7 expression and localization. Experimental Eye Research 175, 44–55.

Lavker, R.M., Dong, G., Cheng, S.Z., Kudoh, K., Cotsarelis, G., and Sun, T.T. (1991). Relative proliferative rates of limbal and corneal epithelia. Implications of corneal epithelial migration, circadian rhythm, and suprabasally located DNA-synthesizing keratinocytes. Investigative Ophthalmology & Visual Science 32, 1864–1875.

Lee, A., Derricks, K., Minns, M., Ji, S., Chi, C., Nugent, M.A., and Trinkaus-Randall, V. (2014). Hypoxia-induced changes in Ca^{2+} mobilization and protein phosphorylation implicated in impaired wound healing. American Journal of Physiology-Cell Physiology 306, C972–C985.

Lister, M.F., Sharkey, J., Sawatzky, D.A., Hodgkiss, J.P., Davidson, D.J., Rossi, A.G., and Finlayson, K. (2007). The role of the purinergic P2X7 receptor in inflammation. Journal of Inflammation 4, 5.

Locovei, S., Scemes, E., Qiu, F., Spray, D.C., and Dahl, G. (2007). Pannexin1 is part of the pore forming unit of the P2X(7) receptor death complex. FEBS Letters 581, 483–488.

Lu, W., Hu, H., Sévigny, J., Gabelt, B.T., Kaufman, P.L., Johnson, E.C., Morrison, J.C., Zode, G.S., Sheffield, V.C., Zhang, X., et al. (2015). Rat, Mouse, and Primate Models of Chronic Glaucoma Show Sustained Elevation of Extracellular ATP and Altered Purinergic Signaling in the Posterior Eye. Investigative Ophthalmology & Visual Science 56 3075–3083.

Mankus, C., Rich, C., Minns, M., and Trinkaus-Randall, V. (2011). Corneal Epithelium Expresses a Variant of P2X7 Receptor in Health and Disease. PLoS ONE 6, e28541.

Mayo, C., Ren, R., Rich, C., Stepp, M.A., and Trinkaus-Randall, V. (2008). Regulation by P2X7: Epithelial Migration and Stromal Organization in the Cornea Investigative Ophthalmology & Visual Science 49, 4384–4391.

Minns, M.S., Teicher, G., Rich, C.B., and Trinkaus-Randall, V. (2016). Purinoreceptor P2X7 Regulation of Ca^{2+} Mobilization and Cytoskeletal Rearrangement Is Required for Corneal Reepithelialization after Injury. The American Journal of Pathology 186, 285–296.

Müller, L.J., Pels, L., and Vrensen, G.F. (1996). Ultrastructural organization of human corneal nerves. Investigative Ophthalmology & Visual Science *37*, 476–488.

Nakajima, R., Kobayashi, T., Moriya, N., Mizutani, M., Kan, K., Nozaki, T., Saitoh, K., Yamato, M., Okano, T., and Takeda, S. (2015). A novel closed cell culture device for fabrication of corneal epithelial cell sheets. Journal of Tissue Engineering and Regenerative Medicine 9, 1259–1267.

Nicke, A., Kerschensteiner, D., and Soto, F. (2005). Biochemical and functional evidence for heteromeric assembly of P2X1 and P2X4 subunits. The Journal of Neurochemistry 92, 925–933.

North, R.A. (2002). Molecular physiology of P2X receptors. Physiological Reviews 82, 1013–1067.

Ormond, S.J., Barrera, N.P., Qureshi, O.S., Henderson, R.M., Edwardson, J.M., and Murrell-Lagnado, R.D. (2006). An uncharged region within the N terminus of the P2X6 receptor inhibits its assembly and exit from the endoplasmic reticulum. Molecular Pharmacology, 69, 1692–1700.

Oswald, D.J., Lee, A., Trinidad, M., Chi, C., Ren, R., Rich, C.B., and Trinkaus-Randall, V. (2012). Communication between Corneal Epithelial Cells and Trigeminal Neurons Is Facilitated by Purinergic (P2) and Glutamatergic Receptors. PLoS ONE 7, e44574.

Philipson, K.D., Nicoll, D.A., and Li, Z. (1993). The cardiac sodium-calcium exchanger. Society of General Physiologists Series 48, 187–191.

Quist, A.P., Rhee, S.K., Lin, H., and Lal, R. (2000). Physiological Role of Gap-Junctional Hemichannels: Extracellular Calcium-Dependent Isosmotic Volume Regulation. The Journal of Cell Biology 148, 1063–1074.

Ratchford, A.M., Baker, O.J., Camden, J.M., Rikka, S., Petris, M.J., Seye, C.I., Erb, L., and Weisman, G.A. (2010). P2Y2 Nucleotide Receptors Mediate Metalloprotease-dependent Phosphorylation of Epidermal Growth Factor Receptor and ErbB3 in Human Salivary Gland Cells. Journal of Biological Chemistry 285, 7545–7555.

Reuter, H. (1991). Sodium-calcium exchange. Ins and outs of Ca^{2+} transport. Nature 349, 567–568.

Robb-Gaspers, L.D., and Thomas, A.P. (1995). Coordination of Ca^{2+} signaling by intercellular propagation of Ca^{2+} waves in the intact liver. The Journal of Biological Chemistry 270, 8102–8107.

Romanov, R.A., Bystrova, M.F., Rogachevskaya, O.A., Sadovnikov, V.B., Shestopalov, V.I., and Kolesnikov, S.S. (2012). The ATP permeability of pannexin 1 channels in a heterologous system and in mammalian taste cells is dispensable. Journal of Cell Science 125, 5514–5523.

Sáez, P.J., Vargas, P., Shoji, K.F., Harcha, P.A., Lennon-Duménil, A.-M., and Sáez, J.C. (2017). ATP promotes the fast migration of dendritic cells through the activity of pannexin 1 channels and P2X7 receptors. Science Signaling 10, eaah7107.

Sanderson, M.J., Charles, A.C., and Dirksen, E.R. (1990). Mechanical stimulation and intercellular communication increases intracellular Ca^{2+} in epithelial cells. Molecular Biology of the Cell 1, 585–596.

Scemes, E., and Giaume, C. (2006). Astrocyte calcium waves: What they are and what they do. Glia 54, 716–725.

Schenk, U., Westendorf, A.M., Radaelli, E., Casati, A., Ferro, M., Fumagalli, M., Verderio, C., Buer, J., Scanziani, E., and Grassi, F. (2008). Purinergic control of T cell activation by ATP released through pannexin-1 hemichannels. Science Signaling, 1, ra6.

Schneider, I., Houston, D.W., Rebagliati, M.R., and Slusarski, D.C. (2008). Calcium fluxes in dorsal forerunner cells antagonize β-catenin and alter left-right patterning. Development 135, 75–84.

Schultz, R.O., Van Horn, D.L., Peters, M.A., Klewin, K.M., and Schutten, W.H. (1981). Diabetic keratopathy. Transactions of the American Ophthalmological Society 79, 180–199.

Smart, M.L., Gu, B., Panchal, R.G., Wiley, J., Cromer, B., Williams, D.A., and Petrou, S. (2003). P2X7 receptor cell surface expression and cytolytic pore formation are regulated by a distal C-terminal region. The Journal of Biological Chemistry 278, 8853–8860.

Sneyd, J., Wilkins, M., Strahonja, A., and Sanderson, M.J. (1998). Calcium waves and oscillations driven by an intercellular gradient of inositol (1,4,5)-trisphosphate. Biophysical Chemistry 72, 101–109.

Söhl, G., and Willecke, K. (2004). Gap junctions and the connexin protein family. Cardiovasc Res 62, 228–232.

Sumi, Y., Woehrle, T., Chen, Y., Bao, Y., Li, X., Yao, Y., Inoue, Y., Tanaka, H., and Junger, W.G. (2014). Plasma ATP is required for neutrophil activation in a mouse sepsis model. Shock 42, 142–147.

Suzuki, K. (2003). Cell–matrix and cell–cell interactions during corneal epithelial wound healing. Progress in Retinal and Eye Research 22, 113–133.

Takai, E., Tsukimoto, M., Harada, H., and Kojima, S. (2014). Autocrine signaling via release of ATP and activation of P2X7 receptor influences motile activity of human lung cancer cells. Purinergic Signaling 10, 487–497.

Trinkaus-Randall, V. (2000) Cornea: Biological Responses. Principles of Tissue Engineering (second edition) 35, 471-491.

Ullah, G., Jung, P., and Cornell-Bell, A.H. (2006). Anti-phase calcium oscillations in astrocytes via inositol (1, 4, 5)-trisphosphate regeneration. Cell Calcium 39, 197–208.

Verhoef, P.A., Estacion, M., Schilling, W., and Dubyak, G.R. (2003). P2X7 receptordependent blebbing and the activation of Rho-effector kinases, caspases, and IL-1 beta release. The Journal of Immunology 170, 5728–5738.

Virginio, C., Church, D., North, R.A., and Surprenant, A. (1997). Effects of divalent cations, protons and calmidazolium at the rat P2X7 receptor. Neuropharmacology 36, 1285–1294.

Volonté, C., Amadio, S., D'Ambrosi, N., Colpi, M., and Burnstock, G. (2006). P2 receptor web: complexity and fine-tuning. Pharmacology & Therapeutics 112, 264–280.

Wang, M., Kong, Q., Gonzalez, F.A., Sun, G., Erb, L., Seye, C., and Weisman, G.A. (2005). P2Y2 nucleotide receptor interaction with αV integrin mediates astrocyte migration. Journal of Neurochemistry 95, 630–640.

Wei, C., Wang, X., Chen, M., Ouyang, K., Song, L.-S., and Cheng, H. (2009). Calcium flickers steer cell migration. Nature 457, 901–905.

Weinger, I., Klepeis, V.E., and Trinkaus-Randall, V. (2005). Tri-nucleotide receptors play a critical role in epithelial cell wound repair. Purinergic Signaling 1, 281-292.

Weissman, T.A., Riquelme, P.A., Ivic, L., Flint, A.C., and Kriegstein, A.R. (2004). Calcium Waves Propagate through Radial Glial Cells and Modulate Proliferation in the Developing Neocortex. Neuron 43, 647–661.

Whitcher, J.P., Srinivasan, M., and Upadhyay, M.P. (2001). Corneal blindness: a global perspective. Bulletin of the World Health Organization 79, 214–221.

Wilson, S.E., and Hong, J.W. (2000). Bowman's layer structure and function: critical or dispensable to corneal function? A hypothesis. Cornea 19, 417–420.

Yang, L., Cranson, D., and Trinkaus-Randall, V. (2004). Cellular injury induces activation of MAPK via P2Y receptors. Journal of Cellular Biochemistry 91, 938–950.

Yin, J., Xu, K., Zhang, J., Kumar, A., and Yu, F.-S.X. (2007). Wound-induced ATP release and EGF receptor activation in epithelial cells. Journal of Cell Science 120, 815–825.

Yip, L., Woehrle, T., Corriden, R., Hirsh, M., Chen, Y., Inoue, Y., Ferrari, V., Insel, P.A., and Junger, W.G. (2009). Autocrine regulation of T-cell activation by ATP release and P2X7 receptors. The FASEB Journal 23, 1685–1693.

Zieske, J.D., Takahashi, H., Hutcheon, A.E., and Dalbone, A.C. (2000). Activation of epidermal growth factor receptor during corneal epithelial migration. Investigative Ophthalmology & Visual Science 41, 1346–1355.

Zimmet, P., Alberti, K.G.M.M., and Shaw, J. (2001). Global and societal implications of the diabetes epidemic. Nature 414, 782.

CURRICULUM VITAE